



THE DEVELOPMENT OF A THERMALLY ACTIVATED,
CONTINUOUSLY SENSITIVE CLOUD CHAMBER, AND
ITS USE IN NUCLEAR PHYSICS RESEARCH.

by

ALEXANDER SUSS LANGSDORF, JR.

A.B., Washington University

1932

Submitted in partial fulfillment of the
requirements for the degree of

DOCTOR OF PHILOSOPHY

from the

MASSACHUSETTS INSTITUTE OF TECHNOLOGY

1937

Signature of Author

Department of Physics, December 9, 1937

Signature of Professor
in Charge of Research . .

Signature of Chairman of Department
Committee on Graduate Students .

√

Phys. Thesis
1937

[For corrections + changes see list at end of thesis.]

38

TABLE OF CONTENTS

	Page
List of Tables and Figures	
Abstract	1
CHAPTER I - THE DIFFUSION CLOUD CHAMBER.	4
Introduction	4
1. The Wilson expansion cloud chamber	5
2. The cloud chamber of long time or continuous sensitivity to ions	10
3. The diffusion cloud chamber	11
4. The design of the diffusion cloud chamber	13
5. The operation of the diffusion cloud chamber	16
6. Criticism of the diffusion cloud chamber described in Section 4	18
CHAPTER II - AN ANALYSIS OF THE OPERATION OF THE DIFFUSION CLOUD CHAMBER	21
1. The problem to be solved	21
2. The diffusion problem	23
3. The temperature distribution problem	27
4. Further analysis of the vapor and gas dis- tribution problem	29
5. Calculations of the diffusion of methyl al- cohol through carbon dioxide under certain specified conditions	30
6. The effects of varying the conditions of operation in the diffusion cloud chamber	34
7. Consideration of factors previously neglected which influence the supersaturation	43
8. Conclusions concerning the choice of operat- ing conditions for the diffusion cloud chamber	49
CHAPTER III - THE DESIGN OF DIFFUSION CLOUD CHAMBERS	50
Introduction	50
1. Various models of the diffusion cloud chamber	50
2. Major design factors	60
A. Visibility of the interior	60
B. Refrigeration of the chamber floor	74
C. Heating the chamber roof and distribution of vapor at the roof	78
D. Vapor supply to the chamber roof	80
E. Prevention of turbulence of gas	84
F. Prevention of leaks	85
3. Minor design factors	87
4. Conclusions	93

TABLE OF CONTENTS (continued)

	Page
CHAPTER IV - THE CONDENSATION OF A SUPERSATURATED VAPOR UPON IONS	94
Introduction	94
1. Thomson's equation	94
2. The kinetic picture of the growth of charged droplets	97
3. Terminology, and calculations for the half-life of ions as a function of supersaturation	99
4. Interpretation of the results of the preceding section	117
5. Variation of the critical supersaturation for ion tracks, S_k with temperature and surface tension	118
6. A correlation of the theories of condensation upon ions and of spontaneous condensation	120
7. Correlation of the theories of condensation with experimental data	122
8. Applications of the analysis of condensation phenomena to the continuous cloud chamber	124
CHAPTER V - THE USES OF A CONTINUOUS CLOUD CHAMBER	128
1. Cosmic ray observation	128
2. Weak radioactivity	128
3. A comparison of the advantages of the continuous cloud chamber with those of other apparatus	129
4. Experiments on the kinetics of condensation, and future development of the cloud chamber itself	129
Appendix I. The spontaneous condensation of supersaturated vapor and related phenomena	130
Appendix II. Various forms of continuous cloud chambers	
Acknowledgments	143
Biography	145
Bibliography	146
Index	

LIST OF FIGURES

	Page
Figure 1	Wilson cloud chambers 7
Figure 2	Wilson cloud chamber photographs 9
Figure 3	Estimated supersaturation 14
Figure 4	Diffusion cloud chamber A 14
Figure 5	Diffusion cloud chamber B 19
Figure 6	Supersaturation for various fluxes 37
Figure 7	Temperature distribution 37
Figure 8	Supersaturation, various temperatures 41
Figure 9	Chamber A photographs 52
Figure 10	Chamber A photographs 53
Figure 10a	Chamber A photographs 55
Figure 11	
Figure 12	Chamber C drawings 57
Figure 13	Chamber C drawings 58
Figure 14	Chamber C drawings 59
Figure 15	
Figure 16	Chamber C photographs 62
Figure 17	Chamber C photographs 63
Figure 18	Chamber C photographs 63
Figure 19	Chamber C drawing 65
Figure 19a	Chamber C drawing 66
Figure 20	Chamber C drawing 67
Figure 21	Chamber C photographs 69
Figure 22	Chamber C drawings 71
Figure 23	A punch 82
Figure 24	A drain tube 82
Figure 25	

Figures continued.

	Page
Figure 26 Charged droplet vapor pressure	96
Figure 27 Half life for methanol	116
Figure 28 Half life for water.	116
Figure 29 Interpolation curve	96
Figure 30	
Figure 31 Graph from Becker	136
Figure 32 Early Wilson cloud chambers	142

LIST OF TABLES

	Page
Table I Supersaturations at various fluxes	35
Table II Supersaturations at various temperatures	40
Table III Functions of q113
Table IV Physical Data114
Table V Values of λ and S115
Table VI Classification of variables126

ABSTRACT.

The diffusion cloud chamber described in this thesis maintains the supersaturation necessary for formation of ion-tracks by the diffusion of an initially saturated vapor vertically downward through a non-condensing gas to a horizontal refrigerated plate. In this way it allows valuable extensions of the cloud chamber technique by overcoming the handicap of a short time of sensitivity to ions which is inherent in expansion cloud chambers.

When methyl alcohol vapor is supplied to the top of the chamber at 70 degrees centigrade and diffuses down to the bottom at -45 degrees, there is an intermediate region sufficiently supersaturated to show the characteristic tracks of cosmic ray primaries and secondaries as well as those due to secondary electrons from gamma-radiation. Turbulence and convection can be avoided, but a continuous rain of condensed droplets probably cannot be completely eliminated.

Calculations have been made to determine what supersaturation can be attained in a diffusion cloud chamber of this type. These calculations are based upon certain simplifying assumptions and are of necessity approximate. However, the manner in which each of the independent and dependent variables influences the supersaturation is illustrated clearly. The calculations permit estimations

of the desirable operating conditions in the cloud chamber previous to their experimental determination.

The construction of each of three models of the diffusion cloud chamber is illustrated by diagrams and photographs. Information of practical value was accumulated in the course of the design, construction, and operation of these chambers, and is recorded here.

A kinetic analysis is made to predict theoretically the supersaturation necessary to produce condensation upon ions in a supersaturated vapor. A thermodynamic analysis of charged droplets predicts a supersaturation sufficient for ion-track formation. A comparison of the two results shows that the necessary supersaturation as determined by the kinetic analysis is approximately the $3/4$ power of the supersaturation sufficient on a thermodynamic basis. This prediction has not yet been experimentally verified.

An earlier kinetic analysis predicts a supersaturation at which spontaneous condensation occurs rapidly without ions. A comparison of this theory and the one presented here leads to the conclusion that cloud chambers cannot show ion-tracks at too high a temperature, a prediction that agrees with experiments.

The theories of condensation of vapors are considered in relation to the phenomena in the continuous cloud chamber.

The further development of the cloud chamber is discussed, and the necessary experimental and theoretical work is briefly outlined.

The uses of the continuous cloud chamber in nuclear research are briefly discussed.

CHAPTER 1 - THE DIFFUSION CLOUD CHAMBER.

Introduction.

The principle topic of this thesis is the presentation of a new form of "cloud chamber" which is continuously supersaturated over extended periods of time. The operation and use of this cloud chamber, which hereafter will be called the "diffusion cloud chamber" are based upon the characteristics of supersaturated vapors in the same way as for the more familiar Wilson expansion cloud chamber. The diffusion cloud chamber was developed as a result of efforts to extend the field of usefulness of the cloud chamber technique by overcoming the handicap of the short active period of the expansion cloud chamber. As a result, the new apparatus has applications similar to those of the Wilson expansion cloud chamber, but nevertheless different in many ways.

In this chapter, a brief description of the Wilson expansion cloud chamber will be made for the benefit of readers unfamiliar with this apparatus. This will be followed by a brief description of the fundamental idea involved in the design of the diffusion cloud chamber, a sketch of the design adopted for it, and a description of how this apparatus acted under typical operating conditions.

In following chapters will be presented the theory of the operation of the diffusion cloud chamber, details of designs of various apparatus built or proposed, descriptions

of experiments performed, and suggestions of appropriate uses in the future. Appendices will present information and suggestions correlated with the design and use of the diffusion cloud chamber, but not directly bearing upon it.

1. The Wilson expansion cloud chamber.

C. T. R. Wilson invented and developed the expansion cloud chamber in the period between 1897 and 1911. In Figure 1 is shown a sketch of his apparatus. It is a cylinder closed by a moveable piston at one end, and covered by a glass window at the other end. The volume inside contains a gas saturated with a vapor such as that of water or a volatile alcohol. This mixture, initially at equilibrium, is suddenly, nearly adiabatically, expanded. As a result the temperature of the mixture drops. A simple analysis shows that at this new lower temperature the amount of vapor present in the mixture is greater than the amount that would be present in equilibrium with liquid at this temperature. One says that the vapor is supersaturated. Quantitatively, the supersaturation, S , is the ratio of the existing vapor concentration to that which would be present at the same temperature in equilibrium with the liquid.

C. T. R. Wilson discovered that for water vapor in the vicinity of 0°C , the supersaturated vapor would condense to a cloud of rain upon dust particles present in the chamber at a small amount of supersaturation (any $S > 1$). But if the chamber is freed of dust, no condensation occurs

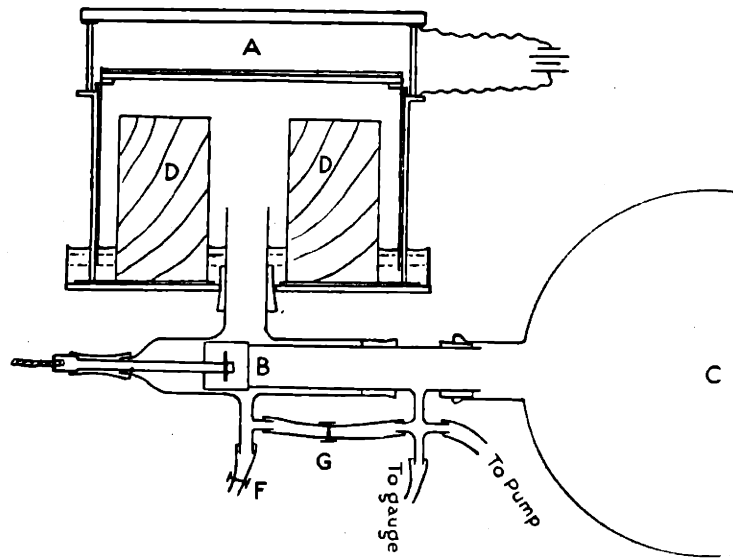
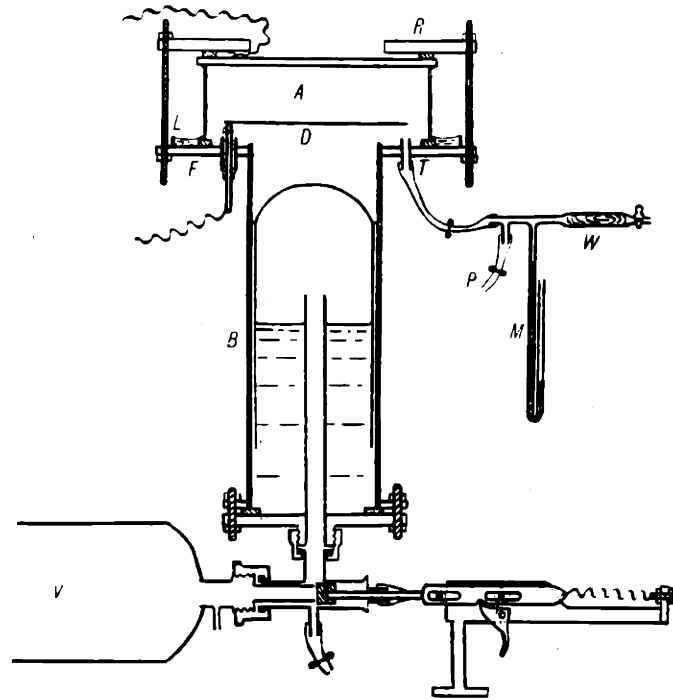


FIG. 1.

FIGURE 1

FIGURE 2.

Ion-tracks as photographed by C. T. R. Wilson.

Top. Secondary electrons produced by x-rays.

Center. Secondary electrons produced by x-rays, etc.,
and a straight track from some high energy
particle.

Bottom. Alpha ray tracks.

Left. A cluster of tracks. This is one of the
earliest published ion-track photographs.

Center. A photograph showing several phenomena
of interest. See

Right. Alpha ray tracks showing delta ray
branches.

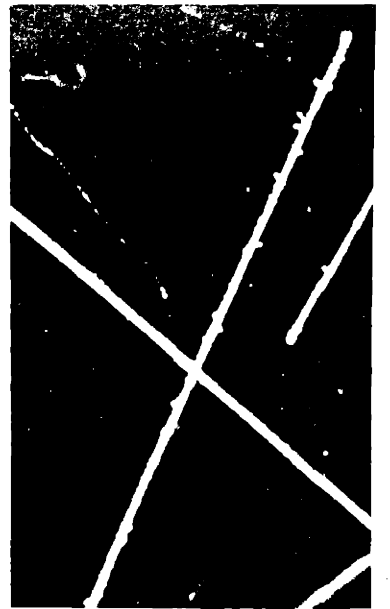
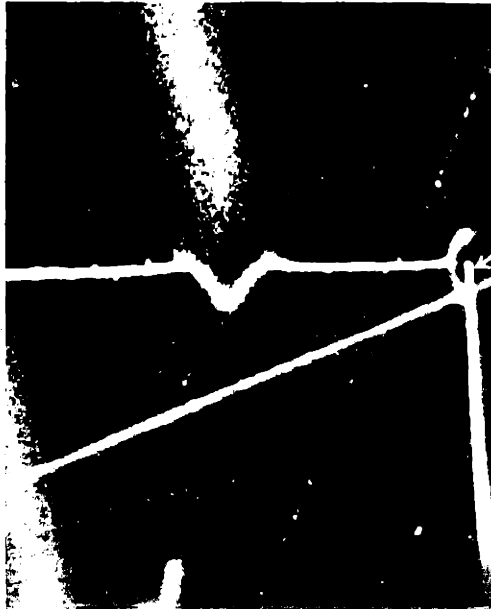
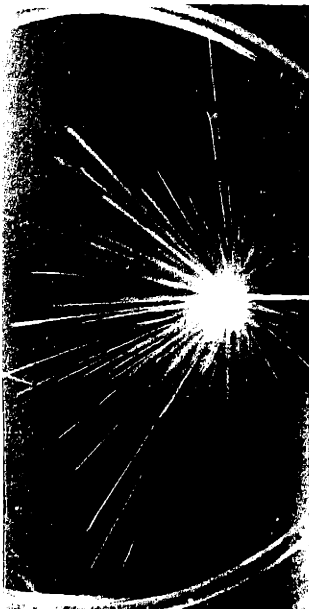
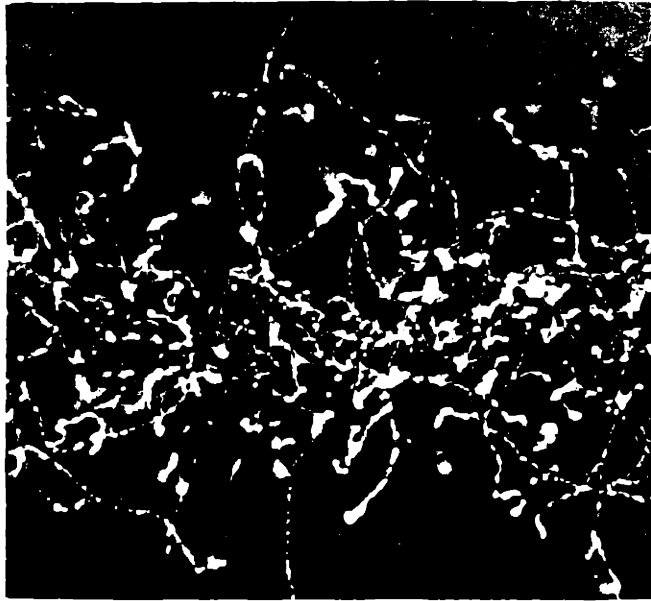


FIGURE 2

until S is about equal to 4. Then the vapor will condense selectively upon ions present in the chamber. This phenomenon is what gives the cloud chamber its greatest usefulness. The droplets which form on the ions can be observed through the glass windows of the chamber and photographed as illustrated by Figure 2. In this way one may obtain much information of value in the field of nuclear physics. C. T. R. Wilson also found that at about $S = 8$ a general cloud condensation set in, which was not limited to condensation upon dust or ions. For the observation of ion-tracks of alpha and beta rays, etc., the adiabatic expansion must be limited so this supersaturation is not reached. For various vapor and gas mixtures, the desirable expansion usually lies between 8 percent and 30 percent by volume.

2. The cloud chamber of long time or continuous sensitivity to ions.

In recent years there has been some demand for maintaining the ability of the vapor in a cloud chamber to condense upon ions over a longer period of time than is usually obtained. With the customary technique of a sudden expansion from one fixed volume to another larger fixed volume, the vapor does not condense upon ions much more than about one-tenth second after the expansion, principally because of loss of supersaturation by condensation on the chamber walls and on other ions, and reheating of the vapor

by conduction and radiation absorption. Then it is necessary to recompress the gas and, for best results, one must wait about ten seconds to obtain equilibrium before another expansion is made. Thus the cloud chamber is only actually operative about one percent of the time. But to study phenomena of low probability and statistically distributed in time, such as cosmic ray bursts and emission from weak radioactive materials, one wants an apparatus operative a large percentage of the time, or continuously. Otherwise it is exceedingly difficult to obtain data of a desirable completeness.

Bearden⁴ found that a slow, large expansion, only approximately adiabatic, would make a suitably designed expansion cloud chamber sensitive to condensation on ions for about two seconds. Hoxton¹ designed an apparatus intended to maintain the needed supersaturation for an extended period. Vollrath² has described a continuously active cloud chamber which he calls a "chemical cloud chamber."

3. The diffusion cloud chamber.

The fundamental idea involved in the apparatus described in this thesis is that in diffusing a vapor through a gas from a region of high vapor density into a region of low temperature, an intermediate region which

⁴ Numbers such as this one refer to the bibliography. Footnotes will be denoted by asterisks.

is supersaturated with vapor can be produced and maintained.

The walls of the region of high vapor density must be kept hot enough so the vapor does not condense there. A supply of vapor must be maintained at all times, from a boiler or other reservoir, flowing into the hot region and maintaining its high vapor density.

To achieve stability against convection, so that the diffusing vapor is not affected by turbulence, two conditions should be fulfilled: the cold region must be cooled by a horizontal refrigerated plane surface beneath the heated region, and the gas thru which the vapor diffuses downward should be more dense than the condensable vapor.

Elementary and approximate reasoning was used at first to justify experimenting with an apparatus to produce supersaturation on the manner just described. This reasoning was as follows:

First assume a vapor diffusing downward from an infinite, hot, horizontal plane surface to an infinite cold horizontal plane surface. Then in diffusing through the gas, the partial pressure of the vapor may be made to vary roughly linearly.* The temperature gradient can also be about linear. That is,

$$(1) \quad p(x) = p_0 + ax$$

$$(2) \quad T(x) = T_0 + bx$$

where x is the height above the floor of the chamber. But

* Pressure is a more convenient variable to use than concentration.

the saturation pressure, p_s , of the vapor is nearly of the form

$$(3) \quad \log \frac{p_s}{p_0} = \frac{\Delta H}{R} \left(\frac{1}{T} - \frac{1}{T_0} \right)$$

which is by no means linear over a wide temperature range. If h is the height of the chamber, we arrange so that the pressure of the vapor at the top, $p(h) = p_0 + a h$, is almost as great as the saturation pressure given by putting T equal to $T(h)$ in the formula for p_s . The supersaturation is then

$$(4) \quad S(x) = p_0(x)/p_s(x)$$

The information contained in these four equations is shown graphically in Figure 3, excepting that p_s (for water) was obtained from experimental data instead of from equation 3. It is to be seen from the graph that there is a region near the cold bottom of the chamber which is highly supersaturated, as desired. These data for a specific case of water diffusing through air indicate that a temperature difference of about 100°C between the hot top and the cold bottom surface is needed to create a supersaturation of $S = 4$. This is the magnitude of supersaturation indicated by the results of C. T. R. Wilson, to be necessary for condensation on ions.

4. The design of the diffusion cloud chamber.

On the basis of the simple analysis just given, an apparatus was designed to permit diffusion of a vapor between

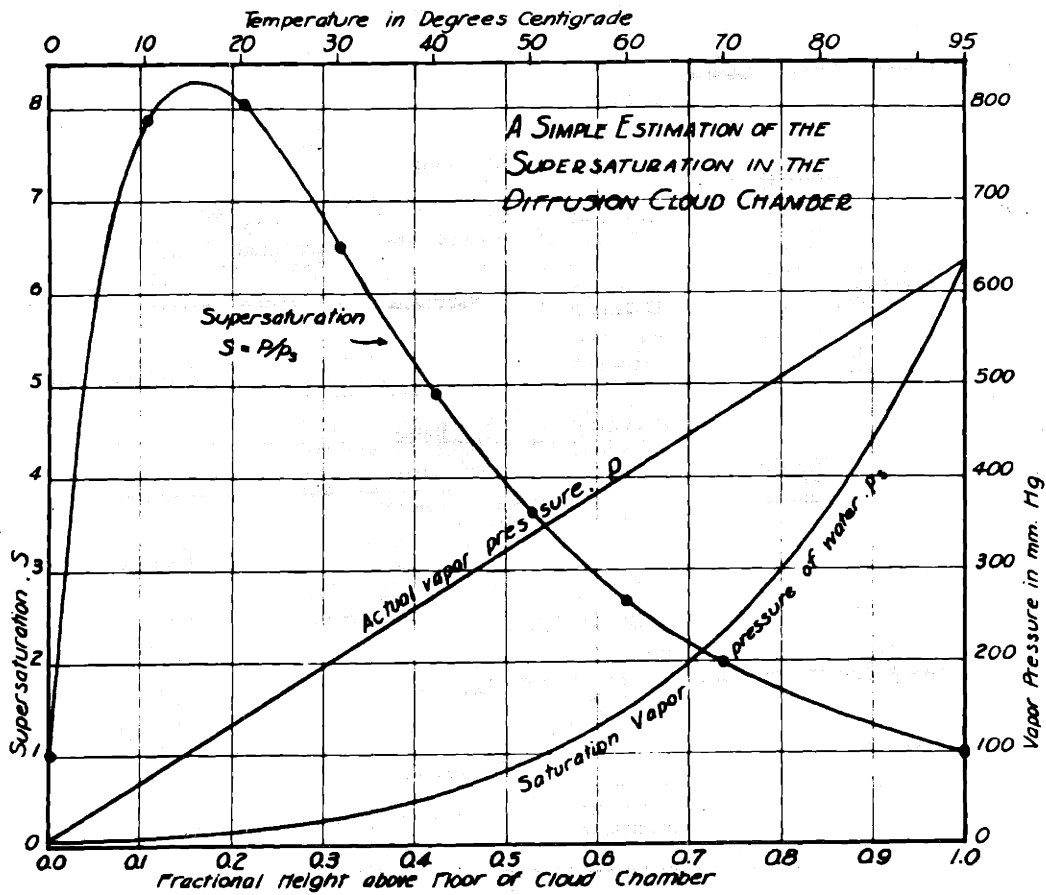
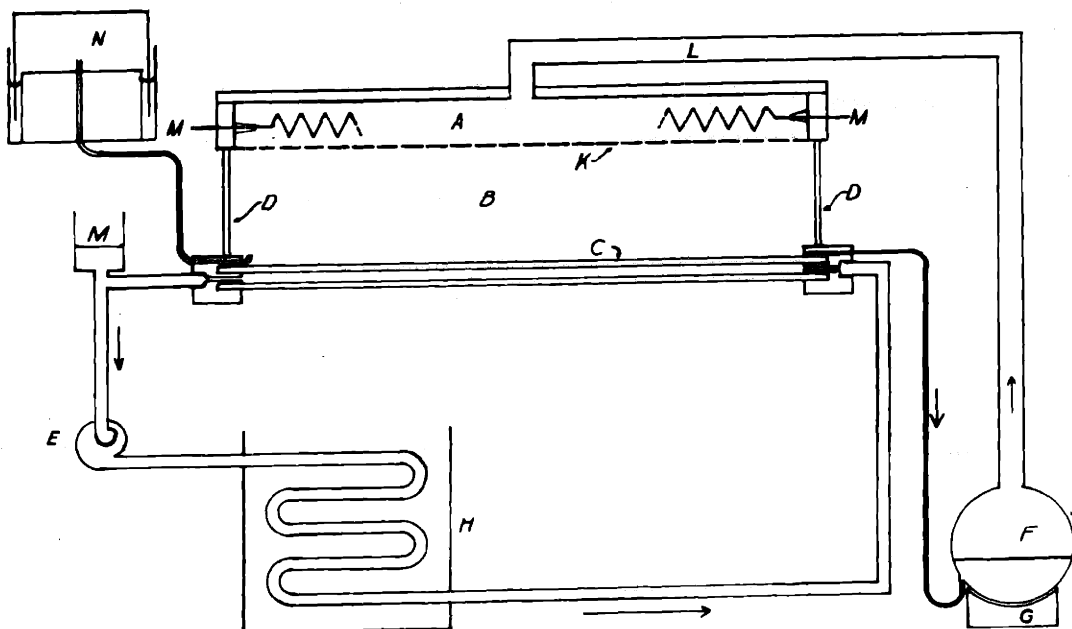


FIGURE 3



SCHEMATIC DIAGRAM OF A DIFFUSION CLOUD CHAMBER
AND ITS PRINCIPAL AUXILIARY PARTS

FIGURE 4

horizontal surfaces maintained at a temperature difference of the order of 100°C . In Figure 4 is a schematic diagram of this apparatus.

The diffusion chamber itself is the volume B, inside a rectangular box whose sides are of pyrex sheet glass, D. The top of the box-like chamber is a metal sheet K, with many small holes (0.015 inch diam. spaced $1/2$ " apart) communicating into the space A. Vapor is introduced into the space, A, from a boiler, F, at any desired rate, and passes through the small holes in K into the chamber, B. The space A, and plate K are kept hot by electric heater wires M mounted in space A.

The floor of the cloud chamber, C, is made of two sheets of glass between which a refrigerating liquid is pumped. The pump E sends this liquid through a cooling coil H immersed in a liquid cooled (by ice or dry ice) as desired.

The vapor from the boiler, after diffusing through the gas in B, condenses on the floor and the liquid drains back to the boiler.

This apparatus, because of its large flat surfaces can operate only very near atmospheric pressure. To allow for changes of volume of the vapor and gas mixture when starting and stopping a run, the gas reservoir N is provided.

More details concerning this apparatus will be found in Chapter III.

5. The operation of the diffusion cloud chamber.

This cloud chamber was successfully operated with methyl alcohol diffusing through carbon dioxide gas, when the top, A, was at about $+70^{\circ}\text{C}$ and the refrigerating liquid in C was at about -40°C . The rate of vapor flow was such that if one assumed pure vapor spread uniformly in a horizontal plane across the chamber, its linear rate of motion downward was of the order of one millimeter per second.

The chamber was illuminated by a beam of light from a 1000 watt incandescent bulb focused through a condenser lens and cooled by a water filter.

When the chamber was being put into operation, and before the temperatures and vapor flow reached the magnitudes specified above, one could observe at first a dense fog of condensed drops in the chamber. These are explainable as resulting from condensation on dust and other small aggregates existing in the fresh gas in the chamber. After a time, this fog would clear up, and be replaced by a sparse rain of large drops. These latter drops were formed throughout the chamber, even near the top, at a rather uniform rate, no matter how long the chamber was kept operating. Ionization (as from radium gamma rays) made no noticeable change in this condensation, nor was it particularly sensitive to the exact degree of supersaturation, as evidenced by the rather constant amount of the rain as the bottom temperature dropped from the vicinity of 0°C to -40°C . The density of this rain was not very great, for with the illuminating beam

of light turned off, the rain became completely invisible; the gas in the chamber became apparently perfectly transparent.

If the top temperature was held at about $+70^{\circ}\text{C}$, and the rate of vapor flow was held at the right value, then as the bottom temperature dropped lower and lower, suddenly a condition was reached near -35°C where ion-tracks could be observed in a narrow region about an inch above the chamber floor, the total depth of the chamber being seven inches. As the floor temperature dropped further, this region increased in thickness and the tracks increased in sharpness and clarity of view. They could be seen quite clearly by eye in spite of the rain, but could not be photographed because of the lack of contrast with the background and the rain. These ion-tracks, of course, fell downward onto the floor of the chamber within one or two seconds.

At all times there were numbers of cosmic ray tracks to be seen. Some of these, running horizontally across the chamber, were visible for twenty inches. A ten microgram sample of radium brought into the vicinity would make visible many "wormy" secondary electron tracks from the gamma rays. But if the radium was held close to the chamber for more than a second, the chamber would become "paralyzed" and cease to show any tracks at all. This "paralyzing" can be explained as due to the using up of the whole vapor supply in condensing on but a few of the many ions present. Occasionally alpha ray tracks were seen when an alpha ray was emitted

upward from radioactive contamination in the liquid on the floor of the chamber.

One might say that under the best conditions the tracks of beta rays in this chamber were almost as easily visible as the tracks of alpha rays in expansion cloud chambers. Nevertheless, lack of contrast balked photography.

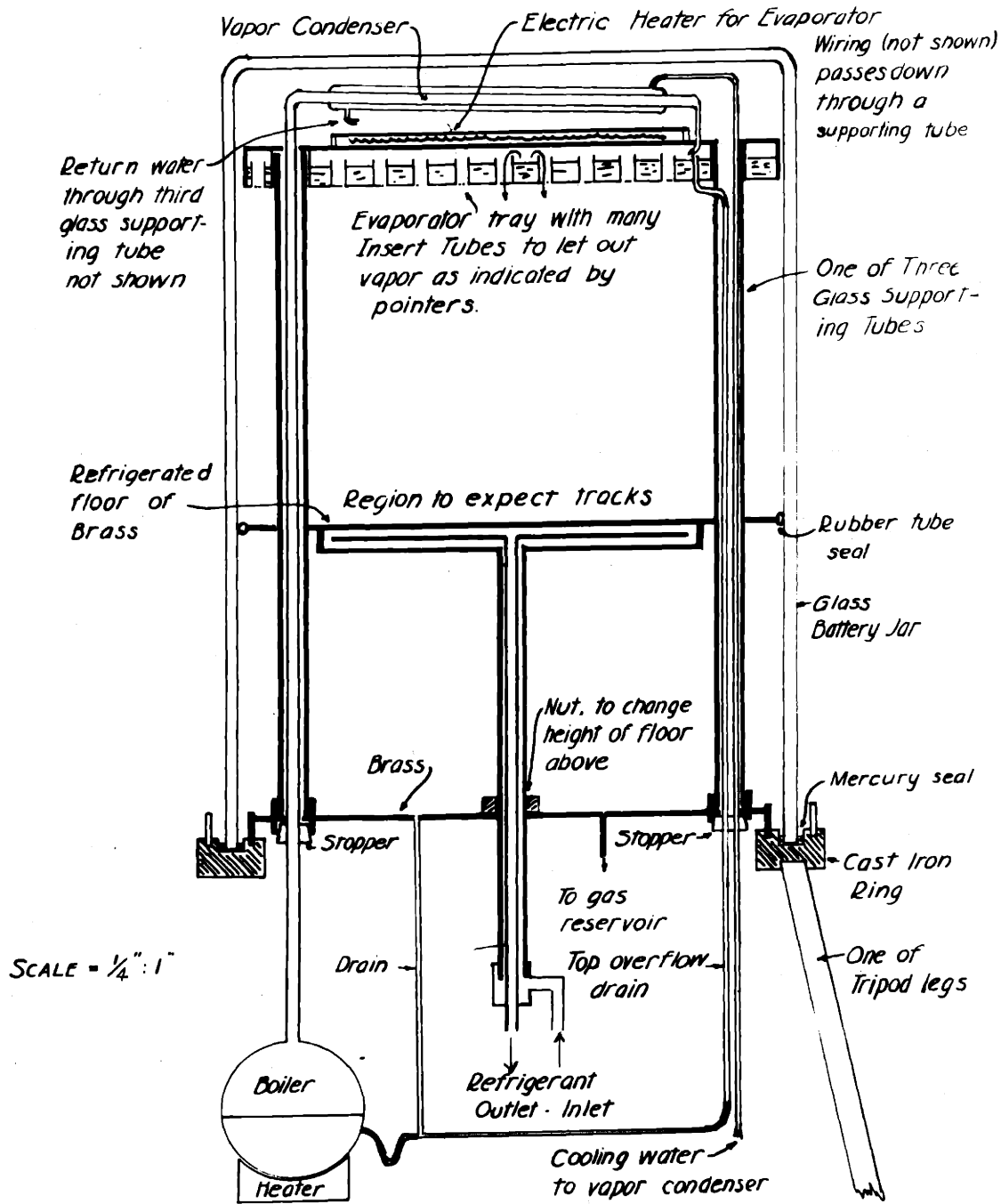
The chamber was operated and showed ion tracks on seven separate days between December 6, 1935 and March 25, 1936, though it was disassembled and reassembled twice in this interval. It only failed to operate during one attempt when a serious leak occurred.

The effects obtained with the apparatus described above are not unique. This was shown in the summer of 1936, when a simple apparatus was assembled and operated at Washington University in Saint Louis.* Tracks were observed when a mixture of water and n-butyl alcohol vapors diffused through a mixture of hydrogen and dichloro-difluoro-methane gases. The top of this apparatus was near 100°C, the bottom near 0°C. The results of this experiment corroborate the preceding results, but the operation was in general inferior to that of the earlier apparatus. *See Figure 5.*

6. Criticism of the diffusion cloud chamber described in section 4.

To use any continuous cloud chamber effectively,

* Acknowledgment is made here of indebtedness to the Physics Department of Washington University for the use of its facilities for this work.



A DIFFUSION CLOUD CHAMBER (B)
FIGURE 5

photographs of the tracks in it must be obtained. To photograph these tracks a dark background and a minimum of spontaneous rainfall are required. The black background was not provided in this apparatus. Moreover, in an effort to find the best operating conditions, a most important variable factor is the total gas pressure in the system. But this first apparatus could only be used at atmospheric pressure. Another desirable feature not present here, would be a device for putting radioactive samples into the chamber while it is operating.

A cloud chamber has been built incorporating changes as just suggested. But the changes incorporated in its design have so far prevented discovery of the conditions to make this chamber show ion tracks.

CHAPTER II - AN ANALYSIS OF THE OPERATION OF THE
DIFFUSION CLOUD CHAMBER.

1. The problem to be solved.

The operation of the diffusion cloud chamber will be analyzed for the idealized case of diffusion between parallel horizontal planes of infinite extent; that is, the effects of the side walls upon heat transfer and removal of vapor by condensation will be neglected. The effects of side walls will be analyzed qualitatively in section 7, below.

Even with this first idealization, the problem that remains defies exact analysis at the present time. The physical properties such as thermal conductivity, diffusivity, and specific heat all vary with temperature, making integration of the differential equations in which they appear very difficult. Furthermore, the physical properties involved are those of supersaturated vapors, and are experimentally undetermined, so that the equation of state and specific heat can only be approximated by uncertain extrapolations. For most of the analysis the equation of state and constant specific heat of a perfect gas will be assumed. Afterwards the effects of deviations will be considered qualitatively.

The problem to be studied is this: Given two parallel horizontal plates of infinite extent, the upper and lower plates at uniform and constant temperatures

T_1 and T_0 respectively, and T_1 greater than T_0 . The plates are a constant distance apart, h . A gas and a vapor are present between the plates at a pressure P_0 . The top plate is permeable to vapor but not to gas; fresh vapor is continually introduced to the space between the plates through the upper plate, whose temperature is held a little above the condensation temperature. Condensation occurs when the vapor reaches the bottom surface. This surface is a liquid film which is held at the constant temperature T_0 .

Only the steady state problem will be studied, in which the vapor diffuses downward with a constant flux, of c_1 grams per cm.^2 per sec. As already pointed out, it is assumed that the vapor is transferred by a pure diffusion; no convection exists except that inherent to the diffusive mass transfer.

Throughout the calculations, it is further assumed that there is no condensation of vapor in the body of the gas between the glass plates. Part of the vapor actually does condense into drops. This effect will be accounted for to some extent later, but will be ignored at first.

The independent parameters will be T_1 , T_2 , P_0 , c_1 , as defined above. Of course, the particular gas and vapor used are subjects of choice also. Numerical calculations will be carried out for the case of methyl alcohol vapor ^{diffusing into} carbon dioxide gas.

The unknowns to be determined are principally $T(x)$, $D_1(x)$, $S(x)$, where x is the position between the parallel plates, measured up from the lower plate, and T , D_1 , and S are the temperature, vapor concentration, and the supersaturation of the vapor, respectively at x . Other quantities of interest to be determined include the amount of heat transfer by conduction, convection, and radiation and the concentration of gas, etc.

The analysis and calculations which follow involve approximations which will be noted as they are made. The analysis will nevertheless give a reasonable picture of the physical situation.

As justification for the calculations to be made one may emphasize that direct measurements of conditions in this type of apparatus are either impossible, or exceedingly difficult; and furthermore, calculations throw considerable light on the phenomena involved. As an example for the experimental difficulties, one may mention the measurement of the temperature of the gas-vapor mixture. No instrument can be introduced into the gas without vapor condensing upon it, liberating latent heat of condensation, and thus raising the temperature above that actually prevailing in the gas.

2. The diffusion problem.

As a basis of the analysis of this problem,^a recent publication on diffusion has been used. This article

by Kuusinen²² showed that for the one dimensional diffusion of a binary mixture, the equations obeyed are of the form

$$(1) \quad c_1 = w D_1 - k \frac{\partial D_1}{\partial x}$$

$$(2) \quad c_2 = w D_2 - k \frac{\partial D_2}{\partial x}$$

$$(3) \quad w = c_1 v_1 + c_2 v_2$$

where c_1 , c_2 are the fluxes of the two materials (in gm. per cm.² per sec.); D_1 , D_2 are the concentrations (in gm. per cm.³); and k is a diffusion constant the same for both directions and both materials; v_1 and v_2 are partial volumes (for perfect gases, the volume of gas per unit of mass* at a total pressure P_0). Then w is the net convection velocity measured in terms of partial(molal) volume.** Under these conditions, k can be (but is not necessarily) a constant for varying composition of the mixture. However, diffusion is a function not of change of concentration, but, in a somewhat more general sense, of pressure. Since the system to

* Kuusinen calls v_1 and v_2 partial molal volumes, but since c_1 and c_2 are to be measured in terms of mass flux, v_1 and v_2 must be "partial volumes" of the constituents per unit of mass rather than per mole so that the units may be consistent.

** Kuusinen's contribution consists in showing clearly how the convective flux must be obtained by considering partial molal volume flux rather than mass flux, number of molecules, etc. This is a detail that has usually been neglected.

be studied is not isothermal, this becomes an important consideration. If the vapor and gas are considered perfect gases,

$$(4) \quad D_1 = \frac{M_1}{RT} p_1 \quad , \quad D_2 = \frac{M_2}{RT} p_2$$

where R is the gas constant per mole, and M_1 and M_2 are the molecular weights of the constituents, p_1 and p_2 their partial pressures so that

$$(5) \quad c_1 = w \frac{M_1}{RT} p_1 - k \frac{M_1}{RT} \frac{\partial p_1}{\partial x}$$

$$(6) \quad c_2 = w \frac{M_2}{RT} p_2 - k \frac{M_2}{RT} \frac{\partial p_2}{\partial x}$$

In the particular problem to be solved here, let subscripts₍₁₎ refer to the vapor, and ₍₂₎ to the gas. Then in the steady state diffusion of vapor c_1 is constant and c_2 is zero. Also, having fixed the temperature at the bottom plate, the lower limit of the vapor pressure of vapor is fixed, so that the initial vapor and gas pressures, p_{10} and p_{20} , are fixed in terms of known physical data. Furthermore, if the perfect gas laws are used,

$$(7) \quad v_1 = \frac{RT}{M_1 P_0} \quad , \quad v_2 = \frac{RT}{M_2 P_0}$$

In Kinetic Theory of Gases, by Loeb, p. 273, (Third Edition) it is stated that the diffusivity varies with temperature as some power between 1.75 and 2.0, and inversely as the pres-

sure. Therefore if k_0 is the diffusivity at a unit pressure of one atmosphere, and at the temperature T_0

$$(8) \quad k = k_0 (1/P_0) (T/T_0)^{\alpha+1}$$

where

$$(9) \quad 1.75 < (\alpha + 1) < 2.0$$

The equations to be solved are now

$$(10) \quad c_1 = c_1 \frac{p_1}{P_0} - \frac{k_0}{P_0} \left[\frac{T}{T_0} \right]^{\alpha+1} \frac{M_1}{RT} \frac{\partial p_1}{\partial x}$$

and

$$(11) \quad 0 = c_1 \frac{M_2}{M_1} \frac{p_2}{P_0} - \frac{k_0}{P_0} \left[\frac{T}{T_0} \right]^{\alpha+1} \frac{M_2}{RT} \frac{\partial p_2}{\partial x}$$

The relation

$$(12) \quad p_1 + p_2 = P_0$$

allows one to determine p_1 from p_2 , so only equation 11 need be integrated directly.

Also T is a function of x which varies from T_0 at $x = 0$ to T_1 at $x = h$, but the exact manner of its variation has not as yet been discussed.

It is desirable, before passing on to the analysis of the temperature distribution, to make a few remarks concerning the validity of equations 5 and 6. These equations may not be strictly correct for diffusion combined with a

temperature gradient, but if the temperature does vary they avoid the absurdity obtained when concentration is used as variable, of indicating a gradient of total gas pressure. It is believed that equations 5 and 6 are sufficiently accurate to be used in the following analysis. The complete analysis of the diffusion would have a complexity not warranted by the inaccuracy unavoidable in other parts of the present analysis. New and unknown quantities would be introduced by a more complete analysis.

For example, consideration of thermal diffusion would necessitate knowledge of the magnitude and form of the forces between the gas and vapor molecules. The thermal diffusion effect tends to create a separation of light and heavy components of a gas mixture, the lighter component concentrating in the hot region. This effect would be expected to decrease the diffusion of a hot vapor into a cold gas of higher molecular weight, below what it would be if the effect did not exist. But the total concentration gradients experimentally produced by thermal diffusion never produce concentration gradients of a magnitude comparable to those involved in the diffusion cloud chamber.²⁶ It would appear, therefore, that this factor is safely to be neglected.

3. The temperature distribution problem.

When equilibrium conditions between the plates have been established, the flux of energy is constant, as is the flux of vapor. The energy is carried by convective trans-

fer of the vapor, molecular transfer of vapor and gas, and radiation. Radiation will not be considered in computing the temperature of the gas; it will be assumed that the emissivity of the vapor and gas is small enough to neglect this factor. Dropwise condensation of vapor, as previously noted, will also be neglected.

The flux of energy resulting from the flux of vapor, c_1 , will be $c_1 H$ where H is the enthalpy of the vapor per gram. If the vapor is considered to be a perfect gas with a constant specific heat, the enthalpy measured from a zero at T_0 will be

$$(13) \quad H = C_p(T - T_0)$$

The flux of heat resulting from molecular transfer is $-K (dT/dx)$. The conductivity K varies with temperature and composition in a manner that is but poorly known in the simplest cases. It would be difficult to justify the added complication of using anything more than a linear approximation,

$$(14) \quad K = K_0 [1 + b (T - T_0)]$$

The total energy flux, neglecting radiative flux, is, then

$$(15) \quad f = c_1 H - K \frac{dT}{dx}$$

Now c_1 and f are negative numbers. For convenience in later work, substitute,

$$(16) \quad F = -f, \quad a = -c_1 C_p, \quad t = T - T_0$$

The energy flux equation is then

$$(17) \quad F = a t + K_0 (1 + bt) dt/dx.$$

For initial conditions $x = 0$, $t = 0$, this gives an integral

$$(18) \quad -ax/K_0 = bt + (1 + Fb/a) \ln (1 - at/F)$$

4. Further analysis of the vapor and gas density distribution problem.

In section 2 the approximate differential equation for the gas pressure, p_g was obtained. (equation 11) It may be put into the following form:

$$(19) \quad A p_g = \left(1 + \frac{t}{T_0}\right)^a \frac{dp_g}{dx}, \quad A = \frac{c_1 R T_0}{M_1 k_0}$$

For equation 18, one may obtain x as a function of T or t , rather than t as a function of x . It is simplest, therefore to make a change of variable here,

$$(20) \quad \frac{dp_g}{dx} = \frac{dp_g}{dt} \cdot \frac{dt}{dx} = \frac{dp_g}{dt} \cdot \frac{(F - at)}{K_0(1 + bt)}$$

and

$$(21) \quad \frac{dp_2}{Ap_2} = \frac{K_0(1+bt) dt}{(1+t/T_0)^\alpha (F-at)}$$

5. Calculations on the diffusion of methyl alcohol through carbon dioxide under certain specified conditions.

In this section numerical results will be presented for certain cases of the diffusion of methyl alcohol through carbon dioxide, on the basis of the preceding analysis.

Physical data have been obtained from various sources. (See references 35 to 38.) The data as presented here have been converted to forms complying with the needs of the equations already given.

Diffusivity for methanol into carbon dioxide.

Experimental data give $k = 0.0880$ in cm^2/sec at 0°C and 1 atm., with $(1 + \alpha) = 2$ in equation 8, within the limit of error, from 0° to 50°C . For lack of any other information, this value of $(\alpha + 1)$ will be used over the whole range of temperatures involved in this problem, from -40°C to $+70^\circ\text{C}$. Then for $T_0 = 273^\circ - 40^\circ = 233^\circ\text{K}$,

$$k_0 = 0.06411, \quad \alpha = 1$$

Specific Heat of Methanol, C_p .

The data of Flock, Ginnings, and Holton⁴⁰ are all that were found. Their data give (dH/dT) along the saturation pressure line for methanol vapor. This function is not the same as C_p , but probably does not differ much from C_p . If this assumption is made, a mean value of C_p for methanol vapor between -40°C and $+70^\circ\text{C}$ may be estimated to be about 0.25 cal./gm.

Heat Conductivity, K .

In the range of 0°C to 100°C the conductivities of methyl alcohol and carbon dioxide are the same within about five percent. This coincidence allows an approximation for K independent of the composition. One obtains

$$K = K_0 (1 + bt) = 2.86 \times 10^{-5} (1 + 0.0048t)$$

where $K_0 = 2.86 \times 10^{-5}$ is the conductivity at -40°C ($t = 0$ at -40°C), and $b = 0.0048$ is the temperature coefficient of conductivity. K is also nearly independent of pressure.

Initial bottom temperature, T_0 is taken as -40°C for a whole series of calculations. The effect of changing the temperature will be considered below.

Pressure, P_0 , will be taken as 1 atmosphere at first, and later the effect of varying it will be demonstrated.

Height of chamber, h, will be taken as 40 cm.

Saturation pressure of vapor at -40°C , is 0.00196 atm. for methanol.³⁵

Final top temperature, will be taken as $+70^{\circ}\text{C}$, so $t_1 = 110$,
 $T_1 = 343.1^{\circ}\text{K}$

Energy flux and material flux.

These two quantities are interrelated by the energy flux equations which have been obtained in section 3.

$$(17) \quad F = at + K_0 (1 + bt) dt/dx.$$

$$(18) \quad -ax/K_0 = bt + (1 + Fb/a) \ln (1 - at/F)$$

The first of these equations states that the energy flux consists of two parts. In this problem both terms on the right side are positive, so that the total energy flux is always greater than the convective heat flux, or

$$(22) \quad F > at = -c_1 C_p t$$

But (at) is a maximum when t is a maximum, that is, $t = t_1$.

For convenience in later calculations, let the factor of proportionality between F and the maximum value at_1 be

$$(23) \quad r = F/at_1 = f/c_1 C_p t_1$$

Then as r varies in value, one is simply indirectly choosing

a value of the flux c_1 . Note that r is of no great significance, but is a convenient parameter relating the total energy flux to the maximum convective energy flux, $c_1 C_p t_1$.

The desirable range of r is that for which the temperature falls off roughly uniformly from top to bottom of the chamber. It may be estimated that this will be the case if only about half the heat is carried convectively at the top of the chamber, that is, $r = 2$; So c_1 and F will be calculated for three values of r : 4, 2, 1.2.

From the integrated equation for x ,

$$(24) \quad -ax/K_0 = bt + (1 + rbt_1) \ln (1 - t/rt_1)$$

At $x = h$, $t = t_1$

$$(25) \quad -ah/K_0 = bt_1 + (1 + rbt_1) \ln (1 - 1/r)$$

which allows the determination of $c_1 = -a/C_p$, and

$$(26) \quad \frac{x}{h} = \frac{bt + (1 + rbt_1) \ln (1 - t/rt_1)}{bt_1 + (1 + rbt_1) \ln (1 - 1/r)}$$

which allows the determination of $x = x(t)$.

If $(t/r t_1)$ is small, the logarithm can be expanded, giving

$$(27) \quad \frac{x}{h} = \frac{t/r t_1}{ah/K_0} \left[1 + (1 + rbt_1) \left\{ \frac{1}{2} \left(\frac{t}{rt_1} \right) + \frac{1}{3} \left(\frac{t}{rt_1} \right)^2 + \frac{1}{4} \left(\frac{t}{rt_1} \right)^3 + \dots \right\} \right]$$

Values of c_1 , F , and x/h for the chosen values of r will be found in Table I.

The gas pressure, p_g

For any chosen value of r corresponding to a chosen c_1 and F , p_g may be found by integration of the equation 21 in section 4. In this problem one has $\alpha = 1$ so that

$$(28) \quad \frac{dp_g}{Ap_g} = \frac{K_o}{F} \frac{(1 + bt) dt}{(1+t/T_o)(1-at/F)} \quad \text{which gives}$$

$$(29) \quad \ln \frac{p_g}{p_{g0}} = \frac{-T_o}{T_o + rt_1} \cdot \frac{RT_o K_o}{M_1 k_o C_p} \left[(1 - bT_o) \ln(1 + t/T_o) - (1 + brt_1) \ln(1 - t/rt_1) \right]$$

This equation has been solved for several cases, and the results are tabulated below in Table I.

6. The effects of varying the conditions of operation in the diffusion cloud chamber.

The tabular data of Table I on supersaturation are reproduced graphically in Figure 6. From this graph it may be inferred that the supersaturation attained increases roughly linearly without the flux of vapor.

Suppose that a minimum supersaturation of 4 is needed to get condensation on ions; then with conditions given by curve I in Figure 6, one would scarcely expect to see ion tracks. By increasing the rate of vapor flow 2.5 times, tracks should be seen for a region about eight centimeters deep, as shown by curve II. Increasing the flow another 2.5 times as for curve III would increase the region of visibility of tracks very little, although the maximum

Table I. Values of p_a/p_{a0} , p_1 , S , and x/h .

r	t	0	11	22	33	44	66	88	110
4	p_a/p_{a0}	1.000	0.980	0.961	0.941	0.921	0.882	0.838	0.796
	p_1	0.0019	0.022	0.041	0.061	0.081	0.120	0.164	0.206
	$S=p_1/p_{1s}$	1.0	4.4	3.6	2.4	1.6	0.7	0.3	0.17
	x/h	0.000	0.071	0.147	0.229	0.319	0.515	0.736	1.000
2	p_a/p_{a0}	1.000	0.961	0.921	0.881	0.839	0.755	0.667	0.576
	p_1	0.0019	0.041	0.081	0.121	0.163	0.246	0.334	0.425
	S	1.0	8.2	7.1	4.8	3.25	1.4	0.7	0.35
	x/h	0.000	0.059	0.123	0.193	0.272	0.452	0.674	1.000
1.2	p_a/p_{a0}	1.000	0.935	0.867	0.798	0.727	0.579	0.419	0.239
	p_1	0.0019	0.067	0.135	0.204	0.274	0.422	0.582	0.761
	S	1.0	13.4	11.8	8.1	5.5	2.5	1.2	0.6
	x/h	0.000	0.037	0.079	0.129	0.187	0.340	0.571	1.000
"	p_{1s}	0.0019	0.0050	0.0114	0.0251	0.0501	0.172	0.496	1.219

When $r = 4$, $c_1 = 1.05 \times 10^{-6}$ gm./cm²/sec, $f = 1.16 \times 10^{-4}$ cal./cm²/sec.

When $r = 2$, $c_1 = 2.56 \times 10^{-6}$ " , $f = 1.41 \times 10^{-4}$ "

When $r = 1.2$, $c_1 = 6.86 \times 10^{-6}$ " , $f = 2.26 \times 10^{-4}$ "

See next page for complete explanation of symbols.

Explanation of symbols in Table I.

p_2 is pressure of CO_2 where temperature at that part of chamber is t degrees above floor temperature.

p_{20} is pressure of CO_2 at the floor of the chamber.

p_1 is actual pressure of methanol in atmospheres.

p_{1s} is saturation pressure of methanol

S is the supersaturation.

x is the height above the floor of the chamber.

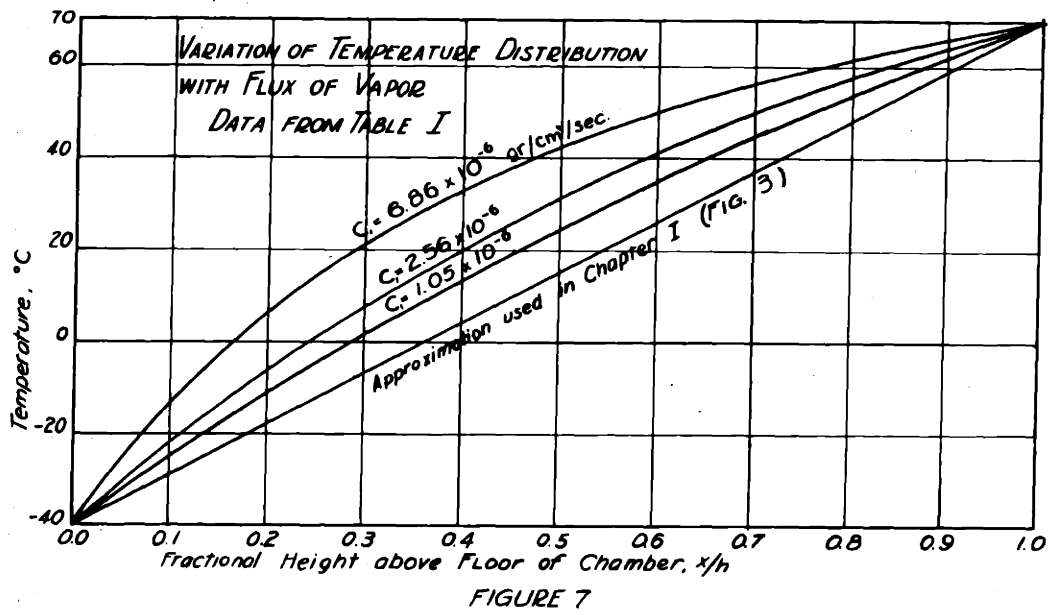
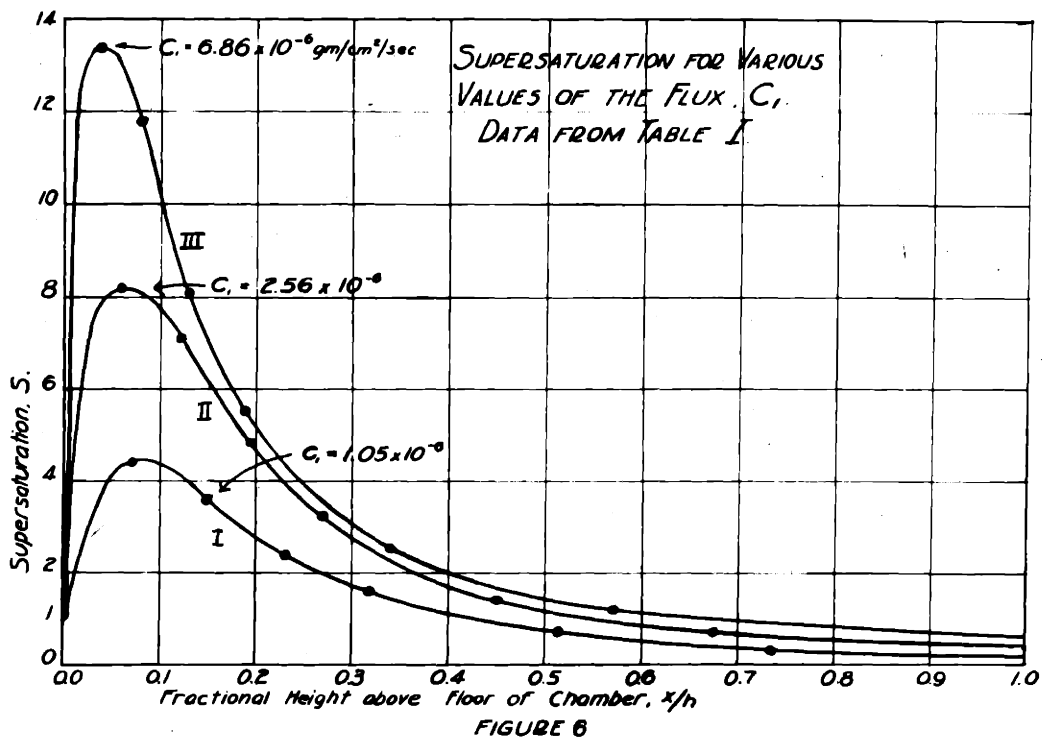
h is the total height of the chamber, $h = 40\text{cm}$.

c_1 is the flux of methanol vapor in grams/cm²/sec.

f is the total energy flux in cal./cm²/sec.

$r = f/c_1 C_p t_1$, $C_p = 0.25 \text{ cal./gm./}^\circ\text{C}$, $t_1 = 110$.

The total pressure in the chamber is $P_0 = p_1 + p_2 = 1 \text{ atm}$.



supersaturation would be increased considerably. But an excessive supersaturation introduces new difficulties because of spontaneous condensation.* One may expect, therefore, that there will be an optimum rate of flux, probably in the vicinity of 2 or 3×10^{-6} gm./cm.²/sec. for the particular conditions for which these calculations have been made.

The graph, Figure 7, made from data in Table I, shows how the temperature varies with height in the chamber. The straight line illustrates the approximation for temperature used in Chapter I. One may observe the magnitude of deviations from this approximation by comparison of the straight line and the curves.

Effect of Varying the Temperatures, T_0 , T_1

To determine the effect of a change in temperature, consider what happens when the temperatures T_0 and T_1 are simultaneously raised 5.5° , and lowered 5.5° from the values used for the preceding calculations.

The diffusivity, k_0 , specific heat C_p , and the heat conductivity K_0 all change by small amounts which can be neglected. The same is true of b and a . The pressure P_0 , chamber height, h , and temperature range ($t_1 = 110$) are all presumed constant at the same values as before. The value of r will be taken as 2 , the middle value in the preceding

* The spontaneous condensation will be considered in more detail below. See also Appendix I.

calculations.* Then it will be noted that the changes in heat and material fluxes, f and c_1 , are negligible. Likewise for the ratio p_2/p_{20} , changes in value are second order effects.

The change in p_{1s} is of major importance. Considering only this change, one can calculate the change in supersaturation as a result of changing temperature, as in Table II following.

The information contained in Table II is repeated graphically on Figure 8. One may conclude from the curves shown that there is an upper limit to the floor temperature for which ion-tracks can be seen. Lowering the floor temperature five to ten degrees below this upper limit should make the formation of visible tracks possible over a considerable region. Still more lowering of the temperature not only increases the peak supersaturation (1.6 times for 5.5° lowering) but also quite appreciably increases the depth of the region sensitive to condensation on ions. Therefore one may expect the chamber to operate best for a floor temperature considerably below the maximum allowable. However, one cannot be sure as to where there might be an optimum floor temperature, because of the conflict of the effect just discussed with the effect of spontaneous rainfall to be discussed below in section 7.

* This simply means one is choosing a particular magnitude of vapor flux, c_1 .

Table II. Values of S for several values of T_0 ;
 $r = 2$, $P_0 = 1$ atm., $t_1 = T_1 - T_0 = 110$

T_0	t	0	11	22	33	44	66	88	110
227.6°K -45.5°C	$P_1 S$	0.0012	0.0032	0.0076	0.0173	0.0363	0.129	0.380	0.989
	P_2	0.9988	0.960	0.920	0.880	0.838	0.754	0.666	0.575
	P_1	0.0012	0.040	0.080	0.120	0.162	0.246	0.334	0.425
	S	1.0	12.5	10.5	6.95	4.45	1.9	0.9	0.43
233.1°K -40°C	$P_1 S$	0.0019	0.0050	0.0114	0.0251	0.0501	0.172	0.496	1.219
	P_2	0.9981	0.959	0.919	0.879	0.837	0.754	0.666	0.575
	P_1	0.0019	0.041	0.081	0.121	0.163	0.246	0.334	0.425
	S	1.0	8.2	7.1	4.8	3.25	1.43	0.7	0.35
238.6°K -34.5°C	P_1	0.0032	0.0076	0.0173	0.0363	0.0692	0.227	0.624	1.51
	P_2	0.9968	0.958	0.918	0.878	0.836	0.753	0.665	0.574
	P_1	0.0032	0.042	0.082	0.122	0.164	0.247	0.335	0.426
	S	1.0	5.5	4.75	3.4	2.4	1.1	0.5	0.28
	x/h	0.000	0.059	0.123	0.193	0.272	0.452	0.674	1.000

The symbols have the same meanings as in Table I. In addition, T_0 is the temperature of the chamber floor, T_1 of the roof.

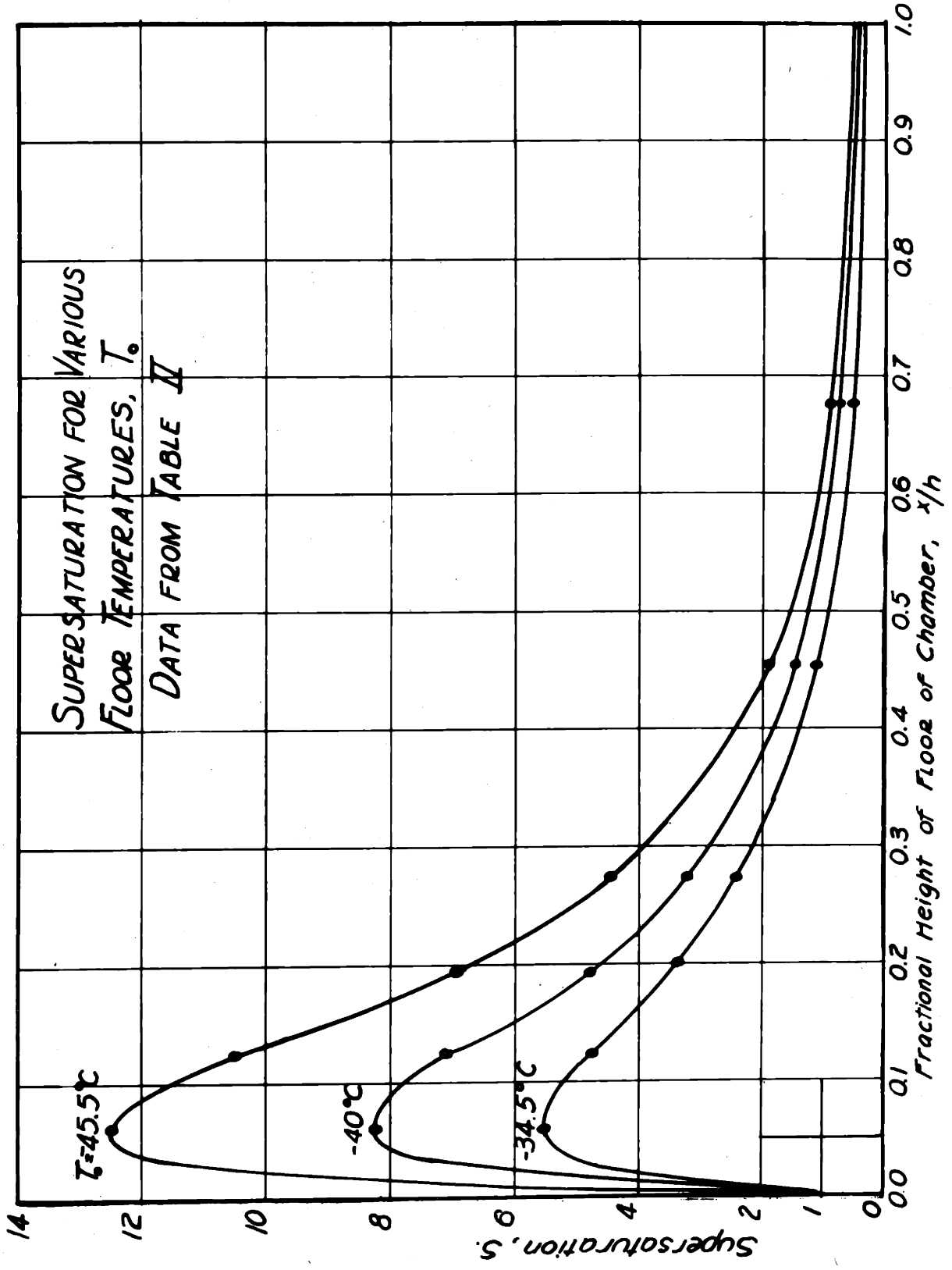


FIGURE 8

Effect of varying the chamber pressure, P_o .

P_o does not appear in the equations for x/h versus t or p_2/p_{2o} versus t . It enters, however, when p_1 and p_2 are calculated.

$$(30) \quad p_2 = \frac{p_2}{p_{2o}} (P_o - p_{1o}) \approx \frac{p_2}{p_{2o}} P_o$$

$$(31) \quad p_1 = P_o - \frac{p_2}{p_2} (P_o - p_{1o}) \approx P_o \left(1 - \frac{p_2}{p_{2o}}\right)$$

(The approximations are good except very near $t = 0$)

Thus it appears that for a given flux of vapor, the supersaturation will be very nearly proportional to the pressure of operation.

Effect of changing from methanol to ethanol as a vapor for the chamber.

Ethanol vapor might be used in this apparatus with carbon dioxide, since the molecular weight of ethanol is but slightly greater than that of carbon dioxide (46 and 44 respectively). In this case all of the physical data of the preceding calculations must be changed. The general effect of the change may be presumed, however, to be an increase in the supersaturation, other things being kept nearly equivalent. For at the same temperature, the saturation vapor pressure of ethanol is only about half that of methanol,

while changes in heat conductivity, heat capacity, diffusivity, etc., are not so large and the effects of some of the changes tend to cancel out, leaving the change in saturation vapor pressure as the major cause of change in supersaturation attained relative to methanol.

Effect of varying the depth of the chamber, h.

For a given value of the ratio r , there is no change in the distribution of temperature or vapor according to the preceding equations, but the heat and material fluxes both decrease in proportion as h increases. One might conclude offhand that the depth of the chamber is not an important variable. However, the total amount of spontaneous condensation may be expected to be proportional to the depth of the chamber. The amount of vapor lost in this condensation is, then, proportional to h , while the total vapor supply is inversely proportional to h . As a result of these superposed effects which decrease the supersaturation below that calculated above, the chamber cannot be expected to show ion tracks if it is too deep. Without complete information on the spontaneous rainfall, it is impossible to predict the optimum depth of chamber to maintain the greatest region sensitive to ions.

7. Consideration of factors previously neglected which influence the supersaturation.

The side walls.

A supersaturated vapor condenses readily upon a

solid or liquid surface. Therefore, near the side walls of the chamber one cannot expect much supersaturation, and so the chamber depth should be considerably less than its horizontal dimensions. A ratio of width to depth of four to one seems to be adequate.

The side wall temperature distribution should be nearly the same as that naturally prevailing in the gas phase, otherwise convection currents will be set up next to the walls, and perhaps extend far out into the chamber.

Deviations of the properties of the vapor for those of a perfect gas.

In this case equation 18 becomes

$$\begin{aligned}
 (32) \quad f &= c_1 H - K \frac{dT}{dx} = c_1 \int_{T_0}^T \left(\frac{dH}{dT} \right)_{p,T} dT - K \frac{dT}{dx} \\
 &= c_1 \int_{T_0}^T \left[\left(\frac{\partial H}{\partial T} \right)_p + \left(\frac{\partial H}{\partial p} \right)_T \frac{dp_1}{dT} \right] dT - K \frac{dT}{dx} \\
 &= c_1 \int_{T_0}^T C_p dT - c_1 \int_{T_0}^T \mu C_p dp_1 - K \frac{dT}{dx}
 \end{aligned}$$

The necessary thermodynamic relations were obtained from the tables by P. W. Bridgman⁴². If the Joule-Thomson coefficient, μ , is positive, as one may expect it to be, the temperature at a point in the chamber will be lower

than if μ is zero. The value of μ is not known for super-saturated methanol vapor, but it would have to be tremendously greater than is usual in order to have any appreciable influence on the conditions in the cloud chamber.

The value of C_p is also influenced by the Joule-Thomson effect.

$$\begin{aligned}
 (33) \quad C_p &= C_v - T \left(\frac{\partial v}{\partial T} \right)_p^2 / \left(\frac{\partial v}{\partial p} \right)_T \\
 &= C_v + (\mu C_p + v) \left(\frac{\partial p}{\partial T} \right)_v
 \end{aligned}$$

To a first approximation, $pv = RT$. Then $(\partial p / \partial T)_v = R/v$, and

$$(34) \quad C_p = (C_v + R) / (1 + \mu R / v)$$

which indicates a reduction in the value of C_p on account of the intermolecular forces. C_v itself may be expected to increase slowly with temperature.

The type of deviation from the state of a perfect gas just considered is such as to influence the temperature distribution analysis. Another type of deviation which affects the analysis of the vapor distribution is concerned with the equation of state and its relation to the diffusion problem. This problem would be quite difficult to analyse.

Also, no experimental information is known to be available on the equation of state of a supersaturated vapor. On the one hand one may expect the deviations from a perfect gas to increase with the supersaturation. On the other hand, in the part of the cloud chamber which is most highly supersaturated, the vapor concentration is low compared to what it is near the top. One may hope that the lowering of vapor pressure will counteract the tendency toward increasing deviations from the perfect gas laws so that the analysis already given is not seriously affected.

The spontaneous condensation.

Of all the factors neglected in the earlier analysis, this is undoubtedly the most important and the most difficult to consider completely. This condensation which occurs all throughout the chamber may be a result of more than one cause. At least part may be ascribed to a spontaneous condensation of the type analysed by Farkas¹⁰, Volmer^{9,10}, Becker¹⁴, and others^{12,13}. The analysis in its complete form as given by Becker is reproduced in Appendix I. Briefly, the result of this analysis is an equation

$$(35) \quad \ln_e S_{cr} = k \left(\frac{\sigma}{T} \right)^{3/2} \cdot \left(\frac{M}{\rho} \right), \quad k \approx 0.5$$

In this equation, S_{cr} represents a "critical" supersaturation, for which about one droplet of condensation is formed in one cm^3 . of volume per second. If this rate of droplet formation

is called J_{cr} , and the rate in general is J , it is shown in the appendix that for a value of S slightly greater than S_{cr} , J may be given approximately by a relation of the form

$$(36) \quad \frac{J}{J_{cr}} = \left(\frac{S}{S_{cr}} \right)^E \quad \text{where} \quad 50 < E < 250$$

That is, the spontaneous condensation increases enormously faster than the supersaturation, beyond the critical value of the latter.

One may conclude that it is impossible to exceed materially the value of supersaturation given by S_{cr} above. For any greater supersaturation will be attended by rapid condensation, reducing the supersaturation back to the vicinity of S_{cr} .

There may be more condensation than is predicted by the theory of Becker. There may be additional condensation on dust or on molecular aggregates introduced in some obscure fashion, perhaps by overheating a vapor like methanol, by contact of vapor with a liquid surface, by evaporation from contaminants of high molecular weight, etc. It is difficult to detect when such effects are present. They are likely to be very elusive. But such causes of condensation must be kept in mind, looked for, and eliminated.

Condensation upon diffused ions, such as might interfere with the operation of a continuous cloud chamber.

In that region of the apparatus above the part where ion tracks are likely to be produced, ions are continually being produced by cosmic radiation and gamma rays from materials in the vicinity. Most of these will be carried down into the region sensitive to condensation on ions, and by causing condensation there, they will decrease the supply of vapor available for ion-track formation. The number of these ions can be expected to be proportional to the depth of the chamber and to the pressure of the gas in it. It would be desirable to remove these stray ions before they enter the sensitive region. A vertical sweeping field between the top and bottom of the chamber might remove up to half of the stray ions. The other half would be swept downward to the sensitive region of the apparatus. A grid of any sort placed in the chamber is not likely to be successful. Condensation upon it is likely to remove more vapor than the stray ions would. However, only experiments can solve this problem conclusively.

8. Conclusions concerning the choice of operating conditions for the diffusion cloud chamber.

In this chapter the value of the supersaturation, S , has been calculated analytically. Then by analogy to the supersaturations found necessary to produce ion-tracks in an expansion cloud chamber, general inferences have been drawn concerning how a diffusion cloud chamber should act, and the proper order of magnitudes of necessary conditions have been estimated.

In Chapter IV condensation phenomena as functions of supersaturation are discussed. In section 7 of that chapter there is further discussion concerning the operation of the diffusion cloud chamber.

CHAPTER III - THE DESIGN OF DIFFUSION CLOUD CHAMBERS.

Introduction.

This chapter presents the most important information that may be of value in designing other diffusion cloud chambers, as gathered from the design, construction, and operation of three models already built.

A composite of experience with all three cloud chambers will be presented rather than great detail upon one of them. Most emphasis will be placed upon the things - sometimes seemingly minor details - which have previously caused most trouble and lost time.

1. Various models of the diffusion cloud chamber.

For the sake of brevity in referring to them, the three models of diffusion cloud chamber will be called simply "chamber A", "chamber B", and "chamber C".

Chamber A was built June to December, 1935. Its construction is illustrated by photographs, Figures 10 & 9, and diagrams, Figures 4, 11, 12, 13, & 14. Its form is essentially that of the sketch (Figure 4) in chapter I, section 4, and is the one whose successful operation is there described.

Chamber B was assembled June to September, 1936. It is shown schematically in Figure 5. The fact that this simple apparatus did show ion-tracks illustrates that once the optimum conditions have been found for running a chamber with a good combination of materials, some such simple, non-

FIGURE 9.

Views of Chamber A.

Top and bottom. - Shows the chamber stripped of its
outer insulating glass windows.

Middle. - View of chamber completely assembled for
operation.

FIGURE 10 - next page over.

Chamber A.

Top. - View of chamber with insulating lid removed to
show insulating window arrangement.

Bottom. - Chamber completely assembled for a run with
light beam turned on.

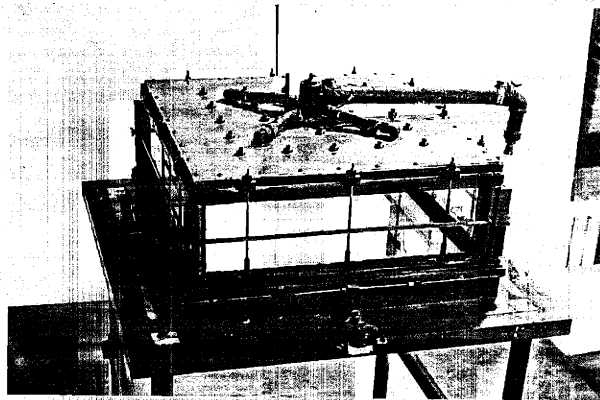
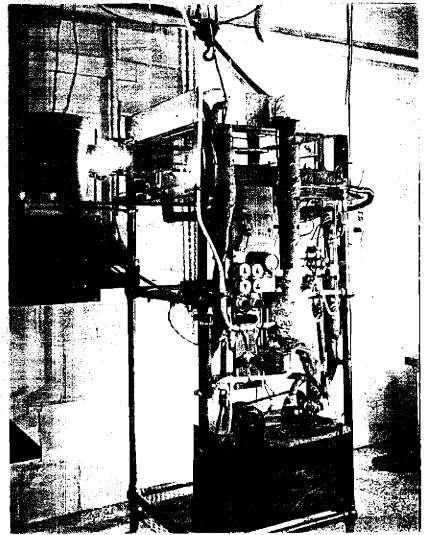
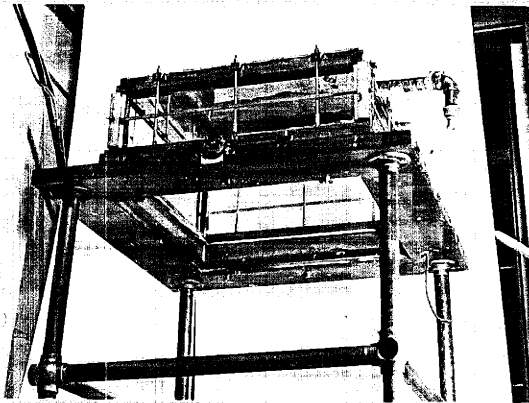


FIGURE 9

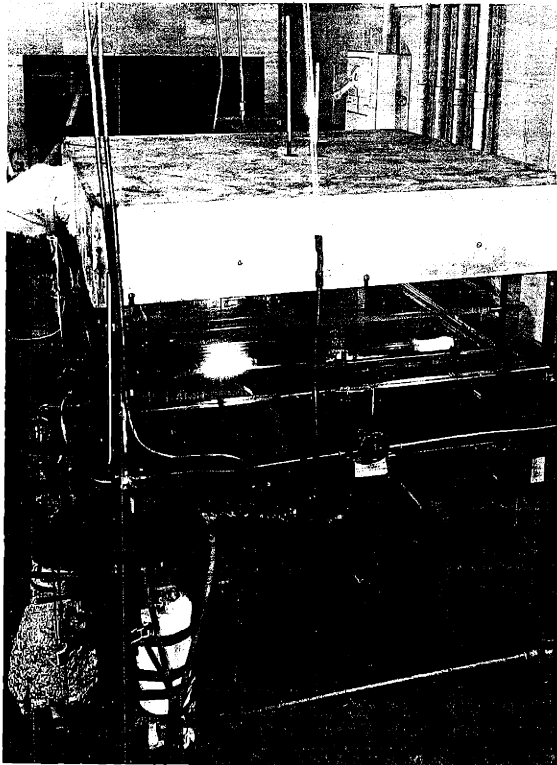
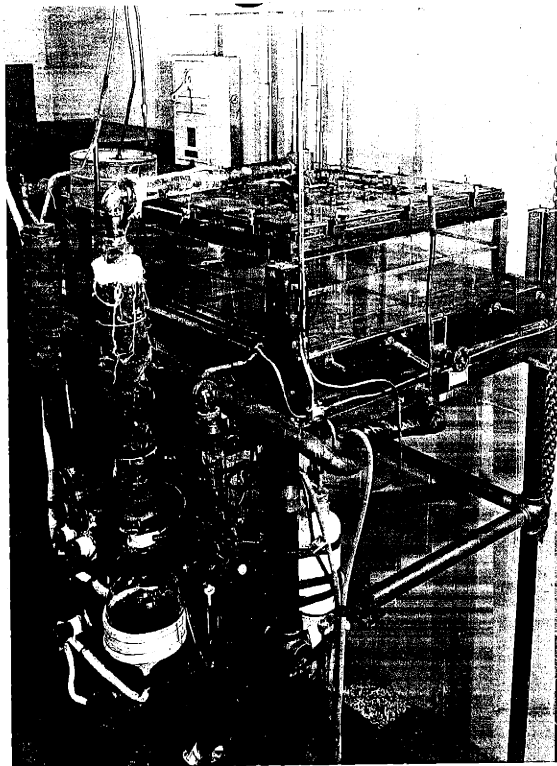


FIGURE 10

FIGURE 10a.

Photographs of chamber A in operation.

The white color of most of the floor is due to frosting on its under side. The vertical streaks are falling drops of condensation.

~~FIGURE 10a~~

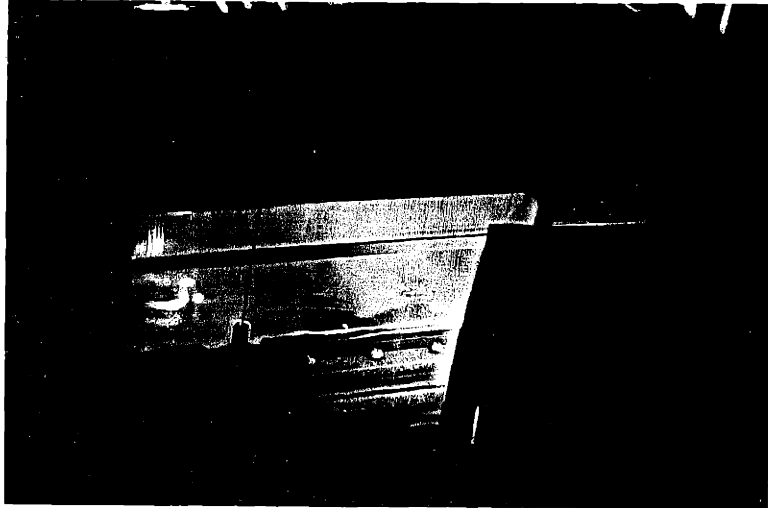


FIGURE 10a.

FIGURES 12 - 13 - 14.

on this page and next two pages

Detail sections of chamber A.

FIGURE 12. shows the essential parts of the structure.

FIGURE 13 shows how a tie-rod holds the various parts together; and also shows an electric heater wire mounted on a porcelain insulator inside the vapor distributor.

FIGURE 14 shows the vapor distributor system and thermometer well also seen in bottom photograph of figure 9, at the center of the top of the chamber.

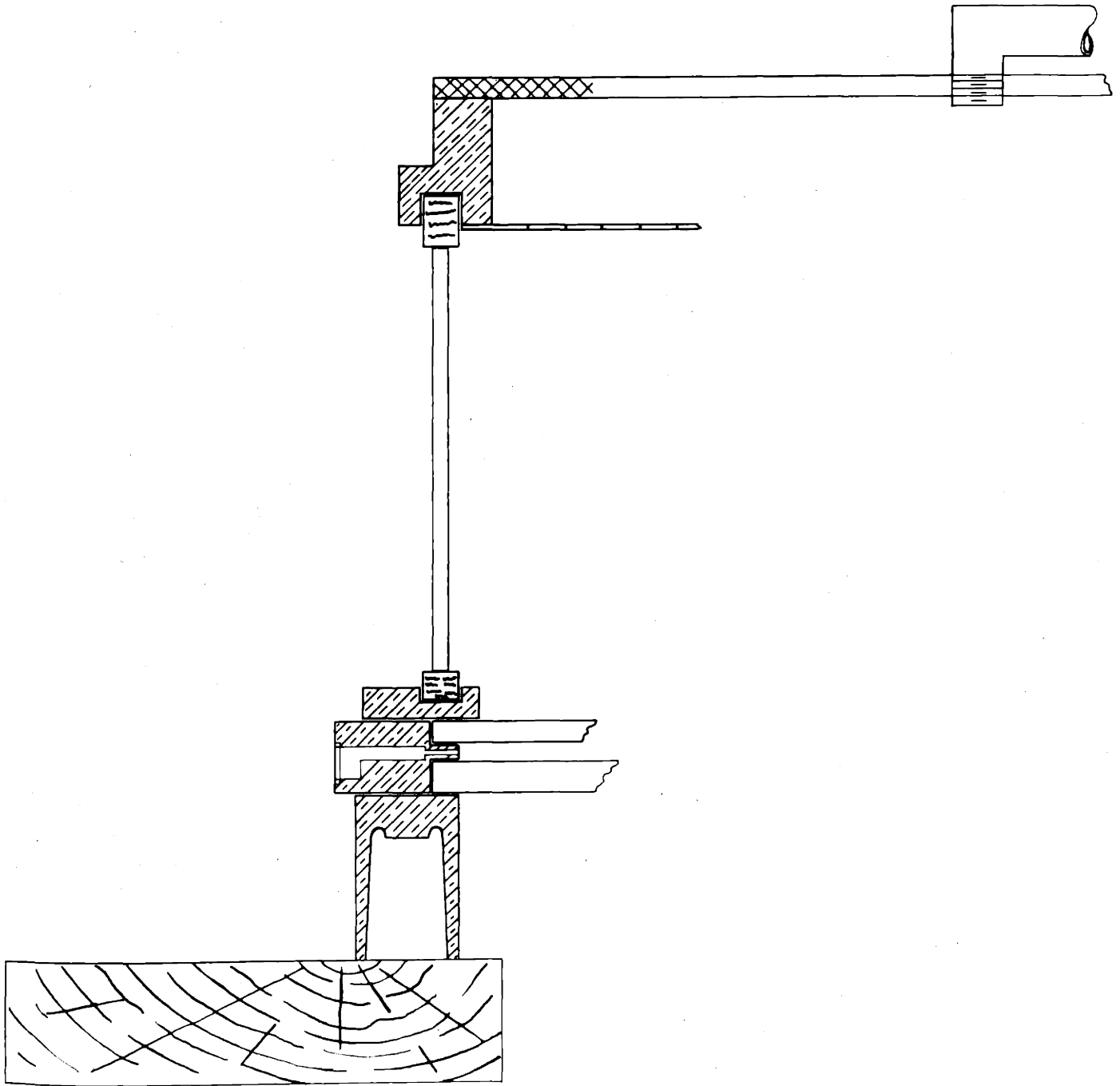


FIGURE 12

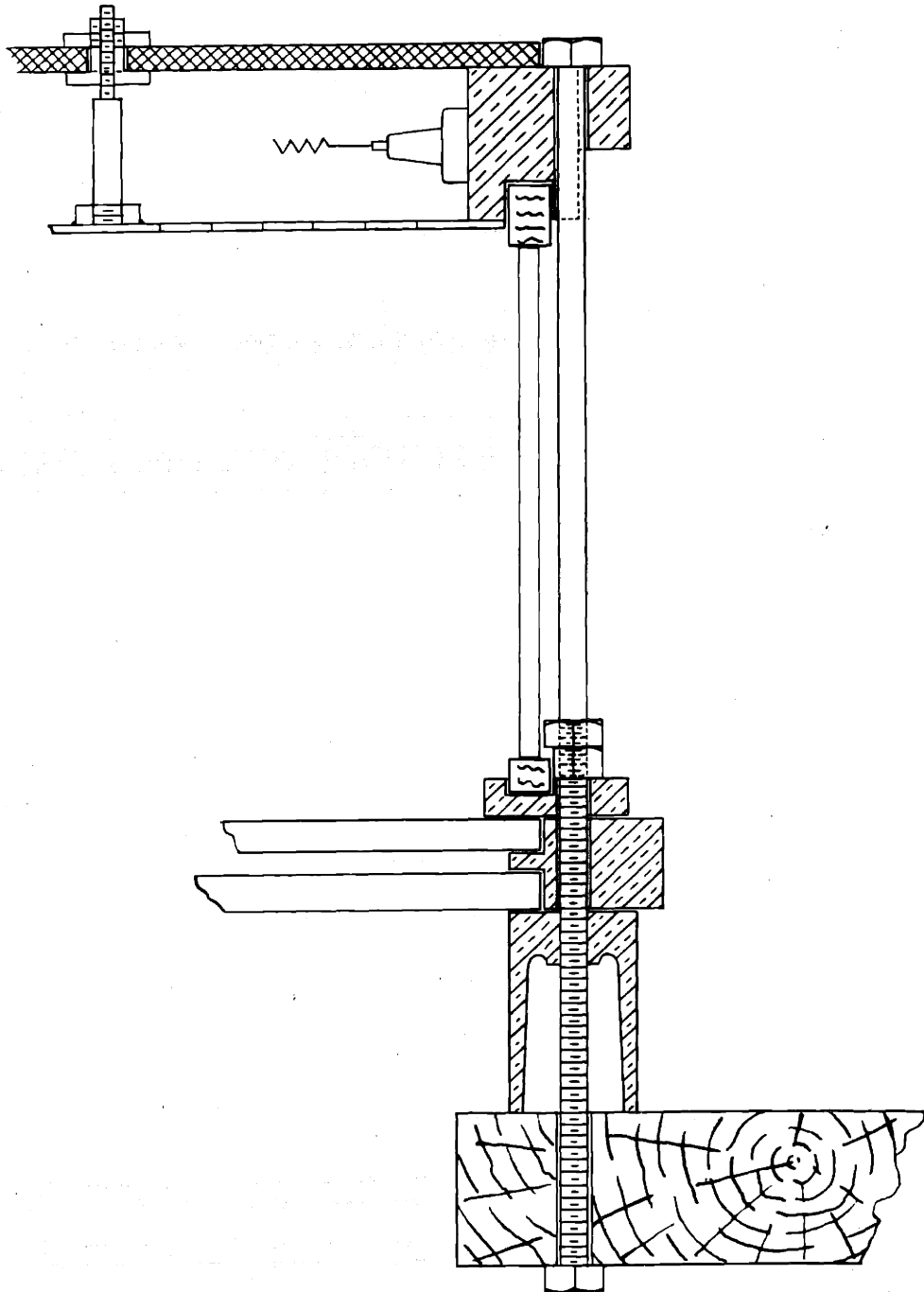


FIGURE 13

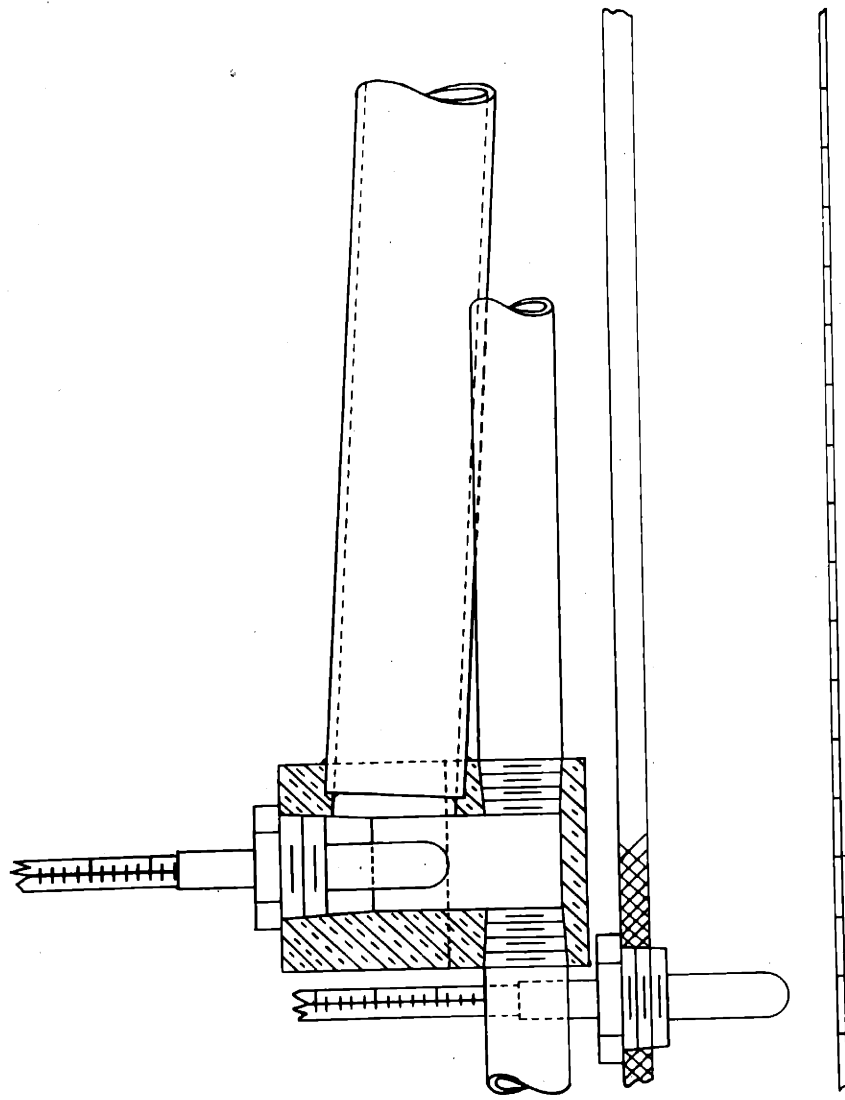


FIGURE 14

flexible apparatus may be made which will be satisfactory for nuclear physics research uses.

Chamber C is illustrated by photographs and line drawings in Figures 16 through 20. It was under construction September 1936 through September 1937. This apparatus was intended to work through a wide range of pressures, and for this reason principally, its construction was the most difficult and the time insufficient to find the conditions for it to show ion tracks.

2. Major design factors.

The major factors which influence design of this type apparatus will be considered in this order:

- A. Visibility of the interior.
 - B. Refrigeration of the chamber floor.
 - C. Heating of the chamber roof and distribution of the vapor at the roof.
 - D. Vapor supply to chamber roof.
 - E. Prevention of turbulence of gas.
 - F. Prevention of leaks.
- 2A. Visibility and photography.

It is essential that one should see what goes on within the cloud chamber. Secondly, one needs photographic records, to make quantitative measurements upon ion-tracks to determine their length, direction, curvature, etc.

A fundamental conflict in the problem of visibility is this: The chamber should have small depth

FIGURE 16.

Views of chamber C from opposite sides.
Pointer referred to in Figures 18 and 21.

FIGURE 17. Next page over.

View of chamber C partly assembled. Pointer on picture points to boiler. Two pointers at left point to motor and pump.

FIGURE 18. Next page over.

Two views of phenomena in cloud chamber C observed when condensation on the roof of the chamber drips down to the floor. The splash produces vortices of fog and a general fogging. The streaks are splashed droplets in mid air. Views are through window marked with arrows in Figure 16, top. See also Figure 21.

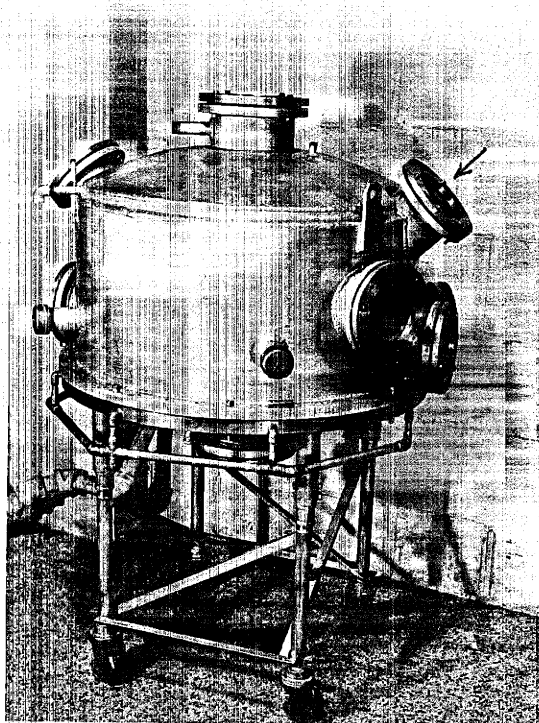
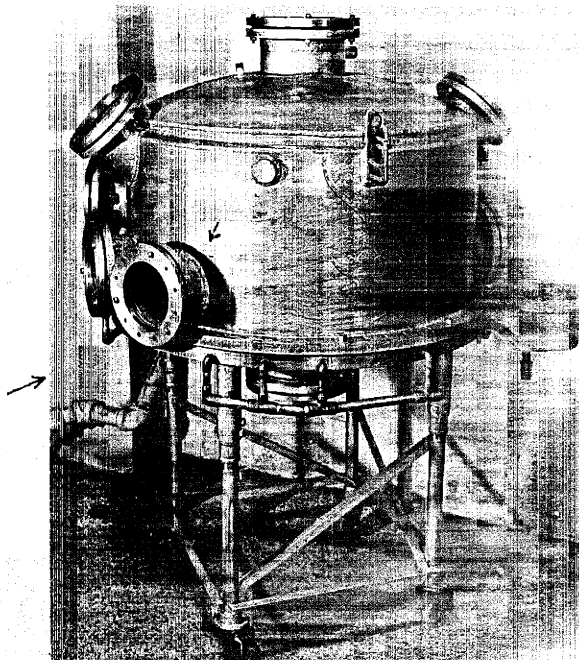


FIGURE 16

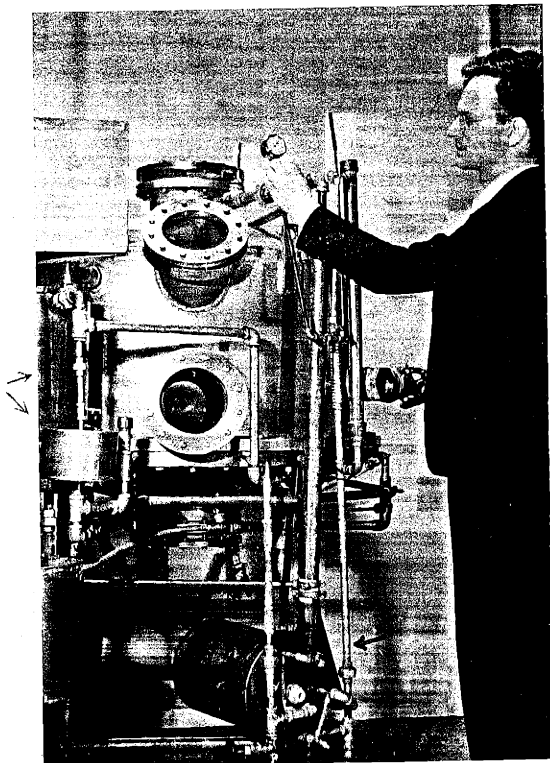


FIGURE 17

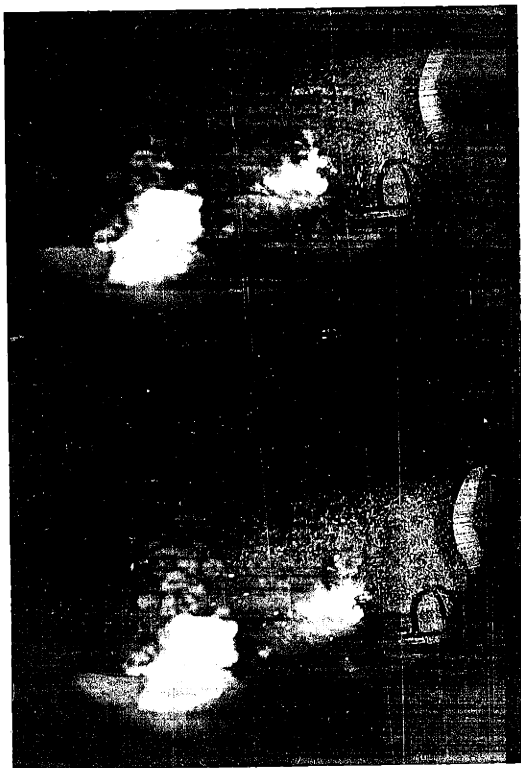


FIGURE 18

FIGURE 19.

Cloud chamber C.

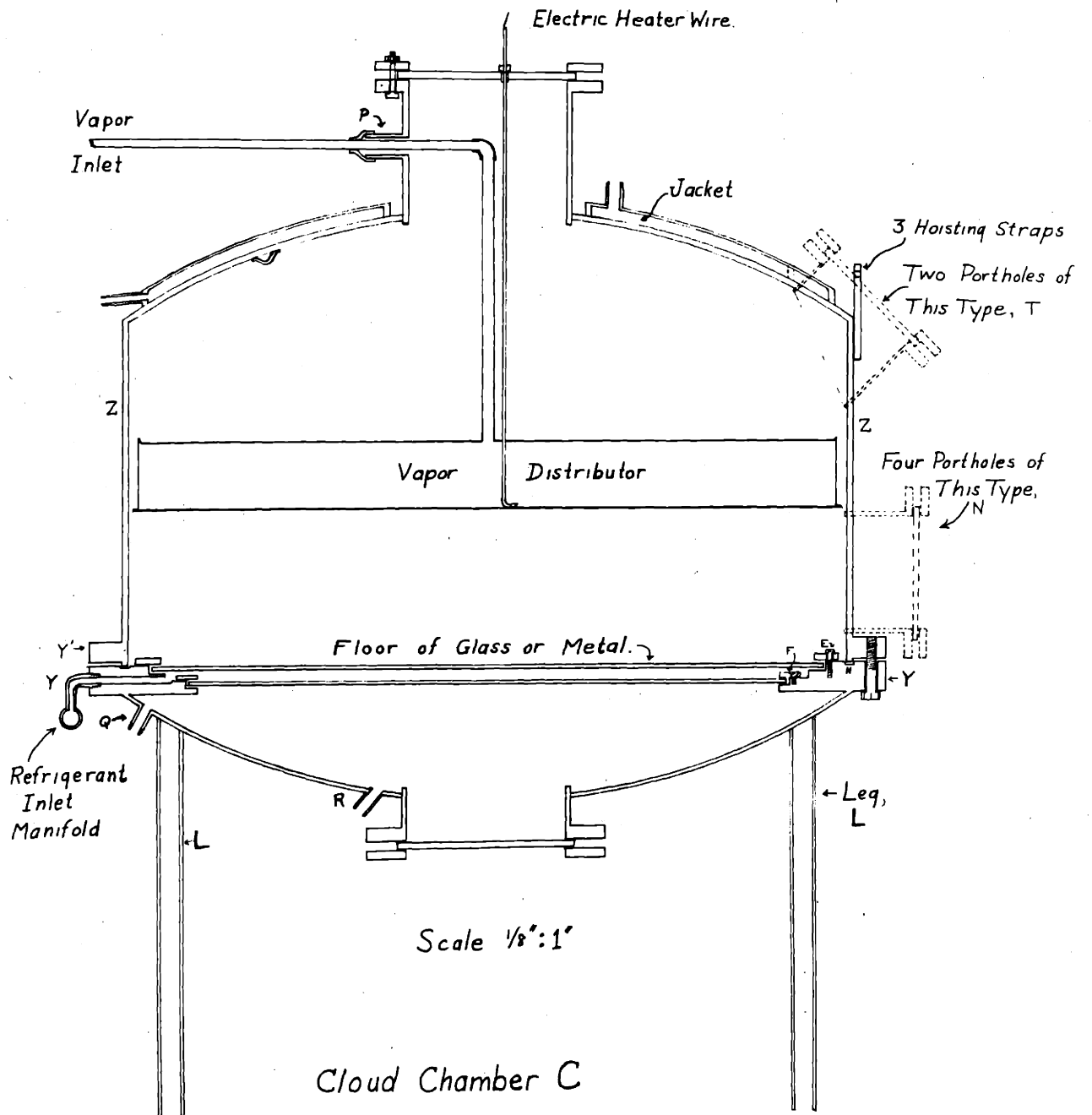
A vertical section through the axis.

FIGURE 19A - next page.

Upper diagram shows plan view looking down on the main flange ring of the lower part of the chamber (indicated by YY in Figure 19)

Lower diagram is opened out view of tank wall, Z-Z.

- A. - Bolt holes for 1/2" bolts holding upper and lower tank parts together.
- B. - drain outlets for chamber floor.
- C. - Refrigerating system inlets.
- D. - Refrigerating system outlets.
- E. - Bolt holes for 1/4" bolts fastening ring that holds down upper floor plate.
- F. - Bolt holes for ring holding down lower floor plate.
- G. - Outer groove for rubber gasket.
- H. - Groove for lead gasket.
- K. - Position occupied by refrigerating system pump - Figure 22.
- L. - Position of legs on tank.
- M-N-T - Positions of portholes as indicates.
- P-Q-R-S - Positions of pipe nipples as indicated.
- T. - see M-N above.
- W. - boiler and lead pipe position (connects with P). See Figure 20 for details.
- Y-Y. - lower and upper main flange rings, respectively.



Scale 1/8":1'

Cloud Chamber C
FIGURE 19.

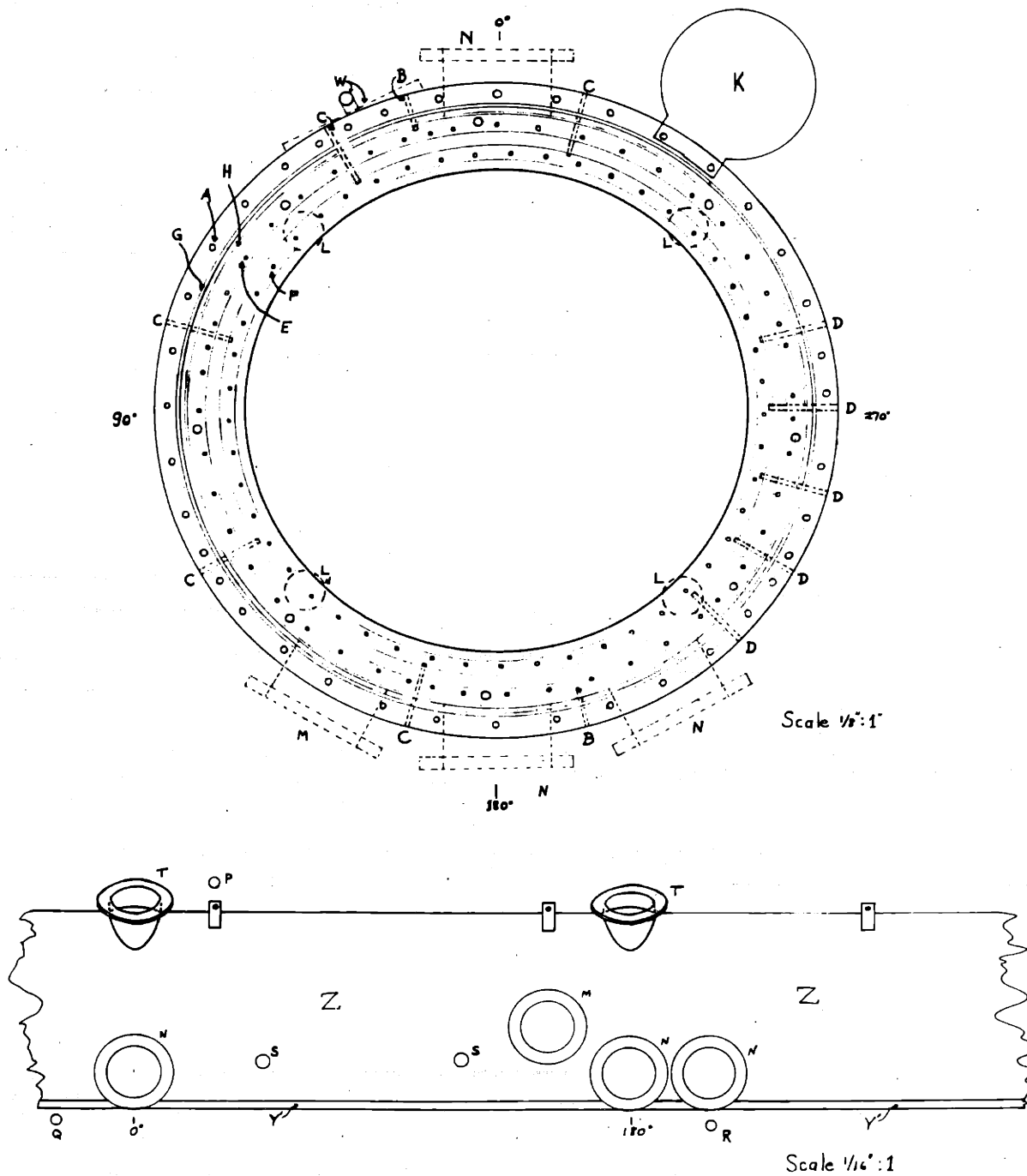
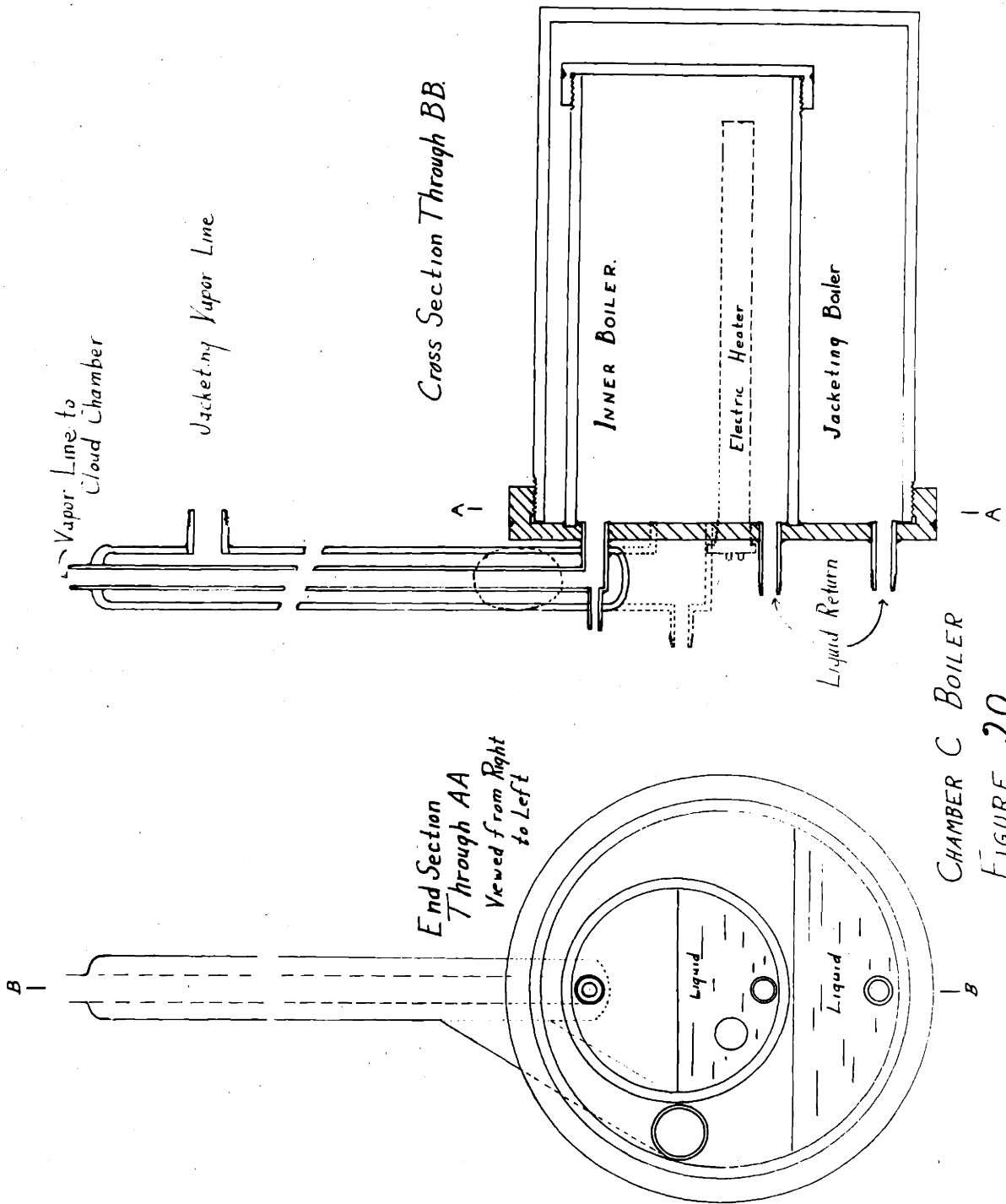


FIGURE 19 A.

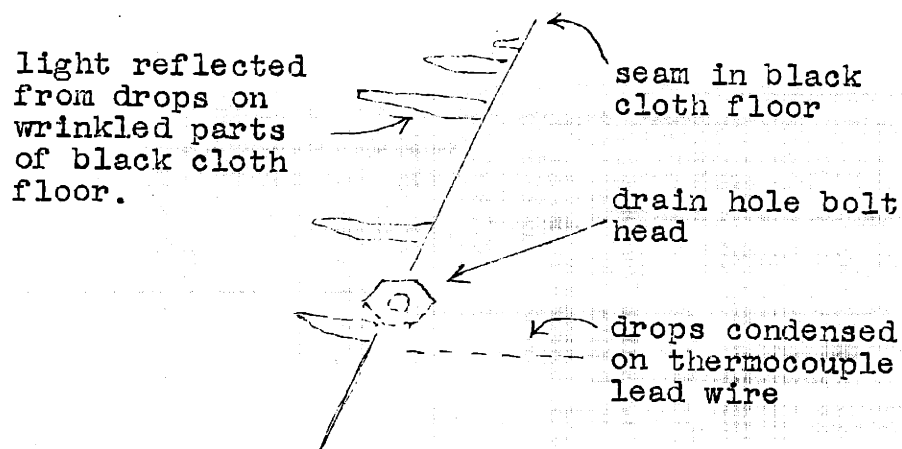


CHAMBER C BOILER
FIGURE 20.

FIGURE 21.

Views through window marked with arrow in Figure 16,
bottom.

The pattern outlined here



is explained as shown.

To the right of the above pattern is a field of droplets illuminated by the arclight beam. The diagonal streaking is a result of their falling vertically downward. The angle of view is about 45° from the vertical, looking down on the rain.

The streak-like and zigzag patterns of cloud in these pictures are associated with drops of condensation falling from the roof.

The general fog in the two center pictures comes from the type of fog in Figure 18, settling downward.

FIGURE 21

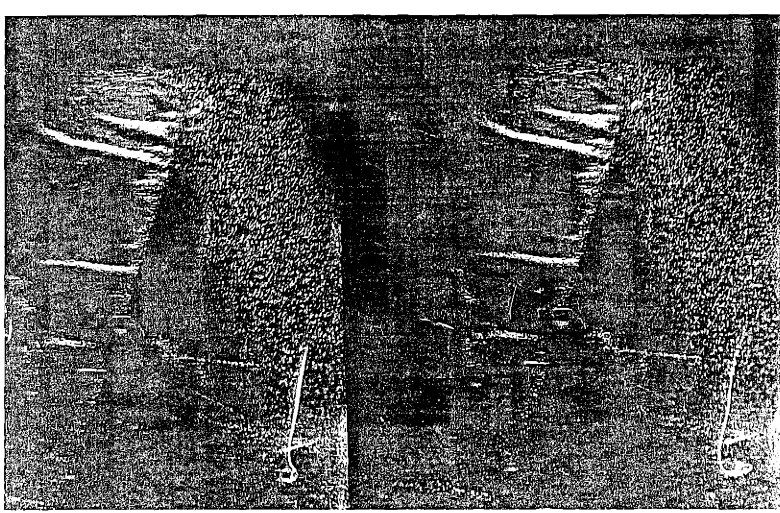
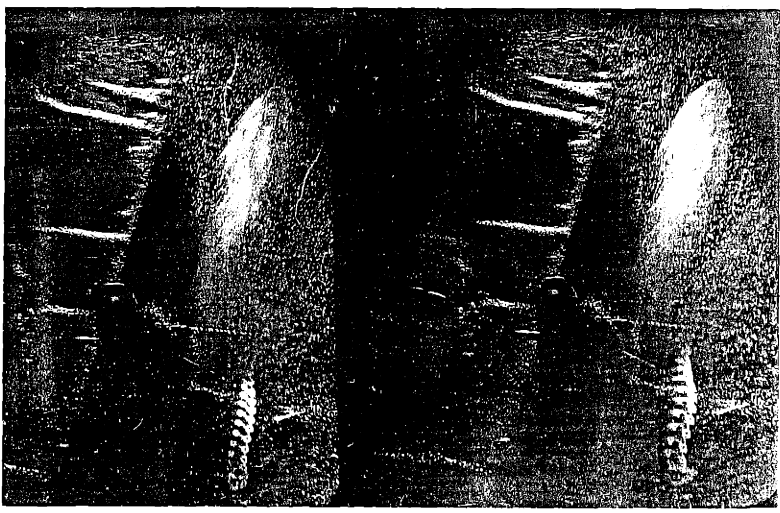
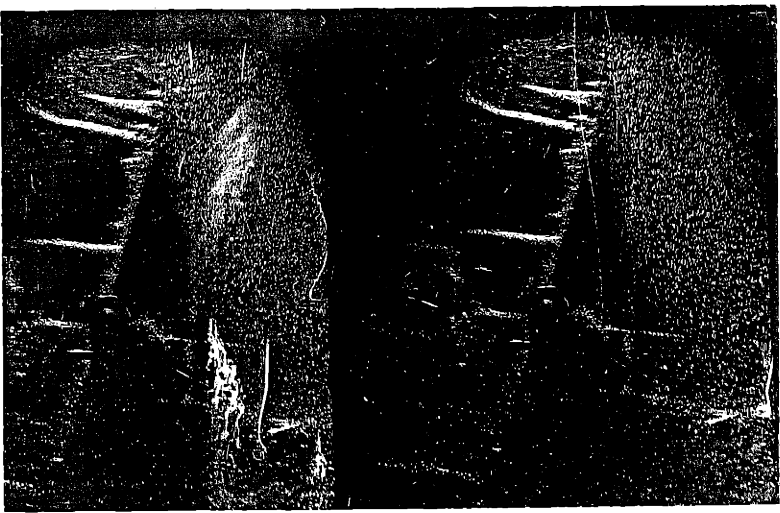
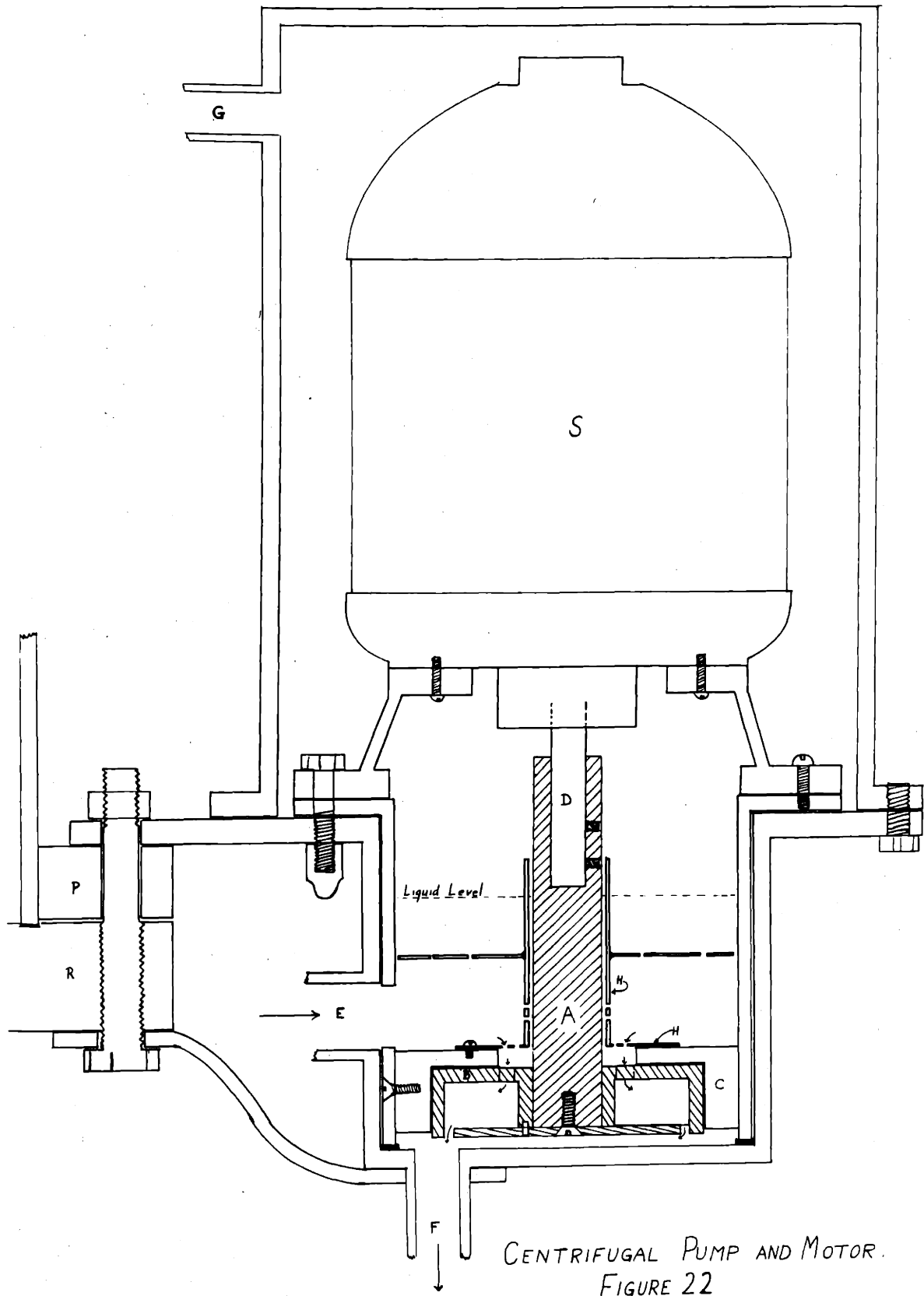


FIGURE 21

FIGURE 22.

Pump (K in Figure 19 A) for cloud chamber C.

- A - stainless steel shaft, press-fitted to brass rotor, B.
- C - Cast iron casing in which rotor B turns.
- D - Motor shaft, fastened to shaft A by set screws.
- E - Inlet pipe for liquid.
- F - Outlet pipe for liquid.
- G - Gas pipe line for pressure equilibration, to main cloud chamber tank.
- H - Baffle plates and tubes to cut out turbulence and swirling, so as to keep gas from being pumped through the pump rotor.
- P - Flange on upper part of tank (Y', in Figure 19A).
- R - Flange on lower part of tank (Y, in Figure 19A).
- S - Motor, 3 phase, 220 volt, 1/6 h.p.



compared to breadth, to avoid turbulence (say 1 to 4 ratio). Then the region sensitive to ions is a very shallow one (in chamber A, one inch deep, 20 inches horizontally) of great breadth. But if one views the tracks through windows in the sides of the chamber, which are the only places where it is easy to put windows, the view of most of the tracks is poor because of foreshortening. A better angle of view through top or bottom, or both, requires glass windows in these places, difficult things to provide effectively. For example, the glass windowed port-holes in the top and bottom of chamber C could not be used. The view from the bottom had to be cut off by a metal chamber floor, and from the top by a metal vapor distribution system.

With water vapor in chamber A, dropwise condensation on the glass sides hampered the view. Alcohols usually gave clear liquid film condensation on windows, but liquid running down the surface often distorted objects in the chamber.

Air moisture formed dew or frost on the outside of cold glass surfaces. This was best avoided by having an extra insulating window. Then a metal surface colder than the inner glass window, if placed in the dead air space, would keep frost off the inner glass. An air blast on the outer surface kept it free of dew.

Observation through the double glass floor of chamber A was hampered because the refrigerating liquid

between the glass plates could not be kept clean. The same difficulty was encountered in chamber C. For this reason (and others) the glass floor technique is to be avoided if other satisfactory methods can be found to make the chamber interior adequately visible. However, with perfectly attainable precautions this type of construction is certainly feasible, and will give a good view of the interior of the chamber. The shallow pool of condensed vapor on the floor of the chamber does not interfere with the view.

It was found that droplets were most brightly illuminated at the smallest angle between the direction of observation and the illuminating light beam. At right angles to the beam it was always hard to get enough light to see or photograph droplets. This is the same experience as is had with expansion cloud chambers.

To illuminate chamber A, a 1000 watt incandescent spot light bulb and a condenser lens gave a beam bright enough for visual observation and crude photography. See Figures ^{9 &} 10. This spot light, however, gave a rather divergent light beam which produced an unnecessarily large amount of scattered and reflected light in the field of view. For use with chamber C, the spot light was replaced by a high intensity motion picture projector arc operating at 60 amperes, 80 volts. This arc supplied as much light as one could want.

The high intensity light source introduces a new

difficulty. For this beam contains energy of the order of hundreds of watts, even after it has passed through one inch of copper sulphate in water solution and through 1 1/4" of ordinary plate glass. In chamber C it was observed that when this beam struck a black cloth wall, the heating produced convection currents which induced cloudy condensation effects far out into the chamber. The beam should pass out of the chamber through windows. Otherwise, even if it does not produce convection currents it is certain to impose an unnecessary load on the floor refrigerating system.

Photographs of phenomena in chamber C were made with the light source just described, on 35 mm. panatomic film in a 5 cm. focal length camera, at an angle of 45° to the beam, in 1/25 to 1/100 second at F 1:9. However, a continuous light source is only needed for visual observation. Photographs could be made just as well or better with a high intensity flash of the type developed by H. E. Edgerton. The intermittent source would cut down the detrimental heat convection effects described above.

2B. Refrigeration of the chamber floor.

The complexity of this problem can vary tremendously according to the design of the apparatus and its intended use. Cloud chamber B, for example, only needed a gear pump to circulate icewater from a vessel of cracked ice, under the metal floor, and back onto the ice.

The most complex case contemplated was the following: It was desired to pump clean butyl alcohol between glass discs 33" in diameter at -50°C , with velocity great enough to keep the temperature gradients small through the floor and across it from side to side. The cloud chamber was to operate at pressures differing from atmospheric, in an atmosphere of carbon dioxide gas. All simpler cases may be derived from this one by appropriate simplifications, of which only the more important will be discussed.

A temperature rise of 4°C for the refrigerating liquid from inlet to outlet seemed to be tolerable without producing turbulence, in chamber A. This implies a tolerable temperature gradient across the chamber floor of the order of 2°C per foot.

A temperature as low as -45°C did not crack a sheet of plate glass. The glass was mounted in rubber gasketed metal frames. Plate glass $1/4$ " thick is moderately strong, but $1/8$ " glass is too weak for a sheet two feet square or larger.

Glass plates 2 feet square (Chamber A) are not as strong as plates 33" in diameter. Either is in serious danger of bursting with a three foot head of water on one side. The volume of space between plates 33" in diameter increases by several quarts on account of bulging when the pressure rises from zero to one foot of water. Metal plates can be bolted together to avoid this bulging.

The edges of round plates (glass or metal) are much more easily sealed than those of square plates.

The two glass plates should be $3/16$ " to $1/4$ " apart, but not so much as $1/2$ " apart, if adequate flow velocity is to be maintained.

The liquid was introduced between the two discs of glass at five points around 180° of the circumference and removed at a cluster of five exits opposite. The flow distribution appeared to be adequately uniform. See Fig. 19a.

With square glass plates (chamber A) the liquid flowed from side to side very simply. With round metal floor plates, liquid could best be introduced at the middle. Glass discs, however, are seemingly better not weakened by a hole through the middle, but no tests were made to find out experimentally. See Figure 24.

If the refrigerated alcohol is to be clean, a gear pump cannot be used. Packing grease and graphite and ground bits of brass from the gear teeth form a dirty colloidal suspension. (Chamber A). Also rust from iron or steel fouls the liquid. (Chamber C).

Lubrication problems in cold alcohol can be satisfactorily avoided by a vertically mounted centrifugal pump with no bearings whatever beneath the liquid surface. The pump which was used with considerable success on Chamber C is shown in Figure 22.

The pump in Figure 22, when first designed sucked bubbles of gas into the liquid. It is shown with the baffle

system which finally avoided this source of gas bubbles.

Another source of gas bubbles in the liquid is that gas which may leak into the pipes. This can happen when chamber C is operated below atmospheric pressure, because this chamber was designed as a sealed unit with the refrigerating liquid at the same pressure as the chamber, in order to avoid a large pressure on the flat floor plates which would inevitably break them, even if of metal and not glass. Chamber C had many parts of the liquid system piping exposed to the atmosphere, so a vacuum leak could seriously displace liquid by air. A pressure leak, if large, might cause a fire, if small it is impossible to find because the liquid evaporates as fast as it leaks. This leads to the rule: As much as possible of the piping (gas as well as liquid) should be enclosed inside the main vacuum or pressure tank and thus minimize leakage of all sorts.

Carbon dioxide is extremely soluble in alcohols at -50°C. Such large quantities will dissolve in the refrigerant butyl alcohol as to interfere with the operation of the cloud chamber. Then, when the alcohol is allowed to warm again after stopping a run, it effervesces, and the carbon dioxide liberated displaces the liquid to quite a large extent. This problem was solved by filling the space over the pump (Figure 22) with nitrogen. This space communicated through a small tube with the main body of the apparatus which was filled with carbon dioxide.

If glass floor plates are used, an otherwise minor feature of design needs special emphasis. Particular care must be taken that the back-pressure at the outlet from the plates be kept very low. To keep this pressure sufficiently low with a liquid flow of about ten gallons per minute, requires liquid outlet piping with a cross sectional area of about three square inches for a length of only two feet. This outlet piping is best horizontal, in order to avoid syphon effects, which have been found to be undesirable.

The motor which drives the liquid circulating pump (Figure 22) for chamber C is enclosed in the system. This motor* has given entirely satisfactory operation as long as liquid alcohol is kept out of the bearings. The technique of sealing the motor into the system and thus avoiding leakage through packing glands is quite satisfactory.

2C. The vapor distribution system and the heating of the roof of the diffusion cloud chamber.

These two phases of the design problem are inseparably bound together. For the vapor must be distributed over the whole roof of the cloud chamber, and the distributor, no matter what its nature, must be hot enough so that vapor does not condense upon it. The top is certain to lose heat by radiation and conduction to the bottom,

* The motor is 1/6 h.p., vertical ball bearing, totally enclosed, 3 phase, 220 volt, squirrel cage rotor, Century Electric Co.

so that heat must be supplied to it.

Only one satisfactory distribution system was developed. This consisted of a brass plate (K, Figure 4.) with small holes ($15/1000$ " in diameter) distributed uniformly over the surface $1/2$ " apart. The total punched out area of the plate was less than $1/10$ of one per cent of the total plate area. The vapor supplied to the space above the plate spread out and flowed quite uniformly through all the holes. Heat was also supplied from the upper side of the plate. To minimize radiation, the lower side of the plate was chrome plated.

In chamber A, the distributor plate was heated by a bare chromel wire strung above it on porcelain insulators (Figures 4 and 13). This method worked and was simple, but was undesirable because of the fire hazard associated with it.

In chamber C, a satisfactory heater design was worked out, although involving difficult construction. In every fourth space between rows of holes, a $1/4$ " copper tube containing an electric heater unit was soldered down to the brass plate. This tube was a single piece about 36 feet long, zigzagged back and forth to cover the whole area of the brass plate nearly uniformly, and the ends of the tube were extended out from the chamber to the atmosphere, through compression fittings. The heater wire was No. 18 B & S Gauge chromel, insulated with two layers of braided asbestos thread. This heater developed an erratic

leakage (resistance of about 3000 ohms, which was probably due to a carbonized lump of cotton in the asbestos. The cotton had not been burned out before drawing the wire into the copper tube in order to avoid breaking the physically weak asbestos. It is suggested that in future construction of such units the cotton be burned out of the inner layer of asbestos before the second layer is woven over it, and so decrease the probability of formation of a complete carbon bridge from heater to ground. This information has been given because commercial heater units of types comparable to this one are not made in lengths approaching 40 feet.

The punching of the many small holes is a problem of sufficient difficulty to be worth mentioning. To have drilled the 4000 holes in the 1/32" brass plate for chamber C as was done for chamber A, would require about 100 hours. However, a punch of the design sketched in Figure 23 can be used to drive cone shaped holes through a 1/32" brass plate, with any diameter desired at the smaller end. No punched plate comparable to that described here is available commercially.

2D. The vapor supply to the chamber roof.

The vapor for chamber A was evaporated from liquid alcohol in a two liter glass flask heated by a steam jacketed oil bath. The evaporation took place with very little turbulent boiling. The rate of vapor flow provided by this boiler was approximately that desired.

FIGURE 23. Punch to put small holes through $1/32$ " brass plate. A schematic diagram.

FIGURE 24. Types of floor drains for double metal floors. A is space between floor plates. I is type used; II is proposed type. Dotted lines indicate drain holes through bolts.

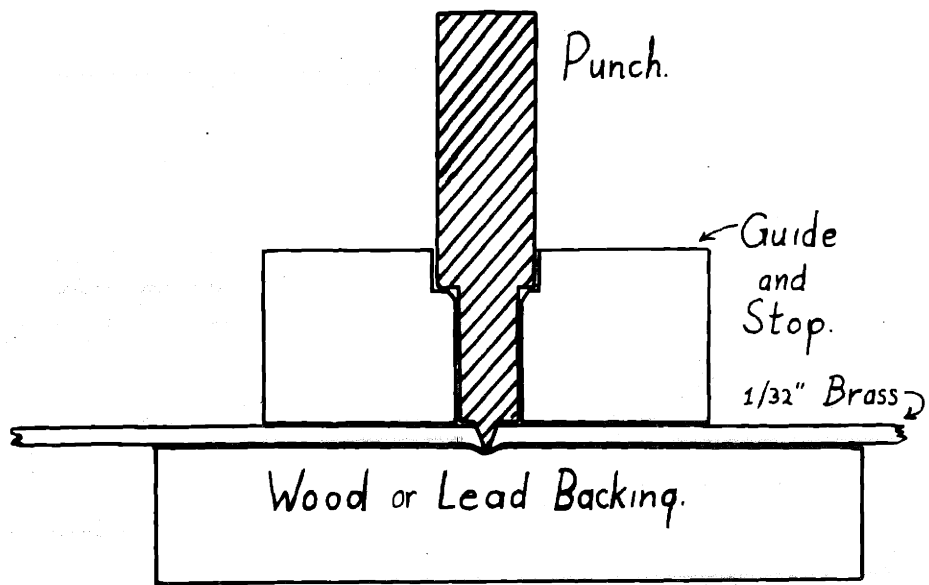


FIGURE 23.

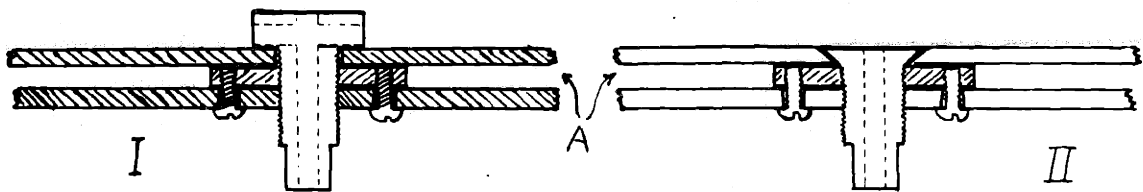


FIGURE 24.

Vapor for chamber B was generated at the roof of the chamber itself, by evaporation from the liquid in the tray (Figure 5). The liquid was heated by an electric heater in the cover of the tray, and the vapor passed down through tubes into the cloud chamber space beneath. The primary fault of this arrangement is that it inflexibly associates the rate of vapor flow and the temperature of the chamber roof. These two variable factors should be kept independent at the present stage of development.

The boiler for chamber C is illustrated by Figure 20. It consists of a section of steel pipe containing a commercial type of electric immersion heater. The rate of heating is variable between zero and 750 watts by the use of a Variac autotransformer. The whole boiler is enclosed in another section of pipe whose purpose is to jacket the vapor supply boiler just at or just above the boiling point temperature. A chief fault of this design is that there is no provision for visual observation of the conditions inside the boiler. Another thing that should have been provided was a vapor flowmeter of some sort in the line between boiler and cloud chamber. For it is highly desirable to have as direct information as possible on every vital functioning part of the entire apparatus, if the phenomena associated with its operation are to be analysed in detail.

The metal boiler used with chamber C is open to suspicion as a cause of the failure of this apparatus to

produce ion tracks. Some chemical action of the metal, which was not present in the glass boiler of chamber A, might produce enough additional molecular aggregates on which condensation occurs, to prevent ion-track formation. Another possible source of these aggregates is an effervescence of gas from the liquid alcohol which drains back into the boiler from the chamber floor. This alcohol may contain a very large quantity of dissolved carbon dioxide. When the liquid is heated, the rapid evolution of the gas may, by splattering, produce condensation aggregates.

However, the suppositions just presented as to sources of condensation nuclei are only two among many possible. A whole field of research upon molecular aggregation of vapors is involved in tracing down possible causes of condensation. This is a nearly unexplored field of research.⁸

2E. Prevention of turbulence and convection.

Chamber A was nearly free of turbulence and convection currents. Its type of construction, with side walls of an insulating material, and with the breadth of the chamber large compared to its height (4 to 1) seems to be the most satisfactory. A ratio of breadth to height of 2 to 1 as tried with chamber B (and for a time with C) is not to be recommended. Also, the metal walls of chamber C would not reach a correct temperature distribution, so that circulation currents had to be stopped by an inner "false wall" of cloth, which acted as an insulating sheath.

Another point to be emphasized is that no extra volume of gas should communicate with the main chamber space, unless through one small tube or hole. Any more extended interconnection is almost certain to lead to destructive circulation currents.

If the vapor is of higher molecular weight than the gas in the chamber, turbulence probably cannot be avoided. Turbulence of a mild sort was evident in chamber A when methanol (m.w. 44) diffused into nitrogen (m.w. 28), but not when methanol diffused into carbon dioxide (m.w. 44).

2F. Prevention of leaks.

Chamber A was operated very near to atmospheric pressure, but even so there were troubles with leakage at some of the many glass to metal joints, and especially at the corners of rectangular joints. It has now been found that pyrex glass cylinders two feet in diameter are made commercially. Such a cylinder and a round chamber floor would simplify design, construction, and sealing of a cloud chamber similar to A.

The vacuum and pressure problems encountered with chamber C are essentially those of high vacuum technique with a few modifications. A particular lesson was learned from chamber C. - Design the apparatus as if it were to work at atmospheric pressure. Then enclose it in a steel tank whose purpose is solely to withstand the pressure forces. - The tank is not to be the cloud chamber itself. Only

the bare minimum of chamber parts should be outside the walls of the pressure tank.

The following experimental information obtained while working with chamber C is presented for the benefit of those who may contemplate construction of a similar chamber.

- (1) The construction of the main flange joint between the top and bottom of the tank was entirely satisfactory. A lead wire in the $1/4$ " x $1/4$ " groove in the lower flange was compressed to a ribbon extending across the whole bottom of the groove. *See Figure 19.*
- (2) The windows of plate glass were entirely leak-proof when fastened between flange rings with wide, soft rubber gaskets (gaskets on both sides to avoid cracking).
- (3) Certain types of fittings are particularly to be avoided wherever they might be subject to pressure gradients. These include pipe unions, valves and valve-stems, sleeve type compression fittings (for copper tubing), compression fittings to hold glass tube liquid level gauges.
- (4) Good arc welding is leaktight. A particular specification not to be overlooked is that pipe nipples welded into a tank must be of good seamless steel tubing. Ordinary iron pipe does not make a satisfactory, tight joint.

(5) The most desirable type of pipe-fittings were found to be the "Streamline" solder type fittings for use with copper pipe. These are made by the Mueller Brass Company. They may be obtained in forged and cast brass and drawn copper. They can be used repeatedly and flexibly. In particular, they have the advantage that where a threaded type assembly would have to have a union joint, these do not. Furthermore, for experimental work, there is the advantage that the pipe system may be cut open anywhere and without delay rejoined, simply by soldering together again with the proper kind of fitting. The only drawback to their use is the fire hazard in reworking a system that has contained flammable materials.

3. Minor design features.

Certain minor details of design cause more difficulties in construction and use of a continuous cloud chamber than might be expected. Some of these are discussed briefly here, along with some other details of design so successful they are worth recommending to others.

3A. Corrosion.

Chamber C was built of ordinary steel plate. In a tank of this size any other material is much more expensive.

The steel will rust badly in the presence of water and air, or even if the air is replaced by carbon dioxide. Rusting is less serious in dry alcohols. The metal surfaces can be quite well protected in the presence of alcohols and water by resin coatings such as Glyptal or Bakelite. The latter is the more resistant to alcohols.

A serious corrosion was encountered in the vessel where the refrigerating alcohol was cooled by dry ice. Heat transfer to the dry ice from the coil through which the refrigerant circulated was facilitated by a liquid in which the cooling coil was immersed. If this liquid was left standing in the vessel when the apparatus was not in use, the copper cooling coil was rapidly corroded. The high concentration of dissolved carbon dioxide accelerated the oxidizing action of air, and the corrosion became very rapid in the presence of carbon tetrachloride that was added to reduce flammability.

3B. Floor drainage.

It is possible to drain the condensed liquid from the horizontal floor of the cloud chamber (either A or C) so that the liquid is less than 1/8" deep. If the floor is made of metal it is simple to do so because a hole can be put through the metal without interfering seriously with the refrigerating system liquid flow. See Figure 24. But if the floor is glass, it is inviting breakage to put a hole in it and to cement a drain tube into the hole. One may drain the liquid over the edge of the glass. This drain must pass through a gap in the frame that holds the glass against the gaskets which seal the refrigerating liquid system. The gap must be large enough to insure that surface tension effects do not stop the liquid flow. In addition, the tubing beyond the initial gap must allow free flow of liquid without possibility of becoming air-bound. Siphons cannot be relied upon because of the gas which comes out of solution and destroys the siphoning column. Mechanical pumps are very likely to become air-bound for the same reason.

3C. Freezing of liquid on the chamber floor.

There is no danger of freezing any alcohols in the temperature range needed in the diffusion cloud chamber, because they may be cooled until their saturation vapor pressures are negligible without freezing. But water must be cooled practically to its freezing point to bring its

saturation pressure down to five millimeters of mercury, just within the possible range of operation. (See Figure 3). The refrigerating liquid will have to be below zero to maintain the surface of water near zero, and then the water is liable to freeze inside the drain pipe. Such a difficulty may undoubtedly be overcome, but methyl alcohol avoids it altogether. This is one reason it was used in chamber A rather than water.

This is an opportune place to mention that formation of snow could be studied in this cloud chamber, by diffusing water vapor to the floor refrigerated to -40°C or colder. The snow could be washed off the floor by a slow flow of alcohol and thus be formed continuously while its formation was being analysed.

3D. Light beam water filter.

The water cell which takes the infrared radiation out of the high intensity arc beam should have a Pyrex window on the side nearer the arc. The water cell can be cooled conveniently by a jacket of flowing water. If the cell wall is made of copper, the cell can contain copper sulphate solution without protection. To prevent corrosion if the cell is made of anything else, a rubber lining can conveniently be cemented to the metal wall with Vulcalock cement made by B. F. Goodrich Co.

3E. Electrical leads.

Electricity may conveniently be brought into the sealed tank through automotive spark plugs. It is best to design the apparatus so that the connections to the plugs inside the tank do not need to be disturbed to open or close any part of the apparatus. However, if it is impossible to avoid the necessity of disconnecting the inside wire connection for disassembly, two-piece spark plugs will permit the disconnection. The operation may be annoying, but it is simple.

3F. Dry ice refrigeration.

The refrigerating system liquid passes through a cooling coil in a vessel containing pieces of dry ice and some liquid to act as a heat transferring agent. Every liquid tried in this vessel foamed up to several times its normal volume. If the vessel was large enough in proportion to the heat transfer rate, the foam broke rapidly enough so it could be ignored. But the heat transfer capacity of a given size of vessel can be increased several times by an air blast from a fan blowing across the foam surface. It is suggested that in future the vessel be closed so the liberated carbon dioxide is taken out of the laboratory through a flue. Then a fan installed in the vessel can make a blast of the liberated carbon dioxide gas itself, and so avoid the unnecessary refrigeration of the air in an air blast.

3G. Heat insulation.

Glass wool* is a convenient and clean insulation for heat or cold which may be handled repeatedly without serious deterioration. It may be used exposed or, preferably, put into moderate sized bags.

Glass windows must be insulated by another glass plate. Windows at low temperatures (-40°C) are best insulated by two extra plates sealed together. A single outer insulating window becomes sweated with moisture rather too easily.

3H. Thermocouples.

Thermocouples should be provided wherever it is of any importance to determine the temperature. Mercury thermometers are extremely inconvenient. Thermocouple leads may be brought out of the tank through spark plugs.

3I. Vapor line heating.

The vapor passing from the boiler to the distributor plate in the cloud chamber must be kept hot. The vapor line may be jacketed by another vapor line. If the line is of metal, the jacket may be assembled out of "streamline" fittings very simply. The vapor line can be electrically heated. In this case it is more difficult to determine the vapor line temperature, but easier to vary it over a wide range.

* "Red top ^{Min} Mineral Wool", United States Gypsum Co.

4. Conclusions concerning diffusion cloud chamber design.

A diffusion cloud chamber might be designed with either of two principal uses uppermost in ones mind. It might be intended only for use as a tool in nuclear research, or it might be intended principally for use in the study of the condensation phenomena themselves. This latter use must, at least for the present, be the one for which a diffusion cloud chamber is constructed. It will be economical to construct an inflexible chamber simply for nuclear research only when experimental conclusions are reached as to exactly what the optimum conditions* for operation may be.

In order to find the best operating conditions to produce ion-tracks, the apparatus must be built flexibly, and this of course makes its construction tend toward complexity. However, whenever a particular set of operating conditions are chosen, the construction can be simplified and the operation made highly automatic.

* It should be made clear that there may be no one optimum set of conditions. In fact, in any design problem one is likely to have to make arbitrary decisions as to where to compromise conflicting effects both of which lead to difficulties.

CHAPTER IV

The condensation of a supersaturated vapor upon ions.

Introduction.

In this chapter the condensation of vapor upon ions will be discussed in some detail, because of its fundamental bearing on the useful operation of all cloud chambers.

In Conduction of Electricity in Gases (Edition III, pp. 325-334) by J. J. Thomson^{16a} there is a rather complete discussion based on thermodynamics, of the properties of electrically charged droplets. Starting from this point, a kinetic analysis of the condensation of vapor upon such droplets should give a more complete theory of the phenomena which occur. Such an analysis is presented in this chapter. It follows and extends the methods of Becker¹⁴ for uncharged droplets.

For a complete understanding of the analysis to be given here, one should refer to Appendix I where Becker's analysis is given for the simpler ~~uncharged~~ problem of the formation of uncharged droplets.

1. Thomson's equation.

The vapor pressure, p_r , in equilibrium over a droplet with an electric charge, e_1 , is given to a good approximation by Thomson's equation.

$$(1) \quad \ln p_r/p_\infty = \frac{M}{\rho RT} \left(\frac{2\sigma}{r} - \frac{e_1^2}{8\pi D^2 r^4} \right)$$

Here D' is the dielectric constant of the vapor, r is the radius of the drop, p_∞ is the normal vapor pressure over a flat surface of the liquid at a temperature T . Also M is the molecular weight, ρ the density, of the liquid in the drop. In deriving this equation certain assumptions are involved: that the surface tension, σ , is independent of drop size, that the vapor is far below the critical pressure, and that there is no electric double layer on the surface of the drop.* For the following analysis these assumptions are implied by the use of this equation in further calculations.

The graph, Figure 26, shows the values of p_r/p_∞ obtained from equation 1 for water and methyl alcohol drops with one unit of charge** and at 0°C . The radius is measured in terms of a dimensionless parameter defined below by equation 11. This graph, as well as equation 1, states that if a charged drop has a radius r , then vapor at a pressure p_r (and at the same temperature***) will be in

* For consideration of dielectric properties of the liquid, see reference 15.

** All the following analysis is intended for drops with charges of one electron unit.

*** Thermal equilibrium may not actually exist when a drop is growing. See reference 28. But in a cloud chamber where the vapor is mixed with a much larger number of molecules of an inert gas, thermal equilibrium is probably near enough to the truth so calculations are not invalidated. See references 11, 12 for experimental confirmation of the theory of condensation of uncharged drops, where thermal equilibrium was also assumed.

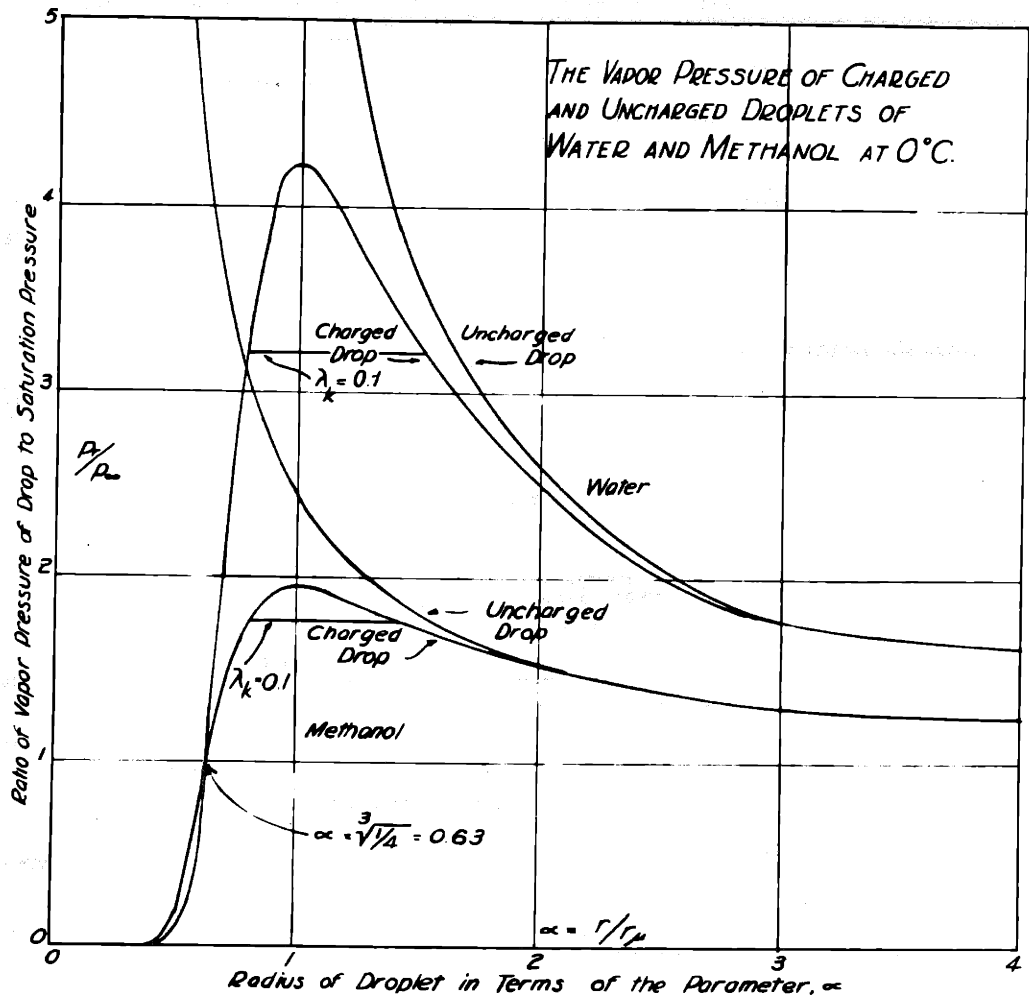


FIGURE 26

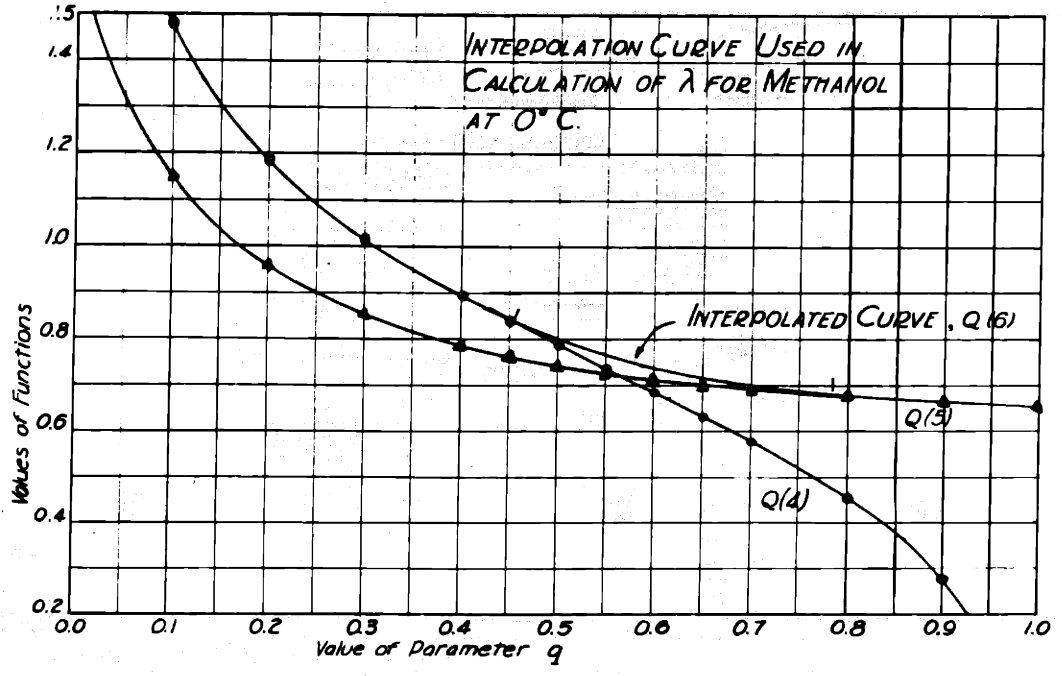


FIGURE 29

equilibrium with it. Note that there is a maximum value of p_r , which will be called the critical pressure, p_μ .

Suppose now that there exists a supersaturated vapor at a pressure p_n , so that

$$(2) \quad S = p_n/p_\infty$$

defines its supersaturation. The "critical supersaturation" will be defined by

$$(3) \quad S_\mu = p_\mu/p_\infty$$

If the actual supersaturation exceeds S_μ , the pressure of vapor is greater than that in equilibrium with any charged drop. In this case one may state with certainty that vapor will sooner or later condense upon any ion in the vapor to produce a large, visible sized drop.

The use that has ~~often~~ been made of the supersaturation value S_μ derived from Thomson's equation has often been such as to imply that this is the necessary supersaturation to make a cloud chamber show ion tracks. It is, rather, a sufficient supersaturation. The necessary supersaturation will be shown to be appreciably less, if the theory to be presented is valid.

2. The kinetic picture of the growth of charged droplets.

Consider a supersaturated vapor whose supersaturation is less than the critical value, S_μ . There are two real values for the radius of a charged drop in equilibrium with this vapor. (See Figure 26). The smaller size (radius r_m) is in stable equilibrium with the vapor, and the larger

size (radius r_n) is in unstable equilibrium. An ion introduced into this vapor may be expected to collect vapor molecules very quickly to form a stable sized drop. This drop will fluctuate in size because of the statistical nature of the individual gains and losses of molecules, and it may eventually grow larger than r_n . Having reached the latter size, it has a large probability of continuing to grow to visible dimensions.

As a measure of the probability of an ion growing to visibility one may use a half-life, λ , which is defined in a manner similar to that used in radioactivity decay problems. That is, one considers a whole group of ions as present in the supersaturated vapor. Then λ is the time interval in which half of the ions are removed from the vapor, by forming large drops which fall out of the vapor volume.

The fluctuations in size of drops which lead to their growth are computed quantitatively by the same method that has been used previously for uncharged drops.^{9,14.} One considers that the "vapor pressure of the drop" is the same thing as the equilibrium vapor pressure over it, p_r . The vapor pressure of the vapor is p_n . Then

$$(4) \quad \frac{\text{probability of losing one molecule}}{\text{probability of gaining one molecule}} = \frac{p_r}{p_n}$$

is the important relation of the statistics to the calculable quantities which is used, and allows one to compute

the probability of a small drop growing larger, until it finally becomes macroscopic.

3. Terminology and calculations for the half-life, λ , as a function of supersaturation.

The terminology has been made as similar as possible to that of Becker¹⁴ (Appendix I). Definitions of most of the symbols follow:

p_z = vapor pressure of a drop containing z molecules.

p_n = the vapor pressure existing in the chamber, a constant.

p_∞ = vapor pressure over a flat surface of liquid at the prevailing temperature.

z = number of molecules in any drop of liquid.

$z = s$ for drops that are removed from the chamber and $s \gg n$ where

$z = n$ for the (larger sized) drop in unstable equilibrium with the supersaturated vapor of pressure p_n .

$z = m$ for the (smaller sized) drop in stable equilibrium with the supersaturated vapor at pressure p_n

Z_z = number of electrically charged drops in 1 cm^3 (all assumed to have one unit of charge only) containing z molecules.

$Z_s = 0$ because of the assumption drops of this size are removed.

Z_m will be assumed to be essentially equal to the number of ions present per cm^3 , and maintained constant.

J = rate at which ionized drops grow to size s and are

removed, and also the rate at which the drops pass from any one size (ν molecules) to the next ($\nu + 1$).

F_ν = surface area of drop of size ν .

$Z'_\nu = F_\nu Z_\nu$ = total surface area of all drops of size ν .

r_ν = radius of a drop containing ν molecules.

$a_0 dt$ = probability of condensation of one molecule on 1 cm^2 in time dt .

$q_\nu dt$ = probability of evaporation of one molecule from 1 cm^2 in time dt .

$\beta_\nu = a_0/q_\nu = p_n/p_\nu$, defining β_ν and relating β_ν to the pressures as in Becker's work, in Appendix I. Also corresponds to equation 4.

σ = surface tension of the drop.

e_1 = charge on drop (assumed equal to one electron charge in this work).

R = gas constant (in dynes, if σ is in dynes).

M = molecular weight of vapor concerned.

N_0 = Avogadro's number.

ρ = density of liquid in drop

D' = dielectric constant of vapor (nearly unity always).

$S = p_n/p_\infty$ defines the supersaturation, S , for a vapor at pressure p_n .

p_μ = maximum possible value of the vapor pressure of a charged drop, which will be called the critical pressure. A drop of this size is called a critical sized drop.

r_μ = radius of a critical sized drop.

μ = number of molecules in a critical sized drop.

$S_\mu = p_\mu/p_\infty$ (see equation 3)

$N_0 p_n / \sqrt{2\pi RTM}$ is number of vapor molecules hitting one cm^2 of area per second, and if the reflection of impinging molecules on a liquid surface is negligible, we get the equation

$$(5) \quad a_0 = N_0 p_n / \sqrt{2\pi RTM}$$

Another equation of value relates the drop radius r to the number of molecules in it:

$$(6) \quad v = \frac{4\pi}{3} r^3 \rho \frac{N_0}{M}$$

The half life of an ion is defined by

$$(7) \quad \lambda = \frac{Z_m}{J} \ln 2$$

By differentiation of equation 1, one obtains the relations

$$(8) \quad r_\mu^3 = \frac{e_1^2}{4\pi D' \sigma}$$

$$(9) \quad \ln \frac{p_\mu}{p_\infty} = \frac{3}{2} \frac{M \sigma}{\rho RT} \cdot \frac{1}{r_\mu} = \frac{\sigma^{4/3}}{T} \cdot \frac{M}{\rho} \cdot \left(\frac{3}{2R}\right) \left(\frac{4\pi D'}{e^2}\right)^{1/3} = 0.0684 \left(\frac{\sigma}{T}\right)^{4/3} \left(\frac{M}{\rho}\right)$$

$$(10) \quad \mu = \frac{4\pi}{3} r_\mu^3 \cdot \frac{\rho N_0}{M} = \frac{e_1^2 \rho N_0}{3D' \sigma M}$$

Define the dimensionless measure of radius, r , as

$$(11) \quad \alpha_{\nu} = r_{\nu} / r_{\mu}$$

Then from Thomson's equation, 1,

$$(12) \quad \ln p_{\nu} / p_{\infty} = \frac{4}{3\alpha_{\nu}} \left(1 - \frac{1}{4\alpha_{\nu}^3} \right) \ln S_{\nu}$$

Now \underline{m} and \underline{n} both correspond to drops in equilibrium with the vapor at pressure p_n , so

(13)

$$\ln p_n / p_{\infty} = \frac{4}{3\alpha_m} \left(1 - \frac{1}{4\alpha_m^3} \right) \ln S_{\nu} = \frac{4}{3\alpha_n} \left(1 - \frac{1}{4\alpha_n^3} \right) \ln S_{\nu}$$

where

$$\alpha_m < 1 < \alpha_n$$

Now define a parameter

$$(14) \quad q = \alpha_m / \alpha_n, \quad 0 < q < 1$$

and then

$$(15) \quad \frac{1}{\alpha_m} \left(1 - \frac{1}{4\alpha_m^3} \right) = \frac{1}{\alpha_n} \left(1 - \frac{1}{4\alpha_n^3} \right) = \frac{q}{\alpha_m} \left(1 - \frac{q^3}{4\alpha_m^3} \right)$$

From this equation one obtains

$$(16) \quad (1 - q) - \frac{1}{4\alpha_m^3} (1 - q^4) = 0$$

which has one trivial solution at $q = 1$ and another for which

$$(17) \quad 4\alpha_m^3 = q^3 + q^2 + q + 1 = 4\alpha_n^3 q^3, \quad \alpha_m = \alpha_n q$$

which relates α_m and α_n parametrically in terms of q .

One may now conveniently proceed to determine J by methods entirely analogous to those of Becker (Appendix I of this thesis). One starts with the same type of equation for J , the rate at which drops pass from one size to the next larger.

$$(18) \quad J = a_0 Z'_j - q_{j+1} Z'_{j+1} \quad (j \geq m)$$

for which family of equations by elimination of all Z' values between m and s one obtains

$$(19) \quad Z'_m = \frac{J}{a_0} \left(\frac{1}{\beta_m} + \frac{1}{\beta_m \beta_{m+1}} + \dots + \frac{1}{\beta_m \beta_{m+1} \dots \beta_{s-1}} \right)$$

$$= \frac{J}{a_0} \sum_{i=m}^{s-1} R'_i = \frac{J}{a_0} R'$$

where R'_i is defined by

$$(20) \quad R'_i = 1/\beta_m \dots \beta_i$$

and R' is defined by equation 19

Then

$$(21) \quad \frac{1}{\beta_j} = \frac{p_j}{p_n} = e^{\frac{4}{3} \ln S_{\mu} \left\{ \left(\frac{1}{a_j} - \frac{1}{a_n} \right) - \frac{1}{4} \left(\frac{1}{a_j^4} - \frac{1}{a_n^4} \right) \right\}}$$

So that

$$(22) \quad R'_i = e^{\frac{4}{3} \ln S_{\mu} \left\{ \sum_m^i \frac{1}{a_j} - \frac{i-m}{a_n} - \frac{1}{4} \left(\sum_m^i \frac{1}{a_j^4} - \frac{i-m}{a_n^4} \right) \right\}}$$

Now note that

$$(23) \quad \nu = \frac{4\pi\rho N_0}{3M} r_{\mu}^3 a^3 = \mu a^3,$$

$$(24) \quad d\nu = 3\mu a^2 da$$

$$(25) \quad i - m = \mu (a_i^3 - a_m^3)$$

So

$$(26) \quad \sum_{\nu=m}^i \frac{1}{a_{\nu}} \approx \int_m^i \frac{1}{a} d\nu = \int_m^i \frac{1}{a} \cdot 3\mu a^2 da = \frac{3\mu}{2} (a_i^2 - a_m^2)$$

$$(27) \quad \sum_{\nu=m}^i \frac{1}{a_{\nu}^4} \approx \int_m^i \frac{1}{a^4} \cdot 3\mu a^2 da = -3\mu \left(\frac{1}{a_i} - \frac{1}{a_m} \right)$$

$$(28) \quad \frac{i - m}{a_n} - \frac{i - m}{4a_n^4} = \mu (a_i^3 - a_m^3) \frac{1}{a_n} \left(1 - \frac{1}{4a_n^3} \right)$$

$$(29) \quad R_1^i = e^{\frac{4}{3}\mu \ln S_{\mu} \left\{ \frac{3}{2} (a_i^2 - a_m^2) + \frac{3}{4} \left(\frac{1}{a_i} - \frac{1}{a_m} \right) \right.}$$

$$\left. - \frac{a_i^3 - a_m^3}{a_n} \left(1 - \frac{1}{4a_n^3} \right) \right\}$$

Now let

$$(30) \quad a = a_n (1 + \omega)$$

$$(31) \quad da = a_n d\omega,$$

$$(32) \quad d\nu = 3\mu a_n^3 (1 + \omega)^2 d\omega$$

and one gets

$$(33) \quad R' = \sum_{i=m}^{s-1} R'_i \approx \int_m^s R'_i d\omega = 3\mu\alpha_n^3 \int_m^s R'(\omega) (1+\omega)^2 d\omega$$

The parentheses $\{ \}$ of the exponent of equation 29 may now be expanded in powers of ω giving:

$$\begin{aligned} & \frac{3}{2} [\alpha_n^2(1+\omega)^2 - \alpha_m^2] + \frac{3}{4} \left[\frac{1}{\alpha_n} \cdot \frac{1}{1+\omega} - \frac{1}{\alpha_m} \right] \\ & - \frac{1}{\alpha_n} \left(1 - \frac{1}{4\alpha_n^3} \right) [\alpha_n^3 (1+\omega)^3 - \alpha_m^3] \end{aligned}$$

(34)

$$\begin{aligned} & = \frac{3}{2} (\alpha_n^2 - \alpha_m^2) + \frac{3}{4} \left(\frac{1}{\alpha_n} - \frac{1}{\alpha_m} \right) - \frac{1}{\alpha_n} \left(1 - \frac{1}{4\alpha_n^3} \right) (\alpha_n^3 - \alpha_m^3) \\ & + \omega \left[\frac{3}{2} (2\alpha_n^2) + \frac{3}{4} \left(\frac{-1}{\alpha_n} \right) - \frac{1}{\alpha_n} \left(1 - \frac{1}{4\alpha_n^3} \right) (3\alpha_n^3) \right] \\ & + \omega^2 \left[\frac{3}{2} (\alpha_n^2) + \frac{3}{4} \left(\frac{+1}{\alpha_n} \right) - \frac{1}{\alpha_n} \left(1 - \frac{1}{4\alpha_n^3} \right) (3\alpha_n^3) \right] \\ & + \omega^3 \left[\frac{3}{4} \left(\frac{-1}{\alpha_n} \right) - \frac{1}{\alpha_n} \left(1 - \frac{1}{4\alpha_n^3} \right) (\alpha_n^3) \right] \\ & + \frac{3}{4\alpha_n} (\omega^4 - \omega^5 + \omega^6 + \dots) \\ & = (\alpha_n - \alpha_m) \left(\frac{\alpha_n + \alpha_m}{2} - \frac{1}{\alpha_m \alpha_n} \right) - \omega^2 \cdot \frac{3}{2\alpha_n} (\alpha_n^3 - 1) \\ & - \omega^3 \left(\alpha_n^2 + \frac{1}{2\alpha_n} \right) + \frac{3}{4\alpha_n} (\omega^4 - \omega^5 + \dots) \end{aligned}$$

So that R' is given by the integral:

$$(35) \quad R' = 3\mu\alpha_n^3 e^{-\frac{4}{3}\mu \ln S_\mu \cdot (\alpha_n - \alpha_m) \left(\frac{\alpha_n + \alpha_m}{2} - \frac{1}{\alpha_n \alpha_m} \right)} \int_m^s (1+\omega)^2 e^{-\frac{4}{3}\mu \ln S_\mu \left[\omega^2 \frac{3(\alpha_n^3 - 1)}{2\alpha_n} + \omega^3 \frac{(\alpha_n^3 + 1/2)}{\alpha_n} + \dots \right]} d\omega$$

This integral can be approximated readily because the coefficient $\frac{4}{3}\mu \ln S_\mu$ is conveniently large, about 20 to 60 in numerical value. The integral will have two limiting values depending on the coefficients of ω^2 and ω^3 . If the expression $\alpha_n^3 - 1$ is not too small, the ω^2 term predominates, and one may make the approximation

$$(36) \quad \int_m^s (1+\omega)^2 e^{-\frac{4}{3}\mu \ln S_\mu \cdot \frac{3(\alpha_n^3 - 1)}{2\alpha_n} \omega^2} d\omega$$

$$\approx \int_{-\infty}^{+\infty} e^{-\frac{4}{3}\mu \ln S_\mu \cdot \frac{3(\alpha_n^3 - 1)}{2\alpha_n} \omega^2} d\omega$$

$$= \left[\frac{2\mu \ln S}{\pi} \cdot \frac{(\alpha_n^3 - 1)}{\alpha_n} \right]^{-\frac{1}{2}} = Q_{1/2}$$

But if $\alpha_n^3 - 1$ is rather small, the ω^3 term comes into prominence, and in the limiting case of $q = 1$, noting that $\omega_m \rightarrow 0$ simultaneously,

$$\begin{aligned}
 (37) \quad & \int_m^s (1+\omega)^2 e^{-\frac{4}{3}\mu \ln S_\mu \cdot \frac{\alpha_n^3 + 1/2}{\alpha_n} \omega^3} d\omega \\
 & \approx \int_0^\infty e^{-\frac{4}{3}\mu \ln S_\mu \cdot \frac{\alpha_n^3 + 1/2}{\alpha_n} \omega^3} d\omega \\
 & = \frac{1}{3} \Gamma\left(\frac{1}{3}\right) \cdot \left[\frac{4\mu \ln S_\mu}{3} \cdot \frac{(\alpha_n^3 + 1/2)}{\alpha_n} \right]^{-\frac{1}{3}} = Q_{1/3}
 \end{aligned}$$

The correct value of the integral term will be denoted by

$$(38) \quad Q_\omega = \int_m^s (1+\omega)^2 \cdot d\omega \cdot e^{-\frac{4}{3}\mu \ln S_\mu \left[\frac{3(\alpha_n^2 - 1)\omega^2}{2\alpha_n} + \frac{(\alpha_n^2 + 1/2)\omega^3}{\alpha_n} + \dots \right]}$$

and $Q_{1/2}$, $Q_{1/3}$ represent the two approximations, as given above. Then Q_ω can be approximated by plotting $Q_{1/2}$ and $Q_{1/3}$, and interpolating a connecting line through the region where both these terms have about the same influence. This has been done and is illustrated in Figure 29.

It is now possible to determine λ from equation 7 by substituting for Z_m its value Z_m' / F_m , and for Z_m' its value from equation 19. Then

$$(39) \quad \lambda = (R' \ln 2) / a_0 F_m$$

The surface area of a drop, F_m is

$$(40) \quad F_m = 4\pi r_m^2 = 4\pi a_m^2 \frac{r_m^2}{\mu}$$

Now substitute into equation 39 from equations 40, 35, and 5.

$$(41) \quad \lambda = \frac{\sqrt{2\pi RT M}}{N_0 p_n} \cdot \frac{\ln 2}{4\pi r_m^2 a_m^2} \cdot Q\omega \cdot \\ 3\mu a_n^3 e^{\frac{4}{3}\mu \ln S_\mu (a_n - a_m) \left(\frac{a_n + a_m}{2} - \frac{1}{a_n a_m} \right)}$$

Note the following simple relations used to put equation 41 into a more usable form (obtained from equations 2, 6, 7, 17)

$$(42) \quad \mu/r_m^2 = 4\pi r_m \rho N_0/3M = 4\pi \rho N_0 e_1^{2/3}/3M(4\pi D^3\sigma)^{1/3}$$

$$(43) \quad a_n^3/a_m^2 = a_m/q^3$$

$$(44) \quad p_n = (p_n/p_\infty) p_\infty = S p_\infty$$

$$(45) \quad \frac{a_n + a_m}{2} - \frac{1}{a_n a_m} = \frac{1-q}{q} \cdot a_m \frac{a_m(1+q)}{2q} - \frac{q}{a_m^2} \\ = \frac{(1-q)^3 (1+4q+q^2)}{8a_m q^2}$$

So that

$$(46) \quad \lambda = \left(\frac{2\pi RT}{M} \right)^{1/2} \cdot \left(\frac{e_1^2}{4\pi D' \sigma} \right)^{1/3} \cdot \frac{\ln 2}{S} \cdot \frac{\alpha_m}{q^3} \cdot Q\omega \cdot e^{-\frac{4}{3} \mu \ln S} \cdot \frac{(1-q)^3 (1+4q+q^2)}{8\alpha_m q^2}$$

or

$$(47) \quad \log_{10} \lambda = \log \left[\ln 2 (2\pi)^{1/2} (4\pi)^{-1/3} R^{1/2} \cdot e_1^{2/3} \right] \\ + \log \left[D'^{-1/3} \sigma^{-1/3} T^{1/2} M^{-1/2} p_\infty^{-1} \right] \\ + \log (\alpha_m / q^3) - \log S + \log Q\omega \\ + \frac{(1-q)^3 (1+4q+q^2)}{\alpha_m q^2} \cdot \frac{\mu \ln S}{6} \cdot \log_{10} e$$

One may obtain $\log S$ by the use of equation 13 and calculate $\log \lambda$ and $\log S$ parametrically in terms of q .

The equation for $\log_{10} \lambda$ contains several functions of the parameter q . For convenience these will be denoted by symbols:

$$(48) \quad Q(1) = \frac{4}{3\alpha_m} \left(1 - \frac{1}{4\alpha_m^3} \right)$$

$$(49) \quad Q(2) = \log (\alpha_m / q^3)$$

$$(50) \quad Q(3) = (1-q)^3 (1+4q+q^2)/q^2 a_m$$

$$(51) \quad Q(4) = \frac{1}{2} \log \left(\frac{2}{\pi} \cdot \frac{a_m^3 - q^3}{q^2 a_m} \right) = \frac{1}{2} \log \frac{a_m^3 - q^3}{q^2 a_m} - 0.098$$

$$(52) \quad Q(5) = \frac{1}{3} \log \left(\frac{4}{3} \cdot \frac{a_m^3 + q^3/2}{q^2 a_m} \right) - \log \frac{1}{3} \sqrt{\frac{1}{3}}$$

$$= \frac{1}{3} \log \frac{a_m^3 + q^3/2}{q^2 a_m} + 0.091$$

In the preceding expression for $\log \lambda$, the term $\log Q_\omega$ is obtained by plotting $Q(4) + (1/2) \log(\mu \ln S_\mu)$ and $Q(5) + (1/3) \log(\mu \ln S_\mu)$ and interpolating in the connecting region to obtain an approximation to the true value of $\log Q_\omega$. This method of approximating the true value of $\log Q_\omega$ is accurate enough for the problem at hand.

Another approximation that simplifies calculation may be made, if one notes that the difference

$$(53) \quad [Q(4) + (1/2) \log(\mu \ln S_\mu)] - [Q(5) + (1/3) \log(\mu \ln S_\mu)]$$

$$= Q(4) - Q(5) + (1/6) \log(\mu \ln S_\mu)$$

is almost entirely a function of q . This fact may be checked as follows:

$$(54) \quad (1/6) \log(\mu \ln S_\mu) = (1/6) \log \left[\frac{\sigma^{1/3}}{T} \cdot \frac{N_0}{R} \sqrt{\frac{e^4}{2D^2 \epsilon}} \right]$$

$$= (1/18) \log \sigma - (1/6) \log T + 0.56$$

For practical cases, σ lies in the range 15 to 80, for which

$$(55) \quad (1/18)\log \sigma = 0.086 \pm 0.02$$

and T lies between about 200° and 373°K ,

$$(56) \quad (1/6)\log T = 0.41 \pm 0.02$$

so that

$$(57) \quad (1/6)\log(\mu \ln S_\mu) = 0.23 \pm 0.04$$

It will be sufficient, therefore, to plot $Q(4) + 0.23$ and $Q(5)$. The smooth interpolated curve can be called $Q(6)$, and then $\log Q_w$ is given by $-[Q(6) + (1/3) \log(\mu \ln S_\mu)]$ with an accuracy of about ± 0.1 unit. Now we may define

$$(58) \quad Q(7) = Q(2) - Q(6) - 3.49$$

Having combined the term $-(1/3)\log(\mu \ln S_\mu)$ with the other logarithms expressing physical constants, one obtains

$$(59) \quad \log \lambda = -\log S - \log (D^{1/9} \sigma^{4/9} M^{1/2} \rho_0 \rho^{-1} T^{-5/6}) \\ + Q(7) + Q(3) \cdot (1/6)\log_{10} e \cdot \mu \ln S_\mu \pm 0.1$$

and

$$(60) \quad \log S = Q(1) \cdot \log_{10} e \cdot \ln S_\mu$$

The three functions, $Q(1)$, $Q(3)$, and $Q(7)$ are tabulated below in Table III. In Table IV appear the

values of physical constants and functions used in the calculations, and in Table V are the computed values of $\log \lambda$ and $\log S$. These data appear graphically in Figures 27 and 28.

TABLE III

Functions of q needed in the computation of $\log \lambda$.

q	$\log Q(1)$	$Q(1)$	$\log Q(3)$	$Q(3)$	$-Q(7) \pm 0.06$
1.0	0	1.0000	$-\infty$	0	3.64
0.98	9.9999	0.9998	5.6944	0.00005	3.62
0.90	9.9976	0.9945	7.8466	0.007	3.53
0.80	9.9893	0.9756	8.8257	0.067	3.41
0.70	9.9730	0.9397	9.4398	0.275	3.29
0.65	9.9610	0.9141	9.6880	0.488	3.22
0.60	9.9458	0.8827	9.9132	0.819	3.17
0.55	9.9269	0.8452	0.1223	1.325	3.07
0.50	9.9036	0.8010	0.3205	2.092	2.99
0.45	9.8751	0.7500	0.5123	3.253	2.90
0.40	9.8400	0.6919	0.7017	5.032	2.81
0.30	9.7439	0.5545	1.0911	12.33	2.57
0.20	9.5918	0.3907	1.5406	34.73	2.22
0.10	9.3100	0.2042	2.1974	157.5	1.62
0	$-\infty$	0.0000	$+\infty$	$+\infty$	$+\infty$

TABLE IV

Data needed in computation of $\log \lambda$.

Property	Methanol at 0°C		Water at 0°C	
	Number	Log (Number)	Number	Log (Number)
σ , dynes/cm.	23.5	1.3711	75.6	1.8785
ρ , gm/cm. ³	0.8101	9.9085	1.0	0
T°K	273.2	2.4364	273.2	2.4364
M,	32	1.5052	18	1.2553
p_{∞} atm.	0.0389	8.5899	0.0060	7.7790
μ	49.5	1.6950	33.8	1.5289
$\ln_e S_{\mu}$	0.6686	9.8252	1.441	0.1586
$\mu \ln_e S_{\mu}$	33.13	1.5202	48.7	1.6875
$\log_{10} e \cdot \ln S_{\mu}$		9.4630		9.7964
$\log_{10} e \cdot \frac{\mu}{6} \cdot \ln S_{\mu}$		0.3798		0.5471
S_{μ}	1.95	0.2904	4.22	0.6257

General Data.

Constant	Number	log (Number)
$\frac{1}{3} \sqrt{\left(\frac{1}{3}\right)}$	0.8930	9.9508 - 10
e_1 (charge)	4.77×10^{-10}	0.6785 - 10
N_0	6.06×10^{23}	23.7828
Conversion atm. to dyn/cm ²	1.0133×10^6	6.0057
R (dynes)	8.316×10^7	7.9199

TABLE V

Tabulation of Calculated Values of $\log S$ and $\log \lambda$.

q	Methanol at 0°C		Water at °C	
	logS	$\log \lambda \pm 0.1$	logS	$\log \lambda \pm 0.1$
1.00	0.2904	1.99-10	0.625	2.52-10
0.98	0.2903	2.01-10	0.625	2.74-10
0.90	0.2888	2.12-10	0.622	2.65-10
0.80	0.2833	2.39-10	0.610	3.00-10
0.70	0.2729	3.03-10	0.588	3.88-10
0.65	0.2655	3.61-10	0.572	4.72-10
0.60	0.2563	4.49-10	0.552	5.97-10
0.55	0.2454	5.79-10	0.529	7.76-10
0.50	0.2326	7.72-10	0.501	0.66
0.45	0.2178	0.60	0.469	5.88
0.40	0.2009	4.97	0.433	11.3
0.30	0.1610	22.8	0.347	37.3
0.20	0.1135	76.8	0.245	116.7
0.10	0.0593	383.1	0.128	436.
0.00	0	∞	0	∞

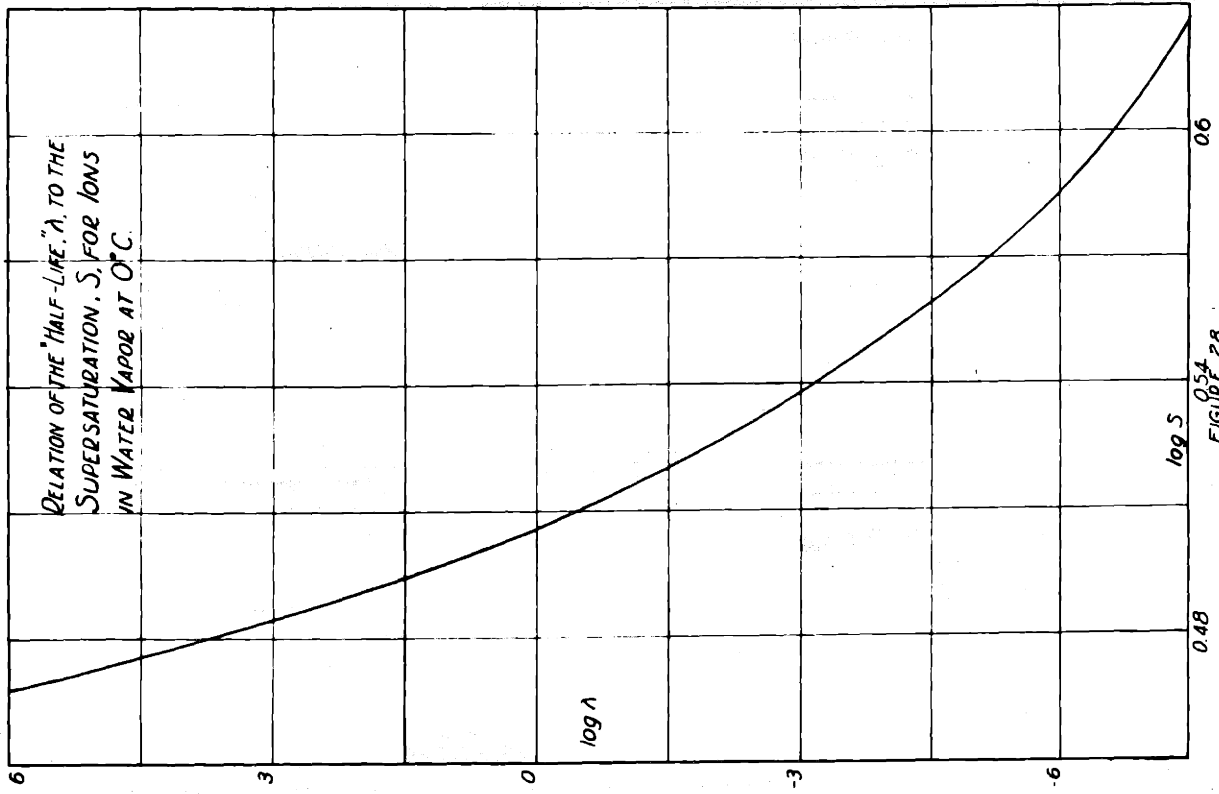


FIGURE 28

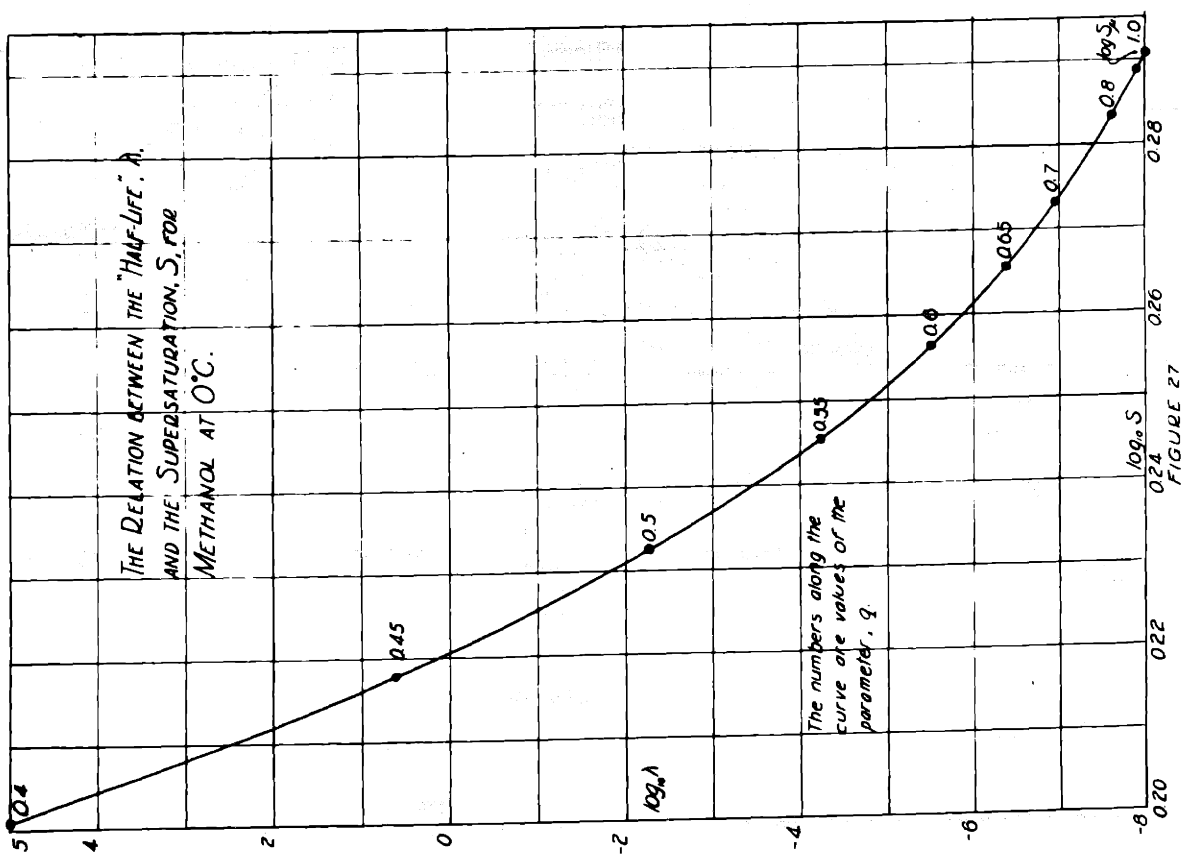


FIGURE 27

4. Interpretation of the results of the preceding section.

One may observe from Figures 27 and 28 that as the supersaturation increases it passes through a region where the half-life of ions, λ , diminishes rapidly from hours to small fractions of a second. Somewhere in this region is the minimum supersaturation for which satisfactory ion-tracks can be formed. This minimum satisfactory supersaturation will be denoted by S_k . Corresponding to it is a maximum half-life, λ_k , for which good ion-tracks appear.

In order to predict theoretically what value S_k should have, one must assume a value of λ_k . Fortunately, a wide variation in one's choice of λ_k affects the value of S_k scarcely at all, so that λ_k only need be determined to order of magnitude.

In an expansion cloud chamber, one ordinarily maintains supersaturation for 1/100 to 1/10 second, so that λ_k should have a value in this range. In a continuous cloud chamber, one might expect to see an ion-track with λ_k as large as one second, without too great a diffusion of ions away from their initial positions. As a mean value $\lambda_k = 0.1$ has been chosen, which should be approximately right for either kind of cloud chamber.

In Figure 26 are two curves drawn to show the vapor pressure in equilibrium with charged drops of water and of methanol at 0°C. In addition there are horizontal line sections drawn in and marked $\lambda_k = 0.1$. These are drawn at a vertical position such that the value of S_k

equals the value of p/p_∞ at this level on the graph. One may now note an analogy to problems in the penetration of a potential barrier. The curve is the barrier hill; the horizontal line marks that level above which a drop has a large probability of hurdling the barrier in a reasonable length of time.

5. Variation of S_k with temperature and surface tension, etc.

The equation

$$(61) \quad \log S_k = Q_k(1) \log_{10} e \cdot \ln S_\mu \\ = Q_k(1) \log_{10} e \cdot 0.064 \frac{\sigma^{4/3}}{T} \frac{M}{\rho}$$

will be sufficient to determine S_k , as a function of the various physical variables if the variation of $Q_k(1)$ with these variables can but be determined. Here $Q_k(1)$ represents that value of $Q(1)$ which gives S_k , and it in turn is determined from q_k .

The value $q = q_k$ is in turn fixed by the functions $Q(3)$ and $Q(7)$ in the expression

$$(62) \quad \log \lambda_k = -\log S_k - \log (D^{1/9} \sigma^{4/9} M^{1/2} p_\infty \bar{\rho}^{-1} T^{-5/6}) \\ + Q_k(7) + Q_k(3) \cdot \frac{\log_{10} e}{6} \mu \ln S_\mu$$

In this expression, one may observe that almost all the variation with temperature and surface tension is confined

to the expression

$$(63) \quad \mu \ln S_{\mu} = \frac{\sigma^{1/3}}{T} \frac{e^{4/3} N_0 \pi^{1/3}}{D^{2/3} R^{1/3}} = 3160 \frac{\sigma^{1/3}}{T}$$

So to a good enough approximation, the variation of q_k with temperature may be determined from

$$(64) \quad Q_k(3) = 0.0267 T/\sigma^{1/3}$$

if the values of the various terms for a typical case (water at 0°C) are substituted. Now for values of q between 0.8 and zero, $dQ(1)/dQ(3)$ is less than 0.2, and in the vicinity of $q = 0.5$ the value of $dQ(1)/dQ(3)$ is about 0.05. So the variation in $Q(1)$ with T will be negligible compared to the direct variation of T as it appears in equation for $\log S_k$. The variation of $Q(1)$ with σ is even more negligible because of the low power with which it appears in the equation for $Q(3)$.

It seems likely that for almost all physical situations, $Q_k(1)$ will lie between 0.7 and 0.8. For water and methanol it is near 0.75. If this latter value is inserted in the equation for $\log S_k$, one obtains a generally applicable equation which is, of course, only approximate,

$$(65) \quad \ln_e S_k = 0.75 \ln_e S = 0.048 \frac{\sigma^{4/3}}{T} \frac{M}{\rho}$$

6. A correlation of the theories of condensation upon ions and of spontaneous condensation.

The supersaturation at which spontaneous condensation appears has been given approximately as

$$(66) \quad \ln_e S_{cr} = 0.55 \left(\frac{\sigma}{T} \right)^{3/2} \left(\frac{M}{d} \right)$$

If the supersaturated vapor is to act as a cloud chamber in which to see ion tracks, it must allow rapid condensation on ions ($S > S_k$) but there must be negligible general fogging ($S < S_{cr}$). There must, therefore, be a finite range of supersaturation between S_k and S_{cr} in which to operate the cloud chamber. From this necessary condition one may deduce an inequality, $S_{cr} > S_k$, and therefore

$$(67) \quad \frac{\ln S_{cr}}{\ln S_k} \cong 11.6 \sigma^{1/6} / T^{1/2} > 1$$

The meaning of this last inequality is that (within the limits of applicability of the equations used in deriving it) the temperature must be less than a certain maximum value T_m if ion-tracks are to be obtainable. Furthermore, the farther T is below this limiting value T_m , the wider the operating region should become, and the better the operation of the cloud chamber. Of course, there are other important practical limiting factors to the operation of a cloud chamber. For example, the vapor density must be high enough to give a reasonable supply of vapor, but low enough

to permit a large admixture of inert gas at the available operating pressure of the apparatus. T_m is given, at least approximately, by

$$(68) \quad T_m = (11.6 \sigma_m^{1/6})^2 = 135 \sigma_m^{1/3}$$

For water T_m is above 100°C and far beyond an experimentally interesting region. For methyl alcohol T_m lies in the vicinity of 80°C by this rough calculation. In general, the lower alcohols, esters, ethers, and other organic liquids have surface tensions in the vicinity of 20 and, therefore, values of T_m of about 90°C .

The temperature limit to cloud chamber operation, T_m , probably cannot be given a sharply defined experimental interpretation. But from the analysis which precedes it, one may infer that the farther below T_m a cloud chamber can be operated, the wider the operating region becomes, and the more satisfactory the tracks will be. For the more one may raise the supersaturation above S_k without getting fog (S_{cr}), the larger the fraction of vapor present which is available for track formation.

Another limiting factor for expansion cloud chamber operation however, is that the vapor pressure of the liquid (p_∞) be large enough to give a sufficient supply of vapor in the first place.

7. Correlation of the theories of condensation with experimental data.

The theory of condensation upon ions has been worked out too recently to be compared with experiments directly. However, the analysis in section 6, which predicts a narrowing of the useful operating range of an expansion cloud chamber with rising temperature, agrees with the experimental results of Powell.³⁹

The theory of spontaneous condensation has been extensively checked with cloud chamber measurements. (See Appendix I, and references 11, 12, 14). In general there is agreement in the values of S_{cr} by theory and experiment to ten percent. The form of variation of S_{cr} with temperature and surface tension is also in generally good agreement. The most serious deviation was for methyl alcohol, for which the theoretical S_{cr} was 1.84 when it was actually 3.2. There has never been a direct measurement correlating the variation in J with S , because of experimental difficulties.

It would not be surprising if it were found that the deviations between theory and experiment were greater for the condensation upon ions than for spontaneous condensation. For in the case of ionized droplets the important sizes are smaller than in the case of uncharged drops. This makes the use of the normal fixed value of surface tension even more uncertain for charged than for uncharged drops.

In addition there may well be electric dipole layers which increase S_k for charges of one sign, decrease it for the other sign.

A new calculation to be performed is suggested by the electric dipole layer effect just mentioned. That is, it should be possible to measure the strength of the dipole layer of a charged drop by the difference in value of S_k for plus and minus charged drops. Having determined the dipole strength of the surface, a corrected value of S_{cr} for uncharged drops should be computed taking this property of the drop into account.

Experiments should be performed comparing theoretical and experimental values of S_k for various materials, and as a function of temperature and surface tension. These experiments can be performed with the expansion cloud chamber. Another experiment can probably be done with the continuous cloud chamber to measure λ versus S . For in this apparatus it is possible to keep S constant within a range of value such that the ions in a track will diffuse a small distance before condensing. Then by calculations from the measured rate of diffusion and distance diffused, one can determine the value of λ . The mean distance diffused can be measured by the effective "thickness" of the track, and the rate of diffusion calculated from data on ion mobilities in electric fields. Perhaps the continuous cloud chamber would also permit a direct measurement of the value of the spontaneous condensation rate, J , after which J can be compared with S .

8. Application of the analysis of condensation phenomena to the continuous cloud chamber.

There is a greater density of spontaneously formed drops in a continuous cloud chamber than in an expansion cloud chamber. That this should be so may be understood if one considers that droplets form at a uniform rate for a given supersaturation, in any fixed volume of large enough size. In an expansion cloud chamber drops form and collect only for the short time the chamber is supersaturated, but in a continuous cloud chamber they collect at the same rate for a much longer time. In fact, they accumulate until an equilibrium concentration is reached at which as many drops fall out of the region as are produced in it. This equilibrium will depend on the rate of formation of drops, J , and on their rate of fall, which in turn depends on their size. The rate of fall is determined by Stokes' law, the growth in size by the rate of diffusion of vapor into the vicinity of the drop.

Then the total concentration, N' of drops in a given volume of the continuous chamber is the sum of the equilibrium concentration of those formed in it and the number passing through, coming from above.

The next step to be taken to extend the analysis of the diffusion cloud chamber should be to calculate this concentration of drops resulting from the spontaneous condensation, and to determine how much this condensation de-

creases the supersaturation below that calculated in Chapter II.

When the calculations have been made, the theoretical droplet concentration, $N'(x)$ should be compared with direct counts of the drop concentration in the chamber. If the actual drop concentration turns out to be much greater than that predicted, it will then be advisable to make a careful search for molecular aggregates. These aggregates may be introduced into the vapor in other ways than the purely kinetic and uncontrollable one described in Appendix I on the basis of which these calculations shall be made.

A summary of all the factors entering into the complete analysis of the diffusion cloud chamber is given in Table VI. The factors especially considered in this section are marked with asterisks. They are the most important factors which have not been given quantitative treatment in this thesis.

TABLE VI

A Classification of the Principal Variables Entering into the Complete Analysis of Diffusion Cloud Chamber Operation and the Associated Phenomena.

A. Independent Variables

1. x = position within chamber, height above floor.
2. h = total depth of chamber.
3. Horizontal dimensions of chamber.
4. T_0 = floor temperature
5. T_1 = roof temperature
6. P_0 = total pressure in chamber
7. c_1 = flux of vapor
8. Vapor composition
9. Gas composition
- *10. I = concentration of diffusely distributed ions.
- *11. G = concentration of aggregates on which condensation occurs.

B. The Normal Intensive Properties of Materials; Dependent Variables.

1. p_{1s} = saturation vapor pressure.
2. H = enthalpy of vapor.
3. σ = surface tension of condensed vapor, or liquid.
4. ρ = density of liquid.
5. M_1 = molecular weight of vapor.
6. M_2 = molecular weight of liquid.
7. k = diffusivity of gas into vapor and vice versa.

8. K = heat conductivity of gas vapor mixture.
 9. η = viscosity of gas vapor mixture.
 10. The equation of state for the vapor and gas.
- C. The primary dependent variables to be analysed.
1. $T(x)$ = temperature distribution.
 2. $P_1(x)$ = vapor distribution.
 3. $P_2(x)$ = gas distribution.
 4. f = energy flux through chamber.
- D. The Phenomena to be Predicted and Compared with Experimental Results. Dependent Variables.
1. $S(x)$ = actual supersaturation attained.
 2. J = Rate of spontaneous condensation of type described by Becker.
 3. λ = half-life of ions.
 4. S_{cr} = supersaturation for which $J = 1$.
 5. S_k = supersaturation for which $\lambda = 0.1$.
 - *6. J' = rate of non-ionic condensation, in drops per cm^2 . per sec. due to aggregates G.
 - *7. N' = drop concentration per cm^3 .
 - *8. $-\Delta p_1$ = decrease in vapor pressure at a given part of chamber resulting from condensation on drops N' .

* The asterisk marks variables whose quantitative estimation remains to be accomplished.

CHAPTER V - THE USES OF A CONTINUOUS CLOUD CHAMBER.

1. Cosmic Ray Observation.

Cosmic ray tracks inevitably appear in any cloud chamber continuously sensitive to condensation upon ions, so that observations upon cosmic rays will be the most obvious application of this type of apparatus. A particular advantage of the continuous cloud chamber for such observations is that it should give a correct statistical weight to the frequency of occurrence of each type of phenomenon recorded. The ion-sensitive region is highly impartial in its action, showing every ion-track that passes through it, so long as there are not too many in a short time interval. The electrical methods are not one hundred percent efficient "counters", involve systematic errors, and give less detailed information upon individual rays that pass through them than the cloud chamber.

2. Weak radioactivity.

The continuous cloud chamber will be useful for the study of very small quantities of beta ray emitting materials. It will eliminate the uncertainty of the Geiger-Müller counter method which cannot distinguish cosmic rays from beta rays. For the cloud chamber allows one to distinguish whether the track comes directly from the source in the chamber, or whether it is only a cosmic ray track in the vicinity of the source.

3. A comparison of the advantages of the continuous cloud chamber with those of other apparatus.

The continuous cloud chamber will share with the expansion cloud chamber the ability to give great detail of information upon an individual ionizing ray. It will share with the electrical methods of studying ionizing rays the ability to record phenomena at random intervals of time. It will have the disadvantage of requiring great amounts of detailed visual observations and measurements, when used for quantitative purposes. For qualitative purposes, it should give quick estimations of the nature of very small radioactive samples. At a glance one should be able to observe alpha, beta, and gamma rays, and get estimates of their energies.

4. Experiments on the kinetics of condensation, and future development of the cloud chamber itself.

In the analysis of the operation of the continuous cloud chamber it has been necessary to study kinetic phenomena of condensation. It should be pointed out that the cloud chamber may be used as a tool for further researches in kinetics as well as for nuclear physics research.

APPENDIX I.

The spontaneous condensation of supersaturated vapor and related phenomena.

Farkas, Volmer, Becker* and others have developed a theory of the condensation of supersaturated vapors based on kinetic theory considerations. This theory is of use in an analysis of the continuous cloud chamber to explain the continuous formation of drops it exhibits. The theory will be presented briefly with some comments upon its validity:

Consider a large chamber containing a supersaturated vapor. The vapor pressure is held constant by adding individual molecules. The droplets of liquid are removed after reaching a large size containing some large number of molecules, s . These drops are counted as they are removed, and the number counted per cubic centimeter per second will be called J , the aggregate-creating-velocity. In this manner one creates a steady state distribution of droplets containing various numbers of molecules, and J is a constant flux of droplets flowing through all sizes from single molecules to the maximum, s .

It is assumed that a droplet containing any number of molecules, \mathcal{N} , can be considered as spherical with a radius r , a surface area F . Then

* See references 9-14.

$$(1) \quad \mathcal{V} = 4\pi r^3 \rho / 3m$$

$$(2) \quad F_{\mathcal{V}} = 4\pi r^2 \quad \text{where}$$

ρ is the density of the liquid drop, m the mass of one molecule. It is further assumed that one may use the thermodynamic relation

$$(3) \quad d\mathcal{V} \cdot k T \ln p_{\mathcal{V}}/p_{\infty} = \sigma dF_{\mathcal{V}}$$

between the increase in number of molecules $d\mathcal{V}$ associated with an area increase $dF_{\mathcal{V}}$, where σ is the surface tension of the drop, $p_{\mathcal{V}}$ the equilibrium vapor pressure over this drop, and p_{∞} the vapor pressure over a flat surface of liquid.

The assumptions just made can later be shown to be sufficiently accurate to allow valid calculations over a considerable range of conditions experimentally attainable. But before proceeding, one assumption tacitly assumed by preceding authors should be emphasized. This assumption is that the droplets are in thermodynamic equilibrium with the surrounding vapor, as indicated when equation (3) was used. It may be seen, on inquiring into the mechanism by which equilibrium is to be maintained, that in a pure vapor with a large latent heat of condensation, there is no adequate means of maintaining thermal equilibrium, and droplets will be hotter than the surrounding vapor.* In spite of this circumstance, the theory here presented agrees with the facts for experiments in a Wilson

* See page for further discussion.

expansion cloud chamber. The way out of the dilemma is pointed by the fact that in this apparatus the vapor molecules are mixed with upwards of twenty times as many inert gas molecules, which by their collisions maintain thermal equilibrium quite closely. One may well expect the theory in its present form to break down in the case of expansion of a pure vapor, such as that of steam in the throat of a nozzle. This latter case will be returned to below.

Proceeding with the present analysis, from equations (2) and (3) one may derive the well-known expression for the vapor pressure of a small drop.

$$(4) \quad \ln p_r/p_\infty = 2\sigma M/\rho RT$$

Let:

(5) $Z_{z'}$ = number of droplets containing z' molecules in the stationary distribution.

(6) $q_{z'} dt$ = probability that one molecule will be lost from 1 cm.² of surface area of a drop of size z' in time dt .

(7) $a_0 dt$ = probability that one molecule will be added to 1 cm.² of surface area of a drop in time dt .

(8) $Z_{z'}^1 = F_{z'} Z_{z'}$ = total surface area of drops containing z' molecules.

$$(9) \quad \beta_{z'} = a_0/q_{z'}$$

Then the stream J becomes

$$(10) \quad J = a_0 Z_{z'-1}^1 - q_{z'} Z_{z'}^1$$

To proceed further let the actual pressure of the super-

saturated vapor be taken as p_n , and make the reasonable assumption (which apparently has not been rigorously justified) that

$$(11) \quad \frac{a_0}{q_{\nu'}} = \frac{p_n}{p_{\nu'}} = \beta_{\nu'}$$

From (10) and (11) one may obtain the family of equations

$$(12) \quad \begin{aligned} Z'_2 &= Z'_1 \beta_2 - J \beta_2 / a_0 \\ Z'_3 &= Z'_2 \beta_3 - J \beta_3 / a_0 \\ &\vdots \\ Z'_{\nu+1} &= Z'_{\nu} \beta_{\nu+1} - J \beta_{\nu+1} / a_0 \\ &\vdots \\ Z'_s &= Z'_{s-1} \beta_s - J \beta_s / a_0 \end{aligned}$$

In this set of equations one can eliminate all intermediate values of Z'_j , between Z'_1 and Z'_s . Furthermore, $a_0 Z'_1$ can be interpreted as double the total number of collisions of vapor molecules with each other, and Z'_s is zero because of the initial condition that drops containing s molecules disappear. Thus one obtains

$$(13) \quad a_0 Z'_1 = J \left(1 + \frac{1}{\beta_2} + \frac{1}{\beta_2 \beta_3} + \dots + \frac{1}{\beta_2 \beta_3 \dots \beta_{\nu'}} + \dots + \frac{1}{\beta_2 \beta_3 \dots \beta_{s-1}} \right)$$

From equations (4) and (11),

$$(14) \quad \frac{1}{\beta_{\nu}} = e^{\frac{2\sigma M}{\rho RT} \left(\frac{1}{r_{\nu}} - \frac{1}{r_n} \right)} = e^{\alpha \left(\frac{1}{r_{\nu}} - \frac{1}{r_n} \right)} \text{ where } \alpha = \frac{2\sigma M}{\rho RT}$$

The n in equation (14) and the following analysis represents that value of ν , the number of molecules in a drop, for which the vapor pressure of the drop equals the vapor pressure p_n existing in the vapor. Such a drop is in unstable equilibrium with the vapor, and is usually called the critical sized droplet. It has equal probability of growing larger or smaller.

Let

$$(15) \quad R_i' = \frac{i}{\beta_2 \beta_3 \cdots \beta_i}$$

and

$$(16) \quad R' = \sum_{i=1}^s R_i'$$

so that equation (13) becomes

$$(17) \quad a_0 Z_i' = J R' = J \sum_{i=1}^s R_i'$$

From (14) and (15),

$$(18) \quad R_i' = e^{\alpha \left(\frac{1}{r_2} + \frac{1}{r_3} + \cdots + \frac{1}{r_i} - \frac{i-1}{r_n} \right)}$$

$$= e^{\alpha \left(\sum_{\nu=2}^i \frac{1}{r_{\nu}} - \frac{i-1}{r_n} \right)}$$

Let

$$(19) \quad x_{\nu} = r_{\nu} / r_n = (\nu/n)^{1/3} \text{ or approximately}$$

$$\nu = n x^3, \quad d\nu = 3n x^2 dx$$

and

$$(19a) \quad A' = \alpha n / 2r_n = F_n / 3kT = \frac{16\pi L}{3} \left(\frac{\sigma}{RT}\right)^3 \left(\frac{M}{\rho \ln p_n/p_\infty}\right)^2$$

Make the approximation

$$(20) \quad \sum_{\nu=2}^i \frac{1}{r_\nu} \approx \frac{1}{r_n} \int_{x_1}^{x_i} \frac{d\nu}{x_\nu} = \frac{3n}{r_n} \int_{x_1}^{x_i} x dx = \frac{3n}{2r_n} (x_i^2 - x_1^2)$$

Also

$$(21) \quad i - 1 = n (x_i^3 - x_1^3)$$

Then

$$(22) \quad R_i' = e^{A' [(3x_i^2 - 2x_i^3) - (3x_1^2 - 2x_1^3)]}$$

Make another approximation,

$$(23) \quad R' \approx \int_1^s R_\nu' d\nu = 3ne^{-A'(3x_1^2 - 2x_1^3)} \int_{x_1}^{x_s} e^{A'(3x^2 - 2x^3)} x^2 dx.$$

In the accompanying figure, Figure 31., taken from Becker's work, it is shown that the integrand

$$e^{A'(3x^2 - 2x^3)}$$

possesses a steep maximum near $x = 1$ in at least some cases such as the one he has chosen. Then let $x = 1 + \xi$ and

$$(24) \quad R' = 3ne^{+A'(1-3x_1^2-2x_1^3)} \int_{x_1-1}^{x_s-1} e^{-A'(3\xi^2+2\xi^3)} (1+\xi)^2 d\xi$$

$$\approx 3ne^{A'} \int_{-\infty}^{+\infty} e^{-3A'\xi^2} d\xi = 3n \sqrt{\frac{\pi}{3A'}} e^{A'}$$

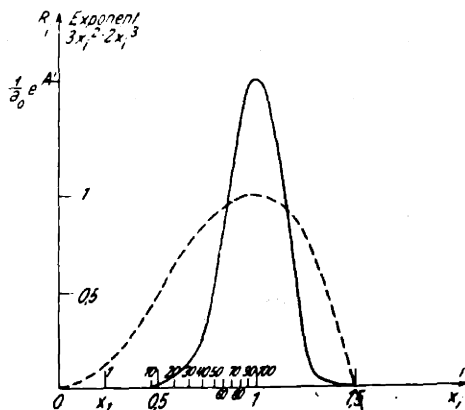


Fig. 1. Die Abhängigkeit des Widerstandes R_i vom relativen Tröpfchenradius x_i .
 (Für den Fall $A' = 10$ und $n = 100$)
 - - - : Verlauf des Exponenten $3x_i^2 - 2x_i^3$

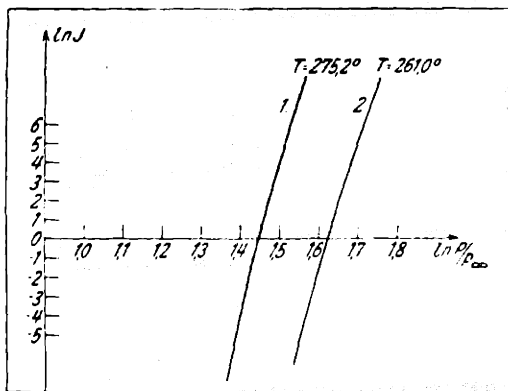


Fig. 2. $\ln J$ als Funktion von $x = \ln \frac{P}{P_\infty}$ für zwei Temperaturen, berechnet für Wasser nach Gl. (13a)

	T	σ [dyn/cm]	x		$\frac{P_n}{P_\infty}$
			berechnet	berechnet	gemessen
Kurve 1 . .	275,2	75,23	1,46	4,30	4,21
Kurve 2 . .	261,0	77,28	1,64	5,14	5,03

A' ergibt sich zu 55 bis 56.

From equations 24 and 17

$$(25) \quad J = \frac{a_0 Z_1'}{n} \sqrt{\frac{A'}{3\pi}} e^{-A'}$$

From (25), by substituting the values of all terms, one may obtain the useable form:

$$(25a) \quad \ln J = \ln[\pi^{-3/2} 8^{-1/2} R T_0 N_0^{1/2}] + \ln[M^{-3/2} L_0^{-1} p_\infty^2 \rho \sigma^{-3/2}] \\ + 2 \ln X + 2X - \frac{16 \pi N_0}{3R^3} \left(\frac{M}{\rho}\right)^2 \left(\frac{\sigma}{T}\right)^3 \frac{1}{X^2}$$

$$(25b) \quad \ln J = 49 + \ln M^{-3/2} L_0^{-1} p_\infty^2 \rho \sigma^{-3/2} \\ + 2 \ln X + 2X - 17.7 \left(\frac{\sigma}{T}\right)^3 \left(\frac{M}{\rho}\right)^2 \frac{1}{X^2}$$

In these equations

$$X = \ln S = \ln p_n/p_\infty$$

L_0 = mean free path of vapor at 0°C , 1 atm.

N_0 = Avogadro's number

and other terms have meanings already defined.

In Figure 30 taken from Becker's work, it is shown graphically how fast J increases with the supersaturation. In an expansion cloud chamber, this can be interpreted to mean that as the expansion ratio is increased, and the supersaturation is correspondingly increased, very suddenly such an expansion will be attained that an appreciable number of drops will be produced in the chamber in a time of the order of 1/100 second, and beyond this expansion the cloud will

rapidly become denser. There is of course some uncertainty in correlating a value of J with what one decides visually to call the "critical" expansion for which visible rain is produced. However, changing the chosen J from 1 to 1000 does not seriously affect the correlation of computed and experimental "critical" expansions and supersaturations.

Having chosen the "critical" J as $\ln J = 1$,

$$(26) \quad X_{cr} = \ln_e S_{cr} \\ = \left(\frac{\sigma}{T} \right)^{3/2} \left(\frac{M}{\rho} \right) \left(\frac{17.7}{48 + \ln \frac{p_{\infty}^2 \rho}{M^{3/2} L_0 \sigma^{3/2}} + 2 \ln X_{cr} + 2X_{cr}} \right)^{1/2}$$

Over a considerable range of variation of the physical conditions, one may use the more approximate relation derived from (26)

$$(26a) \quad X_{cr} = \ln_e S_{cr} \approx k \left(\frac{\sigma}{T} \right)^{3/2} \left(\frac{M}{\rho} \right)$$

where k generally stays within the range of 0.63 to 0.45. Formula (26a) will allow a rapid estimation of X_{cr} from which with (26) a more accurate value can be found.

The results are notably insensitive to error in collision frequency, $a_0 Z_1'$ (i.e., to free path L_0) because of the way this variable enters into the equation. The only dubious quantity of great importance is the surface tension, σ . Fortunately, if the critical sized droplet is large enough so that the normal value of σ for a flat surface applies, any change in σ at smaller sizes is rather unimportant, because

most of the value of the integral for R' comes from drop-lets near to the critical size.

One may derive from equations 25 to 26a a form of relation between J and S which shows clearly how fast J increases as S increases beyond S_{cr} . Let J_{cr} be an arbitrary value of J chosen as the critical value. Then substituting J_{cr} for J and $X_{cr} = \ln S_{cr}$ for X in equation 25a, and subtracting this new equation from 25a,

$$(27) \quad \ln J/J_{cr} = 2 \ln X/X_{cr} + 2(X-X_{cr}) - \frac{16\pi N_0}{3R^3} \left(\frac{M}{\rho}\right)^2 \left(\frac{\sigma}{T}\right)^3 \left(\frac{1}{X^2} - \frac{1}{X_{cr}^2}\right)$$

Now X and X_{cr} have nearly the same values, so approximately

$$(27a) \quad \ln J/J_{cr} \cong 2 \frac{X-X_{cr}}{X_{cr}} + 2(X-X_{cr}) + \frac{16\pi N_0}{R^3} \left(\frac{M}{\rho}\right)^2 \left(\frac{\sigma}{T}\right)^3 \frac{(2X_{cr})(X-X_{cr})}{X_{cr}^4} = 2(X-X_{cr}) \left\{ 1 + \frac{1}{X_{cr}} (1 + 49 + 2 \ln X_{cr} + 2X_{cr} - \ln J_{cr} + \ln \frac{p_{\infty}^2 \rho}{M^{3/2} L_0 \sigma^{3/2}}) \right\}$$

$$(27b) \quad \ln (J/J_{cr}) \cong 2 \left\{ 3 + \frac{1}{X_{cr}} (50 + \ln \frac{p_{\infty}^2 \rho}{M^{3/2} L_0 \sigma^{3/2}}) \right\} \ln (S/S_{cr})$$

X_{cr} usually lies in the range of 0.5 to 2.0, and

$\ln \frac{p_{\infty}^2 \rho}{M^{3/2} L_0 \sigma^{3/2}}$ is considerably less than 50. So the coefficient

of $\ln S/S_{cr}$ lies between 50 and 250 for most conditions, or the exponent E in

$$(28) \quad (J/J_{cr}) = (S/S_{cr})^E \quad (50 < E < 250)$$

lies between 50 and 250. This exponent is in every case a very large number.

FIGURE 32.

Some forms of cloud chambers used by C. T. R. Wilson previous to 1900. Lower two diagrams: chambers used to study effects of ions from x-rays. Upper diagrams: earlier apparatus. Left, a very simple type for use with water. Right, a type in which any of several vapors and liquids may be used, and at various pressures.

Fig. 1.

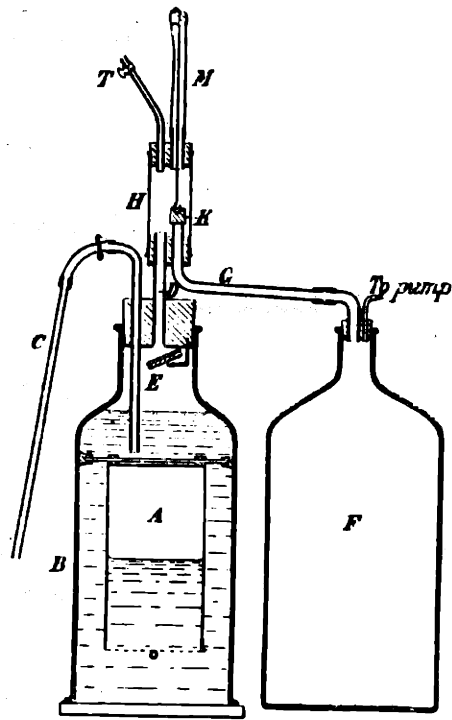


Fig. 2.

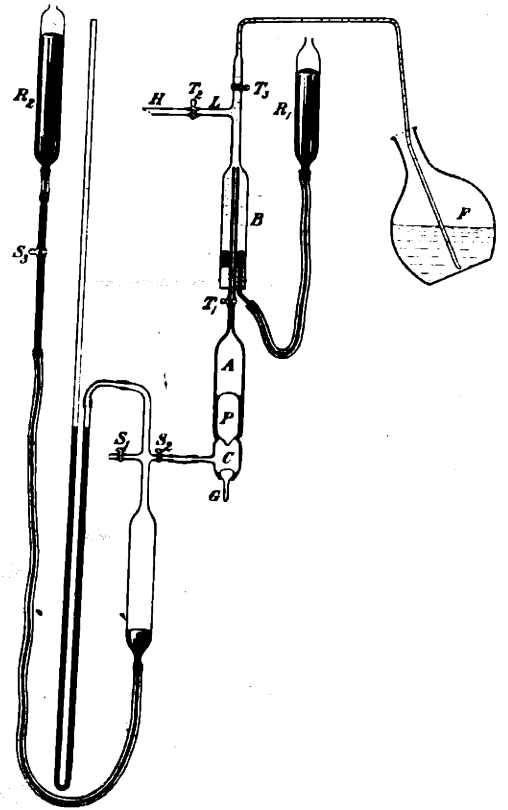


Fig. 2.

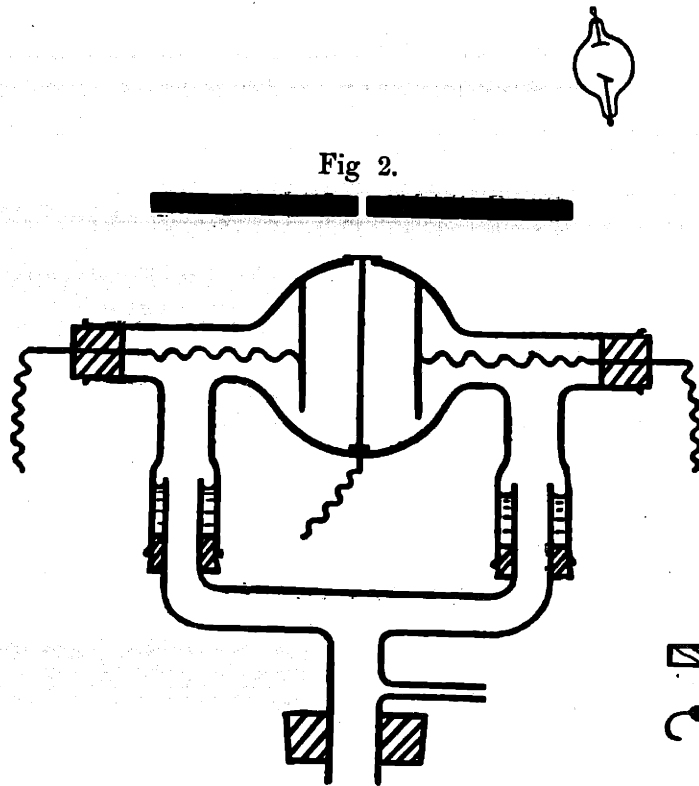


Fig. 1.

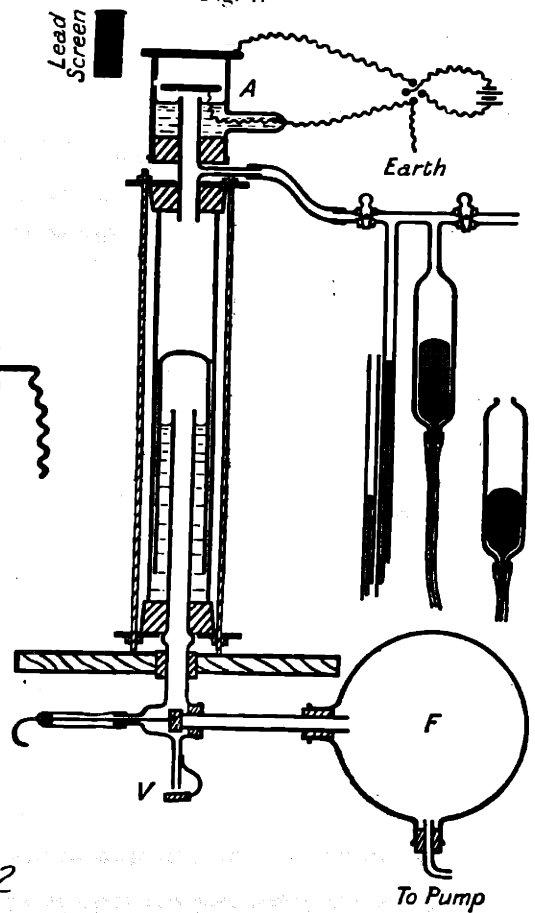


FIGURE 32

ACKNOWLEDGMENTS

I should like to express my deep appreciation to Professor Joseph C. Boyce for his guidance, encouragement, and personal interest in the work during the entire course of development of the diffusion cloud chamber. Also, the original conception of the apparatus was a result of discussions in which he pointed out the valuable uses that a continuously sensitive cloud chamber would have.

Information was received from Professor L. G. Hoxton of the University of Virginia concerning his prior experiments upon the development of a continuous cloud chamber. I wish also to record the independent and approximately contemporary conception of the principle of the diffusion cloud chamber by both Carl D. Anderson at the California Institute of Technology and Richard E. Vollrath at the University of Southern California.

During the early development of this apparatus, suggestions and encouragement were offered by Professors Robley D. Evans, Ralph D. Bennett, J.C. Street, F.C. Stevenson, and many others too numerous to mention.

Professors John C. Slater and Joseph H. Keenan made valuable criticisms of this thesis, especially on the analysis of the cloud chamber in Chapter II.

Mr. Walter Kallenbach of the Physics Department Shop gave valuable cooperation during the design and con-

struction of all apparatus. Mr. Neil Dall of the shop staff contributed innumerable suggestions on construction technique, and his careful, expert work entered in an important way into the successful operation of the original diffusion cloud chamber.

Various manufacturing concerns made gifts of materials, and persons connected with these and other concerns contributed worthwhile information. Among the concerns are the following: The National Carbon Co. (Mr. D. B. Joy and A. B. West), Röhm and Haas Co., United States Gypsum Co., Tubular Rivet and Stud Co., DuPont Viscoloid Co., Jenkins Brothers Co., Kinetic Chemicals, Inc., (Mr. R. J. Thomson).

To all considered in these acknowledgments, and to many others not mentioned, I express gratitude and appreciation, and thank them for every aid in the carrying on of my research and the writing of this thesis.

Alexander Langsdorf, Jr.
Alexander Langsdorf, Jr.

Massachusetts Institute of Technology

December 9, 1937.

BIOGRAPHY.

Alexander S. Langsdorf, Jr. Born in Saint Louis, Missouri, May 30, 1912. Son of Alexander Suss and Elsie Hirsch Langsdorf.

Graduated, Soldan High School in Saint Louis, 1929. Student, Washington University (St. Louis) 1929-1933; A.B. degree 1932. Chemistry major. Summer courses, University of Colorado, 1930, Columbia University, 1931. Graduate student, Massachusetts Institute of Technology, 1933-1937.

Honors: The National Honor Society (High School, 1929), Phi Eta Sigma (Freshman honor society, 1930), Pi Mu Epsilon (Mathematical Society, 1931), Phi Beta Kappa (1932), Sigma Xi (Associate membership, 1933).

Publications: "Optical Rotation of Unpolarized Light." with L. A. DuBridge, J.O.S.A. 24, 1 (1934).

Industrial experience: assistant in research laboratories, Monsanto Chemical Co., summers of 1934 and 1936.

Teaching fellowship, Massachusetts Institute of Technology 1936-37.

BIBLIOGRAPHY.

Continuous cloud chambers and nearly continuous cloud chambers.

1. L. G. Hoxton. Proceedings of the Virginia Academy of Science, 1933-34, Abstract 9, page 23.
"A Continuously Operating Cloud Chamber."
(Secretary's office: 12th and Clay Streets, Richmond, Va.)
2. R. E. Vollrath. R.S.I. 7, 409 (1936).
"A Continuously Active Cloud Chamber."
This is a chemically activated system.
3. H. Brinkman. Proc. Roy. Acad. Amsterdam 39, 1185-86 (1936). In English.
"A Continuously Acting Cloud Chamber."
This is an expansion chamber operating twenty times per second.
4. J. A. Beardon. Phys. Rev. 45, 758A (1934).
"A Wilson Chamber with an increased time of sensitivity."
5. T. Shimizu. Proc. Roy. Soc. 99, 425 (1921).

Expansion cloud chambers.

6. C. T. R. Wilson.
This is an incomplete list of his more important publications on cloud chambers.
 - (a) Proc. Camb. Phil. Soc. 8, 306 (1895).
 - (b) Proc. Camb. Phil. Soc. 21, 405 (1922).
 - (c) Proc. Roy. Soc. A59, 338 (1896).
 - (d) Proc. Roy. Soc. A86, 360 (1912).
 - (e) Proc. Roy. Soc. A85, 285 (1911).
 - (f) Proc. Roy. Soc. A87, 277 (1912).
 - (g) Proc. Roy. Soc. A104, 1, 192 (1923).

- (h) Phil. Trans. Roy. Soc. A189, 265-307 (1897).
- (i) Phil. Trans. Roy. Soc. A192, 403 (1899).
- (j) Phil. Trans. Roy. Soc. A193, 289 (1899).
- (k) Phil. Mag. 7, 681-690 (1904).
- (l) Phil. Mag. 23, 499 (1912).
- (m) Proc. Roy. Soc. A142, 88 (1933).
- (n) Proc. Roy. Soc. A148, 523 (1935).

7. A complete bibliography on expansion cloud chamber theory, design, and use would be of great length and of no direct bearing on this thesis. A list of names of some persons who have published articles on the expansion cloud chamber is given here, as a brief key to the literature:

Anderson, Carl	Locher, G. L.
Barus, C.	Loughridge, D.
Beardon, J. A.	Mott-Smith, L. M.
Blackett, P. M. S.	Philipp, K.
Brode, R.	Powell, C. F.
Crane, H. R.	Richardson, H. O. W.
Curtiss, L. F.	Shimizu, T.
Dahl, O.	Skobelzyn
Feather, N.	Snoddy, L. B.
Freitag, N.	Street, J. C.
Herzog, G.	Thomson, J. J.
Johot, F.	Wilson, C. T. R.
Kurie, F. N. D.	Wilson, J. G.

See also 39.

Physical phenomena of supersaturation and theories concerning condensation of supersaturated vapors.

8. Owen, G. and Hughes, A. L.
- (a) Phil. Mag. 14, 528-538 (1907).
"Condensation nuclei produced by cooling gases to low temperatures."
 - (b) Phil. Mag. 15, 746-761 (1908).
"On molecular aggregations produced in gases by sudden cooling."

9. M. Volmer and A. Weber. Zeits. f. Phys. Chem. (Hereafter abbreviated Z. f. P. C.) 119A, 277 (1926). Droplet formation in the supersaturated state.
10. L. Farkas. Z. f. P. C. 125A, 236 (1927). Velocity of droplet formation in supersaturated vapors.
11. M. Volmer and H. Flood. Z. f. P. C. 170A, 273 (1934). Droplet growth in vapors.
12. L. Flood. Z. f. P. C. 170A, 286 (1934). Growth of droplets in supersaturated mixtures of ethyl alcohol and water vapors.
13. H. Flood and L. Tronstad. Z. f. P. C. 175A, 347-353 (1936). Surface tension of heavy water determined by droplet growth in its supersaturated vapor.
14. R. Becker and W. Döring. Ann. d. Phys. 24, 719-752 (1935). Kinetic theory analysis of droplet formation in supersaturated vapors. (A most important article. Also refers to other papers.)
15. E. Hückel. Physik. Zeits. 37, 137 (1936). A correction to Thomson's Theory of condensation on ions.
16. J. J. Thomson.
 - (a) Conduction of Electricity in Gases, Third Edition, pp. 325-334.
 - (b) Applications of Dynamics to Physics and Chemistry (1890), pp. 162-175.
On Theory of Condensation on ions, etc.
17. Frumkin. Acta Physicochim. U. S. S. R. 3, 783-790 (1935). A correction to Kelvin's equation for very small drops.
18. Gorbalschew. Kolloid Z. S. 73, 263-267 (1935). A critical treatment of Kelvin's equation.
19. (a) J. L. Shereshefsky and S. Steckler. J. of Chem. Phys. 4, 108 (1906).
(b) D. J. Woodland and E. Mack, Jr. J. Amer. Chem. Soc. 55, 3149 (1933).
Studies of drops evaporating in a Millikan oil drop type apparatus.

20. Sir W. Thomson (Kelvin) Proc. Roy. Soc. Edinburgh 7, 63 (1870).

References on diffusion and heat transfer in gases, etc.

21. G. Ackermann. Forschungsheft 8B, No. 382, pp 1-16 (1937).
Simultaneous heat and material transfer with large temperature and partial pressure differences.
22. K. Kuusinen. Ann. d. Phys. 24, 445, 447 (1935).
Definition of diffusion constants. (An addition to and correction of earlier work).
23. P. D. Crout. Journal of Math. and Physics 15, 1, 124 (1936).
Applications of kinetic theory to problems of evaporation and sublimation.
24. E. R. Gilliland. Ind. and Eng. Chem. 26, 681 (1936).
Diffusion Coefficients in Gaseous Systems. (33 references).
25. J. Jeans. Dynamical Theory of Gases. (1921).
26. L. B. Loeb. Kinetic Theory of Gases. (1934).
27. I. Amdur. Journal of Chem. Phys. 4, 339 (1936).
Viscosity and Diffusion Coefficients of Atomic Hydrogen and Deuterium.

Studies of condensation in steam jets and steam atmospheres.

28. A. Stodola. Steam and Gas Turbines (McGraw Hill 1927). Translated from 6th German edition by L. C. Loewenstein. Vol. II, pp. 1034-1075.
29. J. I. Yellott. Trans. Amer. Soc. Mech. Eng. 56, 411-430 (1934).
An optical method of studying condensation of steam in orifices. Includes a good bibliography of 61 articles.

30. J. T. Rettaliata. Trans. A. S. M. E. 58, 599-605 (1936).
Expansion of steam in rough nozzles.
31. J. I. Yellott and C. K. Holland. Trans. A. S. M. E. 59, 171-185 (1937).
Condensation in orifices. Photographs. Bibliography of 18 articles.
32. C. Barus. Phil. Mag. 38, 19 (1894).
33. R. von Helmholtz. Ann. d. Phys. 32, 1 (1888).
34. J. Aitken. Trans. Roy. Soc. Edin. 16, 14 (1888).

Physical Properties of methanol, carbon dioxide, water, etc.

35. Fiock, Ginnings, and Holton. Bureau of Standards Journal of Research 6, 881-900 (1931).
Data on methanol include vapor pressure, specific volume, heat content of liquid and saturated vapor, and latent heat of vaporization.
36. Landolt, Bärnstein, Roth, Scheel. Physikalisch-Chemische Tabellen.
37. P. W. Bridgman.
A Condensed Collection of Thermodynamic Formulas. (Harvard University Press, 1925).
38. Beilstein's Handbuch der Organischen Chemie.
39. C. F. Powell. Proc. Roy. Soc. 119, 553-577 (1928).
Condensation Phenomena at Different Temperatures.

Corrections and Changes in Thesis

Alexander Langsdorf, Jr.

M. I. T., 1937

Appended February 4, 1938

Note that the page numbering of these corrections may be in error by as much as two pages because of different page numbering in different copies of the thesis. The context is sufficient to locate where the correction should be.

Page

- 8 Facing page 9, 3rd line from bottom. After "See" put "Proc. Camb. Phil. Soc. 21, 408 (1922).
- 9 Figure 2. Top photograph from PRS, 87A, 292 (1912); Center photograph from PRS, 104A, 212 (1923); Bottom left from PRS, 87A, 292 (1912); Bottom center and right, Proc. Camb. Phil. Soc. 21, 408 (1922).
- 22 Fifth line from bottom put T_0 in place of T_2 .
- 23 Line 18, first word. "of" in place of "for".
- 27 Line 22, end of section 2. Put "that this factor may safely be neglected" in place of "...that this factor is safely to be neglected."
- 44 Line 10. Put "from" in place of "for" so that heading reads "Deviations of the properties of the vapor from those of a perfect gas."
- 32 Line 14. Scratch the word "heat" in the expression "the total energy flux is always greater than the convective heat flux."
- 38 Line 5. The expression should be $2 \text{ or } 3 \times 10^{-6} \text{ gm./cm}^2/\text{sec}$. The exponent six may have been omitted.
- 46 Line 8. First word should be "concentration" instead of "pressure".
- 46 Line 9. Put a comma between "laws" and "so".
- 74 Third line from bottom. Scratch last word in line, "when".
- 84 Line 9. The expression should be "when methanol (m.w. 32) diffused into nitrogen (m.w.28), ". The 32 was erroneously typed 44.
- 96 Line 13. Put "produce a large drop, that is, one of visible size" in place of "produce a large, visible sized drop".
- 97 Line 3. Put "a drop of stable size" in place of "a stable sized drop".
- 97 First sentence of last paragraph of Section 2. Put "The fluctuations in size of drops upon which their growth is conditioned are computed quantitatively..." in place of "The fluctuations in size of drops which lead to their growth are computed quantitatively...."
- 98 Line 10. The symbol being defined is " p_s = vapor pressure over a flat surface of liquid at the prevailing temperature." (It may have been wrongly written p_v .)
- 102 Equation 18. The "q" should have subscript " $\frac{1}{2} + 1$ " which may have been omitted.

118 Line 3. Put "So to a sufficient...." in place of "So to a good enough...."

118 Equation 65 should read " $\ln_e S_K = 0.75 \ln_e S_\mu = \dots$ "

130 Next to bottom line. Replace asterisk by 28, and scratch reference at bottom of page.

131 Line 8. Scratch sentence "This case will be returned to below."

131 Equation 4. Insert r_2 so that the equation reads

$$\ln p_2/p_0 = 2\sigma M/\rho RT r_2$$

141 Figure 32. Top left photograph, Phil. Trans. Roy. Soc. London, 189A, 263 (1897). Top right, ditto, 189A, 276 (1897); Bottom left, ditto, 193A, 297 (1900); Bottom left, ditto, 193A, 291 (1900).

146 Reference 6d is erroneous. Scratch.

147 Reference 6j is erroneous. Scratch.

Note also: Appendix II and the Index have not yet been appended. Also Figures 11, 15, 25 and 30 do not exist.

CORRECTIONS AND NOTES FOR THESIS
ON THE CONTINUOUSLY SENSITIVE CLOUD CHAMBER

July 28, 1938

Alexander Langsdorf, Jr.

Note that the page numbering in various copies of the thesis may differ by one or two pages from that given below. The context will show where to apply the correction indicated.

Page 95, Figure 29. The interpolation shown in this figure is wrong. See below under page 106.

Page 101. Equation 15 should be:

$$\frac{1}{\alpha_m} \left(1 - \frac{1}{4\alpha_m^3}\right) = \frac{1}{\alpha_n} \left(1 - \frac{1}{4\alpha_n^3}\right) = \frac{q}{\alpha_m} \left(1 - \frac{q^3}{4\alpha_m^3}\right)$$

Page 104, equation 34. The simplification carried through here was facilitated by the substitution:

$$\frac{1}{\alpha_n} \left(1 - \frac{1}{4\alpha_n^3}\right) (\alpha_n^3 - \alpha_m^3) = \frac{1}{\alpha_n} \left(1 - \frac{1}{4\alpha_n^3}\right) \alpha_n^3 - \frac{1}{\alpha_m} \left(1 - \frac{1}{4\alpha_m^3}\right) \alpha_m^3 \quad \text{etc.}$$

Page 104, equation 34, continued. Note also that

$$\frac{3}{4\alpha_n} (\omega^4 - \omega^5 + \dots) = \frac{3}{4\alpha_n} \frac{\omega^4}{1 + \omega}$$

Page 106, equation 38. The brackets should be $(\alpha_n^3 - 1)$ and $(\alpha_n^3 + \frac{1}{2})$.

The square powers given were erroneous.

The determination of Q_ω as described just after equation 38 is not satisfactory. Values of Q_ω have been found by numerical integration, as follows:

$\mu \ln S_p$	q	Q_ω
33.13	0.7	0.27
"	0.8	0.31
"	1.0	0.30
48.7	0.7	0.22
"	0.8	0.27
"	1.0	0.26

The following approximation is probably satisfactory:

For $Q_{\frac{1}{3}}(q) < Q_\omega$ ($q = 1$) = C, a constant,

use $Q_\omega = Q_{\frac{1}{3}}(q)$

For $Q_{\frac{1}{3}}(q) > C$, (i.e., approximately from $q = 0.7$ to $q = 1.0$)

use $Q_\omega = C$, a constant.

Page 107, equation 45. This should be:

$$\begin{aligned}
 (\alpha_n - \alpha_m) \left(\frac{\alpha_n + \alpha_m}{2} - \frac{1}{\alpha_n \alpha_m} \right) &= \left(\frac{1-q}{q} \right) \alpha_n \left(\frac{\alpha_n (1+q)}{2q} - \frac{q^2}{\alpha_n} \right) \\
 &= \frac{(1-q)^3 (1+4q+q^2)}{8\alpha_m q^2} = \frac{Q(3)}{8}
 \end{aligned}$$

